Title: Cross-scale assessment of environmental variation on the rabies virus reservoir *Desmodus rotundus*

Paige Van de Vuurst McClure

Thesis submitted to the faculty of the Virginia Polytechnic Institute and State University
in partial fulfillment of the requirements for the degree of:

Doctorate of Philosophy
in
Translational Biology, Medicine, and Health

Luis E. Escobar, Chair

Andrea S. Bertke

Cassidy Rist

Eric M. Hallerman

Julia M. Gohlke

December 5th, 2024

Blacksburg, Virginia, United States

Keywords: Ecological Niche Modeling, Spillover, Climate Change, RABV, *Desmodus rotundus*, Population Genetics

Cross-scale assessment of environmental variation on the rabies virus reservoir *Desmodus rotundus*

Paige Van de Vuurst McClure

ABSTRACT

Anthropogenic impacts on the natural world are a topic of continued assessment and scientific concern. Human activity has been shown to impact multiple ecological components, with changes to disease dynamics caused by human activity being linked to disease emergence and pandemic risk. In Latin America, the rabies virus (RABV) is regularly transmitted by the common vampire bat (*Desmodus rotundus*). Rabies virus is extremely lethal, killing nearly 100% of infected individuals. *Desmodus rotundus* is a sanguivorous (blood-feeding) species that can easily transmit RABV to their prey during normal feeding behaviors, thereby acting as a wildlife reservoir and known host for the virus. Previous research has found that vampire bat-transmitted RABV has increased in prevalence and geographic distribution in association with changes to landscape and climate. As such, the *D. rotundus*-RABV disease system exemplifies many of the factors identified as foundational to the broader elucidation of disease emergence from pathogens of wildlife origin. This dissertation demonstrated how environmental variation associated with human activity may impact *D. rotundus* at the population level, the impacts of landscape factors on spillover transmission risk, and the broader climatic drivers of host distribution across a continent. In doing so, this cross-scale assessment filled key research gaps in our current understanding of emerging infectious diseases of bat origin.

Cross-scale assessment of environmental variation on the rabies virus reservoir *Desmodus rotundus*

Paige Van de Vuurst McClure

GENERAL AUDIENCE ABSTRACT

Human activity has had and will continue to have large impacts upon the natural world. Our choices of how to use the land and our contribution to changing climate can have negative impacts upon the health of ecosystems and animals. By changing where certain animals can live, our actions can increase the risk of new pathogens being transmitted to other animal species, or even to humans. The common vampire bat (*Desmodus rotundus*) is an example of one such animal. Vampire bats feed upon the blood of other mammals by biting. The nature of their feeding makes them very effective transmitters of the rabies virus, which is nearly 100% fatal. In Latin America, vampire bats regularly transmit rabies virus to livestock, which causes negative impacts to animal welfare, public health, and the economy. Previous research has found that the impact of vampire bat-transmitted rabies virus has increased because of changes to the landscape and climate. As such, the vampire bat-rabies disease system provides a study system through which we can understand how human activity impacts the spread of wildlife pathogens. This dissertation assessed how environmental variation associated with human activity impacts the population genetics of vampire bats, what factors increase or decrease rabies virus transmission from vampire bats to other species, and how changes to climate may shape the future distribution of vampire bats across the Americas. In doing so, this research answered many of the questions that were previously unanswered about this bat-disease system, and potentially others wildlife-mediated systems.

DEDICATION

I would like to dedicate this dissertation to every person who has supported me, shaped me, defended me, and allowed me stumble through their orbit in these last three decades that I have been alive. I have never been the best at knowing how and when to say 'thank you', but I hope that I have let you know the depth of my gratitude. To my family and friends, who have never hesitated to lend me their ears to listen or shoulders to lean on, I hope you know how beautiful you are. A heart is a heavy burden to carry alone, and for some reason you all have chosen to help me carry mine. I hope that I have in some way helped you to carry yours. To every mentor and teacher that has taken the time to hold my hand and guide me through this process, I hope and pray that this world gives you the same kindness and reassurance that you have given me. To my students and colleagues, thank you for teaching me more than I could ever hope to impart. To my husband Jon, who is the light I sail home to whenever I am lost, you are the safest harbor I have ever known and I unquestionably could not have done this without you. Lastly, I would like to dedicate this dissertation to all of the young people in the world who dare to dream of better things in a world so full of sound and fury. Daring to be alive when the world would rather tear you to pieces is no small act of bravery and you, my dear, are stronger than you know.

ACKNOWLEDGMENTS

I would like to extend my sincere acknowledgement to the Unidad de Planificación Rural Agropecuario and the Instituto Colombiano Agropecuario Epidemiological Surveillance and Animal Health Technical Direction for their invaluable collaboration, their generous sharing of data, and insightful comments. Specifically, I would like to acknowledge Daniel Aguilar Corrales, Andrés Felipe Rodríguez Vásquez, Cesar Andrés Cortes Bello, Carolina Linares Chaparro, Jaime Unriza Vargas, and Zulma Rojas-Sereno. I would also like to acknowledge Antoinette Piaggio and Annie Tibbels for the provision of samples for the completion of this dissertation. Special acknowledgment should also be given to the efforts of Carley Elliot, Quan Dong, Kaitlyn Enstice, Carlos Hinajosa, Julia Alexander, Katelyn Domke**,** Juan Camilo Quintero, Laura Valentina Ávila Vargas, Karen Daniela Sarmiento Arias, Nicolas David Sanabria Rivera, Analorena Cifuentes, Diego Soler-Tovar, Shariful Islam, Connor Hughes, Reilly Brennan, and Paanwaris Paansri. Studies for this dissertation were supported by the National Science Foundation CAREER (2235295) and HEGS (2116748) awards, by the National Institute of Allergy and Infectious Diseases of the National Institutes of Health under award number K01AI168452, and by seed grants from Virginia Tech Institute for Critical Technology and Applied Science, Pandemic Prediction and Prevention Destination Area, and Center for Emerging, Zoonotic, and Arthropod-borne Pathogens. The content is solely the author's responsibility and does not necessarily represent the official views of the National Institutes of Health.

TABLE OF CONTENTS

DEDICATION...……...…….…..……...……Page iv

ACKNOWLEDGMENTS…….…….……..…Page v

PREFACE AND ATTRIBUTION……...Page 7

INTRODUCTION…….……...……...……Page 8

CHAPTER 1: Assessing the effects of environmental variation on population genetic structure of *D. rotundus*….…….……...…Page 15

Tables and Figures……...……...…Page 30

CHAPTER 2: Drivers of rabies virus spillover risk distribution from bats to livestock in Colombia…….……..……Page 53

Tables and Figures…….……Page 67

CHAPTER 3: Vampire bats, emerging disease, and future climate change…….Page 80

Tables and Figures……...……..……Page 97

CONCLUSION...……...……...…..…Page 112

PREFACE AND ATTRIBUTION

Committee chair Luis E. Escobar (LEE) and committee members Andrea S. Bertke (ASB), Cassidy Rist (CR), Eric M. Hallerman (EMH), and Julia M. Gohlke (JMG), each contributed significantly to this dissertation and reviewed its contents before submission. LEE acted as the project design supervisor and facilitator, and contributed to the analytical framework of the study and the writing of each dissertation chapter for publication. ASB, CR, EHM, and JMG provided crucial guidance on the research methods, design, and interpretation of this work. ASB and EMH facilitated and guided research methods and interpretation of Chapter One, with EH and LEE contributing to the final draft of this chapter. LEE and CR contributed to the analysis and interpretation of Chapter Two and LEE and JMG contributed to the analytical methods and interpretation of Chapter Three. All Committee members served as editors for the chapters and provided key guidance on the written presentation of this work. Paige Van de Vuurst McClure (PVM), the student, acted as the lead author and research for this dissertation.

Chapters Two and Three of this dissertation were co-authored and submitted to journals for peer review prior to its defense. Chapter submission titles and authors are as follows:

- Chapter Two: Submitted to PLOS Neglected Tropical Diseases as an independent research article under the title "Drivers of rabies virus spillover risk distribution from bats to livestock in Colombia"
    - Authors: Paige Van de Vuurst, Cassidy Rist, Tatiana Medina-Rodriguez, Andres Felipe Osejo-Varona, Diego Soler-Tovar, and Luis E. Escobar

- Chapter Three: Submitted to Scientific Reports as an independent research article under the title, "Vampire bats, emerging disease, and future climate change".
    - Authors: Paige Van de Vuurst, Julia M. Gohlke, and Luis E. Escobar

INTRODUCTION

Anthropogenic impacts on the natural world are a topic of continued assessment and scientific concern. Human activity has been shown to impact multiple ecological components, with changes to disease dynamics caused by human activity being linked to disease emergence and pandemic risk [1,2]. Land use change, including the conversion of natural habitats to urban or agricultural landscapes, is widely considered to be a contributor to zoonotic disease risk in humans [3,4]. Similarly, anthropogenic climate change has been shown to increase the risk of cross-species pathogen transmission (i.e., spillover) [5,6]. Climate change has already contributed to fundamental shifts in the underlying socioeconomic and environmental determinants of health worldwide [7,8]. The differences between the best-case scenarios of climate change, where warming is kept to or below 2°C of pre-industrial temperatures, and the worst-case scenarios where warming meets or exceeds 5°C, are drastic [9]. Preventing climate change or stopping warming is no longer an option, as the deadlines to fully mitigate climate change have become untenable [10]. According to the ERA 5 dataset [11], 2024 will be the hottest year on record and the first year to completely exceed the 1.5°C of warming from pre-industrial levels threshold. Furthermore, climate change impacts on human and animal health are not evenly distributed geographically [12]. Tropical ecosystems are among the most impacted by emerging infectious diseases due to landscape and climate change [12–14]. Low-income countries in the tropics are at even greater risk of emerging diseases [15,16]. As such, the study of how human activity impacts ecosystem degradation and associated zoonotic spillover risk in the tropics is critically important for forecasting disease emergence. Nevertheless, quantitative evidence assessing ecosystem degradation and wildlife health is limited, especially in the tropics, where diseases are expected to

emerge at a faster rate [12] and where habitat degradation is occurring at an unprecedent pace [17–20].

Over the next century, shifts in environmental and climate conditions are expected to alter the global distribution of many wildlife species and their associated pathogens [21–23]. One taxonomic group which functions as a key reservoir of impactful zoonotic pathogens is bats, which can carry and transmit pathogens that cause virulent disease in humans and other mammals [24,25]. Many infectious agents, such as Marburg virus, Nipah virus, Hendra virus, and Middle East respiratory syndrome coronavirus (MERS-CoV), have emerged via pathogen spillover transmission from bats to livestock [26–28], with secondary transmission to humans causing zoonotic outbreaks [25]. Scientific concern exists regarding the impacts of landscape and climate change on bat health and associated disease emergence [29–32]. Currently, we lack a comprehensive understanding of how variation in landscape features and climate may influence the ecology of bats and other wildlife in general.

In tropic and subtropical Latin America, rabies virus (RABV) is regularly transmitted by the common vampire bat (*Desmodus rotundus*) [33,34]. Rabies virus is extremely lethal, killing nearly 100% of infected individuals [35]. *Desmodus rotundus* is a sanguivorous (blood feeding) species that can easily transmit RABV to their prey during normal feeding behaviors [36], thus acting as a wildlife reservoir and known host for the virus. Previous research has found that vampire bat transmitted RABV has increased in prevalence and geographic distribution in association with changes to landscape and climate [37–39]. As such, the *D. rotundus*-RABV disease system exemplifies many of the factors identified as foundational to the broader elucidation of disease emergence from pathogens of wildlife origin. The effective prevention and management of spillover transmission of zoonotic pathogens relies upon understanding of how spillover occurs

and how environmental factors modulate the likelihood of transmission.

The goal of this dissertation was to assess how ecosystem degradation will impact wildlife hosts at the population level (Chapter One), the impacts of landscape factors on spillover transmission risk (Chapter Two), and the broader climatic drivers of host distribution across a continent (Chapter Three). In doing so, this cross-scale assessment filled key research gaps in our current understanding of emerging infectious diseases of bat origin. To accomplish this goal, we combined field-based sampling and wet-lab analysis of population genetics with computational ecology. To assess population diversity and geneflow of *D. rotundus* (Chapter One), we utilized multiple microsatellite DNA markers with known polymorphism to identify how environmental variation impacts host populations across an elevational gradient in Colombia. Colombia is a diverse country in terms of climatic, biodiversity, and topographic variation. Colombia is also heavily affected by RABV, with multiple RABV outbreaks occurring every year in specific sites [40]. As such, abundant high-quality RABV data are available. We then used ecological niche modeling to generate estimates of RABV spillover risk using comprehensive data generated by collaborators in Colombia for the last decade and a variety of potential drivers (Chapter Two). Finally, we forecasted *D. rotundus'* expected distribution across the Americas using diverse global climate models across a range of possible future climate change scenarios (Chapter Three).

References

1. Jones BA, Grace D, Kock R, Alonso S, Rushton J, Said MY, et al. Zoonosis emergence linked to agricultural intensification and environmental change. Proc Natl Acad Sci USA. 2013;110: 8399–8404. doi:10.1073/pnas.1208059110

2. Morens DM, Fauci AS. Emerging pandemic diseases: How we got to COVID-19. Cell. 2020;182: 1077–1092. doi:10.1016/j.cell.2020.08.021

3. Gibb R, Redding DW, Chin KQ, Donnelly CA, Blackburn TM, Newbold T, et al. Zoonotic host diversity increases in human-dominated ecosystems. Nature. 2020;584: 398–402. doi:10.1038/s41586-020-2562-8

4. Gottdenker NL, Streicker DG, Faust CL, Carroll CR. Anthropogenic land use change and infectious diseases: A review of the evidence. Ecohealth. 2014;11: 619–632. doi:10.1007/s10393-014-0941-z

5. Carlson CJ, Albery GF, Merow C, Trisos CH, Zipfel CM, Eskew EA, et al. Climate change increases cross-species viral transmission risk. Nature. 2022;607: 555–561. doi:10.1038/s41586-022-04788-w

6. Filho WL, Ternova L, Parasnis SA, Kovaleva M, Nagy GJ. Climate change and zoonoses: A review of concepts, definitions, and bibliometrics. Int J Environ Res Public Health. 2022;19. doi:10.3390/ijerph19020893

7. Watts N, Amann M, Arnell N, Ayeb-Karlsson S, Beagley J, Belesova K, et al. The 2020 report of The Lancet Countdown on health and climate change: responding to converging crises. Lancet. 2021;397: 129–170. doi:10.1016/S0140-6736(20)32290-X

8. IPCC. Climate change 2014 impacts, adaptation, and vulnerability Part B: Regional aspects: Working group ii contribution to the fifth assessment report of the intergovernmental panel on climate change. Barros VR, Field CB, Dokken DJ, Mastrandrea MD, Mach KJ, Chatterjee M, et al., editors. Working Group II Contribution to the Fifth Assessment Report of the Intergovernmental Panel on Climate Change. New York, NY: Cambridge University Press; 2014. doi:10.1017/CBO9781107415386

9. Hausfather Z. Explainer: How 'Shared Socioeconomic Pathways' explore future climate change. In: Carbon Brief - Clear on Climate. 2018 [cited 12 May 2020]. Available: https://www.carbonbrief.org/explainer-how-shared-socioeconomic-pathways-explore-future-climate-change/

10. Hausfather Z. Analysis: When might the world exceed 1.5C and 2C of global warming? In: Carbon Brief - Clear on Climate. 2020 [cited 10 Aug 2024]. Available: https://www.carbonbrief.org/analysis-when-might-the-world-exceed-1-5c-and-2c-of-global-warming/#:~:text=Similarly%2C if future emissions remain,between the 2030s and 2050s

11. ERA 5 Dataset. Copernicus: 2024 virtually certain to be the warmest year and first year above 1 . 5°C. In: Copernicus Climate Change Services. 2024 [cited 11 Nov 2024]. Available: https://climate.copernicus.eu/copernicus-2024-virtually-certain-be-warmest-year-and-first-year-above-15degc#:~:text=According to Samantha Burgess%2C

Deputy,according to the ERA5 dataset.

12. Jones KE, Patel NG, Levy MA, Storeygard A, Balk D, Gittleman JL, et al. Global trends in emerging infectious diseases. Nature. 2008;451: 990–993. doi:10.1038/nature06536

13. Messina JP, Brady OJ, Golding N, Kraemer MUG, Wint GRW, Ray SE, et al. The current and future global distribution and population at risk of dengue. Nat Microbiol. 2019;4: 1508–1515. doi:10.1038/s41564-019-0476-8

14. Hansen G, Cramer W. Global distribution of observed climate change impacts. Nat Clim Chang. 2015;5: 182–185. doi:10.1038/nclimate2529

15. Bathiany S, Dakos V, Scheffer M, Lenton TM. Climate models predict increasing temperature variability in poor countries. Sci Adv. 2018;4: e5809. doi:10.1126/sciadv.aar5809

16. Pörtner, D.C. Roberts, M. Tignor, E.S. Poloczanska, K. Mintenbeck, A. Alegría, M. Craig, S. Langsdorf, S. Löschke, V. Möller, A. Okem BR. Sixth Assessment Report (AR6) of the IPCC. H.-O. Pörtner DCR, E.S. Poloczanska, K. Mintenbeck MT, A. Alegría, M. Craig, S. Langsdorf, S. Löschke, V. Möller AO, editors. Managing the risks of extreme events and disasters to advance climate change adaptation: Special report of the Intergovernmental Panel on Climate Change. 2022. doi:10.1017/CBO9781139177245.003

17. Kim DH, Sexton JO, Townshend JR. Accelerated deforestation in the humid tropics from the 1990s to the 2000s. Geophys Res Lett. 2015;42: 3495–3501. doi:10.1002/2014GL062777

18. Lawrence D, Vandecar K. Effects of tropical deforestation on climate and agriculture. Nat Clim Chang. 2015;5: 27–36. doi:10.1038/nclimate2430

19. Hoang NT, Kanemoto K. Mapping the deforestation footprint of nations reveals growing threat to tropical forests. Nat Ecol Evol. 2021;5: 845–853. doi:10.1038/s41559-021-01417

20. Escobar H. Deforestation in the Brazilian Amazon is still rising sharply. Science. 2020;369: 613. doi:10.1126/science.369.6504.613

21. Williams JE, Blois JL. Range shifts in response to past and future climate change: Can climate velocities and species' dispersal capabilities explain variation in mammalian range shifts? J Biogeogr. 2018;45: 2175–2189. doi:10.1111/jbi.13395

22. Hof C, Araújo MB, Jetz W, Rahbek C. Additive threats from pathogens, climate and land-use change for global amphibian diversity. Nature. 2011;480: 516–519. doi:10.1038/nature10650

23. Haver M, Le Roux G, Friesen J, Loyau A, Vredenburg VT, Schmeller DS. The role of abiotic variables in an emerging global amphibian fungal disease in mountains. Sci Total Environ. 2022;815. doi:10.1016/j.scitotenv.2021.152735

24. Irving AT, Ahn M, Goh G, Anderson DE, Wang LF. Lessons from the host defences of bats, a unique viral reservoir. Nature. 2021;589: 363–370. doi:10.1038/s41586-020-03128-0

25. Letko M, Seifert SN, Olival KJ, Plowright RK, Munster VJ. Bat-borne virus diversity, spillover and emergence. Nat Rev Microbiol. 2020;18: 461–471. doi:10.1038/s41579-020-0394-z

26. Han HJ, Yu H, Yu XJ. Evidence for zoonotic origins of Middle East respiratory syndrome coronavirus. J Gen Virol. 2016;97: 274–280. doi:10.1099/jgv.0.000342

27. Epstein JH, Field HE, Luby S, Pulliam JRC, Daszak P. Nipah virus: Impact, origins, and causes of emergence. Curr Infect Dis Rep. 2006;8: 59–65.

28. Han HJ, Wen H ling, Zhou CM, Chen FF, Luo LM, Liu J wei, et al. Bats as reservoirs of severe emerging infectious diseases. Virus Res. 2015;205: 2–6. doi:10.1016/j.virusres.2015.05.006

29. Piccioli Cappelli M, Blakey R V., Taylor D, Flanders J, Badeen T, Butts S, et al. Limited refugia and high velocity range-shifts predicted for bat communities in drought-risk areas of the Northern Hemisphere. Glob Ecol Conserv. 2021;28: e01608. doi:10.1016/j.gecco.2021.e01608

30. García-Morales R, Badano EI, Moreno CE. Response of neotropical bat assemblages to human land use. Conserv Biol. 2013;27: 1096–1106. doi:10.1111/cobi.12099

31. Streicker DG, Recuenco S, Valderrama W, Benavides JG, Vargas I, Pacheco V, et al. Ecological and anthropogenic drivers of rabies exposure in vampire bats: Implications for transmission and control. Proc R Soc B Biol Sci. 2012;279: 3384–3392. doi:10.1098/rspb.2012.0538

32. Becker DJ, Nachtmann C, Argibay HD, Botto G, Escalera-Zamudio M, Carrera JE, et al. Leukocyte profiles reflect geographic range limits in a widespread neotropical bat. Integr Comp Biol. 2019;59: 1176–1189. doi:10.1093/icb/icz007

33. Anderson A, Shwiff S, Gebhardt K, Ramírez AJ, Shwiff S, Kohler D, et al. Economic evaluation of vampire bat (*Desmodus rotundus*) rabies prevention in Mexico. Transbound Emerg Dis. 2014;61: 140–146. doi:10.1111/tbed.12007

34. Velasco-Villa A, Mauldin MR, Shi M, Escobar LE, Gallardo-Romero NF, Damon I, et al. The history of rabies in the Western Hemisphere. Antiviral Res. 2017;146: 221–232. doi:10.1016/j.antiviral.2017.03.013

35. Brunker K, Mollentze N. Rabies Virus. Trends Microbiol. 2018;26: 886–887. doi:10.1016/j.tim.2018.07.001

36. Páez A, Polo L, Heredia D, Nuñez C, Rodriguez M, Agudelo C, et al. Brote de rabia humana transmitida por gato en el municipio de Santander de Quilichao, Colombia, 2008. Rev Salud Pública. 2009;11: 931–943. doi:10.1590/S0124-00642009000600009

37. Piaggio AJ, Russell AL, Osorio IA, Jiménez Ramírez A, Fischer JW, Neuwald JL, et al. Genetic demography at the leading edge of the distribution of a rabies virus vector. Ecol Evol. 2017;7: 5343–5351. doi:10.1002/ece3.3087

38. Benavides JA, Valderrama W, Streicker DG. Spatial expansions and travelling waves of rabies in vampire bats. Proc R Soc B. 2016;283: 20160328. doi:10.1098/rspb.2016.0328

39. Van de Vuurst P, Qiao H, Soler-Tovar D, Escobar LE. Climate change linked to vampire bat expansion and rabies virus spillover. Ecography. 2023; e06714. doi:10.1111/ecog.06714

40. PANAFTOSA. Sistema de Información Regional para la Vigilancia Epidemiológica de la Rabia (SIRVERA). Vet Med Assoc. 2021;237: 646–657. doi:https://doi.org/10.2460/javma.237.6.646

CHAPTER 1: Assessing the effects of environmental variation on population genetic structure of *Desmodus rotundus*

Abstract

Tropical ecosystems worldwide are subject to emerging infectious disease risk, principally due to landscape degradation and climate change. Rabies virus (RABV) is a neglected tropical disease predominantly spread from bats to other species in Latin America by the common vampire bat (*Desmodus rotundus*). Transmission of RABV among *D. rotundus* individuals and colonies is a function of individual dispersal and gene flow, patterns of which can be inferred from population genetic structure. To assess how landscape heterogeneity may impact population structure of *D. rotundus*, we conducted a cross-elevation assessment of population genetics for this species in Colombia using nuclear microsatellite DNA markers. We quantified genetic variance and geographic distribution of genetically clustered individuals across the landscape of Colombia with a comparator group of *D. rotundus* individuals from Mexico. We found genetic structure within our collection of samples and inferred patterns of dispersal and migration between *D. rotundus* populations. Limited differences were observed between inferred populations regarding genetic variance, climate of occupancy, or landscape characteristics. Our results support previous hypotheses of male-biased and resistance-mediated patterns of dispersal for *D. rotundus,* and informs future research on the role of genetic connectivity upon RABV transmission between *D. rotundus* colonies.

Introduction

Ecosystem degradation can impact the spatial distribution and overall health of wildlife species [1,2]. Negative impacts upon wildlife health can increase the risk of pathogen spillover transmission from wildlife to livestock and humans [3]. Pathogen spillover transmission between species has been linked to some of the most lethal zoonotic disease outbreaks in human history [4]. Some examples include Ebola virus, Nipah virus, Avian Influenza, and SARS-COV-2 [5–12]. More specifically, spillover transmission from wildlife to livestock via disruption of multiple biological processes [3] has led to precipitous impacts upon animal health, food security, and human well-being due to economic losses and disease emergence [4,13]. Interactions among humans, livestock, and wildlife populations within disturbed ecosystems are expected to facilitate pathogen spillover transmission [11,14], and, by extension, to influence the risk of disease emergence in domestic animals and humans.

Viral shedding from wildlife increases when host immune competencies decline in disturbed ecosystems, resulting in greater host viral loads and discharge [15–18]. Wildlife mortality in disturbed ecosystems may reduce host abundances and decrease geneflow between populations, which in turn may decrease genetic diversity within the remaining wildlife populations [11,16,19]. Furthermore, genetic diversity has been linked to pathogen prevalence and virulence in wildlife hosts [20]. As such, ecosystem degradation can indirectly affect pathogen transmission dynamics in wildlife. Similarly, deforestation isolates wildlife populations [21–23], which could reduce geneflow, eroding genetic diversity within populations [21,24] and potentially lead to the loss of alleles and haplotypes affecting immune competence [25]. Ecosystem degradation continues at an accelerated rate in the Neotropics [26], suggesting that the effects of landscape and climatic degradation could be important drivers of zoonotic disease emergence in this region.

Tropical ecosystems are highly impacted by landscape degradation and climate change, elevating the risk of emerging infectious disease [27–29]. Low-income countries in the tropics are at great risk of emerging diseases borne by bats [30,31]. Hence, the study of how tropical ecosystem variation impacts the distribution and health of free-ranging bats is critically important for forecasting disease emergence. Rabies virus (RABV) is a prevalent and highly impactful bat-borne pathogen [32,33] predominantly spread from bats to other mammalian species in Latin America by the common vampire bat (*Desmodus rotundus*) [34]. RABV outbreaks in humans and livestock regularly occur in tropical and subtropical regions of Latin America [35], where human infection regularly follows outbreaks in livestock [36]. Spread of RABV among vampire bats may be a function of individual dispersal and gene flow, patterns of which can be inferred from population genetic structure. Furthermore, assessing population genetic structure can bypass the need for lengthy telemetry- or mark-recapture-based assessments of bat movement [37,38]. To assess how landscape heterogeneity may impact population structure of *D. rotundus*, we conducted a cross-elevational assessment of population genetics for this species in Colombia using nuclear microsatellite DNA markers. We evaluated genetic diversity, population structure and its spatial distribution among sampling locations across an elevational gradient. Our objective was to assess whether population genetic diversity and structure of *D. rotundus* populations varied across space, or was related to any environmental factors that could be used in the future to infer RABV transmission dynamics. Studies were conducted in Colombia, which has large environmental gradients within a relatively small study area, has endemic circulation of RABV, and where ecosystem degradation is ongoing at an unprecedented rate since the cessation of armed conflict in 2016 [39].

Methods

Experimental Design

Genetic variation of *Desmodus rotundus* was estimated from DNA isolated from 81 tissue samples collected during field sampling conducted in June and July of 2022 and 2023 (Table 1). Sampling of *D. rotundus* individuals was performed in RABV-endemic areas across an elevational gradient from low (< 500 meters), to moderate (500-1000 meters) to high (> 1000 meters) elevation. This elevational gradient was used as a proxy for multiple climatic and landscape factors which we related to population genetic variation of *D. rotundus*. Climatic measures included temperature, humidity, and landscape features such as cover type and associated land use (i.e., rural, agricultural, suburban, urban, undeveloped) for each sample site. Each sampling site was at least 20 km from other sampling sites, a distance comparable to *D. rotundus* home ranges [40,41].

Tissue Collection

Desmodus rotundus individuals were collected using 12×2.6-meter mist nets with a mesh size of 36 mm (Avinet Research Supplies, Inc., Portland, ME). Nets were opened 15 minutes before sunset and remained open for at least five consecutive hours (3900 m^2 sampling effort/site). Sampling was scheduled between the last and the first quarter of the lunar cycle to maximize periods of *D. rotundus* activity [42]. Capture and handling protocols followed guidelines of the American Society of Mammalogists [43], as approved by the Institutional Animal Care and Use Committee at Virginia Tech (IACUC approval # 21-138). Tissue samples from each captured individual were collected via either 1-mm wing punch, or from pectoralis muscle dissected from deceased individuals. Samples were stored in 1.8-ml cryogenic tubes and frozen at -20ºC after collection.

Samples were then placed in long-term storage in -80°C at La Salle University in Bogota, Colombia. Complementarily, five samples from a prior study collected in Colombia between 2019 and 2022 were provided by the Humboldt Institute (Bogota, Colombia) (Table 1). These samples were frozen at -80ºC after collection.

Molecular Methods

To estimate genetic similarity within and among *D. rotundus* populations, we followed molecular genetic protocols established by Streicker et al. (2016) and Piaggio et al. (2008). From tissue samples of each individual captured, we extracted DNA using the DNeasy Blood & Tissue Kit (Qiagen) and quantified double-stranded DNA using a µLite PC spectrophotometer (BioDrop, Cambridge, UK) at La Salle University in Bogota, Colombia. For each individual, we then amplified 12 nuclear microsatellite loci previously developed by Piaggio et al. (2008). The 12 loci were amplified using polymerase chain reaction (PCR) protocols [46] for the Promega GoTaq Gold PCR core system [47]. As a comparator, we amplified DNA from six *D. rotundus* individuals collected in western Mexico in 2007 by Piaggio et al. (2008) (Table 1, Figure 1). Each 25-µl PCR reaction consisted of 1.0 µl 25 mM $MgCl_2$, 5.0 µl of 5X colorless GoTaq Flexi buffer, 0.5 µl of 10 mM PCR nucleotide mix, 1.0 µl of 10 µM forward and reverse primer, 0.125 µl of GoTaq DNA polymerase, 2.0 µl of template DNA (<0.25 µg /25 µl), and 14.375 µl of nuclease-free water. The PCR thermal cycling profile consisted of initial denaturation at 95°C for 10 min; followed by 35 cycles of 94°C for 30s, 52°C for 45s, and 72°C for 45s; and a final extension at 72°C for 10 min. Samples then were held at 12°C for at least 15 min prior to being placed in storage at 2°C [48]. All reactions were performed in a Bio-Rad T100 thermal cycler. PCR amplification products were sent to the Cornell Institute of Biotechnology Resource Center for fragment-size analysis in 96-well

plates. We used the *Fragman* package (version 1.0.9) [49] in R statistical software version 4.1.0 [50] to automate peak calls for determining amplification fragment sizes for alleles at each of the 12 loci for each *D. rotundus* individual. Allele lengths were confirmed via a visual inspection of peaks for each locus in GeneMarker version 2.6.3 software [51].

Data Analysis

We used *PopGenReport* version 3.1 [52] in R version 4.1.0 to assess segregation of any null alleles at each locus using the Brookfield method [53,54]. We confirmed null allele frequencies using the Oosterhout method in Micro-Checker software version 2.2.3 [55–57]. Data for loci with null allele frequencies greater than 0.5 were removed from subsequent analyses.

We applied discriminant analysis of principal components (DAPC) [58] to identify clusters of genetically related individuals (i.e., populations) within our collection of samples. DAPC applies a multivariate method to identify clusters using sequential *K*-means without prior assumption of the number of populations or conformance of genotype frequencies to Hardy-Weinberg conditions [59,60]. Functionally, one can then identify the best-supported number of clusters by viewing the Bayesian information criterion (*BIC*) for each increasing number of *K*. We also used Structure software [61] for an alternative approach to cluster analysis that maximized conformance to Hardy-Weinberg genotype frequencies within and contrast among inferred clusters, applying the ln $P(D|K)$ criterion of Pritchard et al. (2000) and the delta K (*dK)* method of Evanno et al. (2005) to identify the best-supported value of *K*. We applied the *poppr* package version 2.9.6 [62] to conduct analysis of molecular variance (AMOVA) within individuals, among individuals within clusters, and between clusters.

For each cluster identified by DAPC, we used *hierfstat* version 0.5-11 [63] and *dartRverse* version 2.0 [64] to quantify allelic richness, observed and expected heterozygosities, inbreeding coefficient (F_{IS}, [65]). We used N_e Estimator [66] to estimate effective population size (N_e) using 0.05 as the lowest allele frequency. N_e was estimated using the Waples correction [67,68] to mitigate downward bias. We used the *poppr* package [62] to assess divergence from Hardy-Weinberg equilibrium (HWE) for each sample site and population. We used *dartRverse* to quantify genetic distance between sampling sites and populations using the F_{ST} and G'_{ST} metrics [69,70].

We applied a Mantel (1967) test to assess the relationship between genetic distances and geographic distances among our Colombian samples using Euclidean distance, F_{ST}, and G'_{ST} in the *PopGenReport* and *dartRverse* packages [52,64]. A Mantel test also was used to assess isolation-by-distance among our collection of samples from Colombia, and the relationship between the elevation of sample sites and genetic distance. To assess whether fine-scale genetic structure was a function of sex, we conducted a one-tailed permutation test to identify autocorrelation coefficients (r) for each sex [72]. We then estimated 95% bootstrap confidence intervals (100 replications) around the value of r for each sex at different distance-classes based on our sample sites. We assessed equilibrium levels of migration between populations and collection sites in Colombia using both Wright's F_{ST} equation for effective migration (m) [73,74] and direct identification of within sampled generation migrants in GeneClass 2.0 [75]. Effective migration or "equilibrium" migration rates can be interpreted as mean number of individuals migrants per generation across ecological time is calculated using F_{ST}, a metric of genetic differentiation [76,77]. In contrast, migrant identification in GeneClass2 directly identifies first-generation migrants and estimates the likelihood that these migrants originated from other sampled populations [75].

We used multiple *t*-tests to assess whether there were any differences between the values of associated climate or landscape metrics at the location of capture for each *D. rotundus* population in Colombia. These included annual average temperature (°C), annual average precipitation (mm), cattle density (individuals per km^2), and elevation (m). Climate and landscape variable data at the associated sampling sites were collected from the NASA Socioeconomic Data and Applications Center (SEDAC) [78], Gridded Livestock of the World Database [79], and the WorldGrids Archived database [80] at 1-km spatial resolution. Temporal range of the climate and landscape data were from 2016-2020.

Results

Genetic variation within a total of 92 *D. rotundus* individual samples was assessed; 86 of the samples were collected in Colombia, while six collected in Mexico were regarded as a comparator group. Of the samples collected in Colombia, 79 had known sex, comprising 22 females and 57 males. All microsatellite loci proved polymorphic, with numbers of alleles ranging from three to 16. Private alleles, i.e., alleles only found in specific populations or at specific sampling sites [81,82], were observed in all populations (Table 2). There was evidence of divergence of genotype frequencies from HWE expectations for sampling sites Auga de Dios, Pipiral, and Puente Quetame (Table 2). All microsatellite loci had null allele frequencies below 0.5, except for locus *Dero_H02F_C03R* (Figure S1), data for which was excluded from subsequent analysis.

Analysis of *BIC* for increasing numbers *K* of DAPC clusters indicated greatest support for three clusters within the dataset (Figure S2). This inference was supported by results of Structure

analysis, with delta *K* supporting presence of three clusters among the sampling sites (Figure S3). The clusters were partitioned geographically (Figure 4). Population One encompassed the Mexico samples provided by A. Piaggio (United States Department of Agriculture) used as a comparator. Two populations were distributed across Colombia, with most of Population Two occurring in high-elevation portions of Colombia east of the central Andes Mountain passage (Figure 4). Population Three was distributed across the elevational gradient in montane central and western portions of Colombia (Figure 4). We used the three clusters identified from the DAPC analysis as hierarchical strata (i.e., populations), while respective sampling sites were considered subpopulations to calculate descriptive genotypic metrics (e.g., allelic variation, heterozygosities, and genetic distances) across both sampling sites and inferred populations. Observed heterozygosity (H_o) was less than expected heterozygosity (H_e) for all sampling sites and populations (Table 2).

Results of AMOVA analysis showed significant genetic variance (27.7%, p=0.01) within the respective sampling sites (Table 3). There was also significant variance between sampling sites within populations (5%, p=0.01), and between populations in Colombia (14.9%, p=0.01) (Table 3). Populations Two and Three from Colombia had similar mean numbers of alleles per locus (7.4 and 7.1, respectively) and allelic richness (4.9 and 4.5) (Table 2). The comparator group from Mexico had lower allelic richness (4.2), although that population had a smaller sample size (Table 2). The inbreeding coefficient F_{IS} for all populations was between 0.31 and 0.33, indicating an excess of homozygotes above Hardy-Weinberg expectations [53], suggesting inbreeding or family structure. Estimated effective population sizes for the populations in Colombia were 16.9 for Population Two and 41.6 for Population Three (Table 2). High genetic distances (F_{ST} ~ 0.30, G'_{ST} ~ 0.80) were observed between Population One in Mexico and Populations Two and Three in

Columbia (Table 4). Genetic distances between Populations Two and Three in Colombia were comparatively low (F_{ST} = 0.12, G'_{ST} = 0.34). The estimate equilibrium rate migration across an ecological time-scale (i.e., effective migration) between Populations Two and Three was 1.83 individuals per generation. Effective migration between sites indicated that there was high migration (>1 individuals per generation) between sites that were closer together (< 120 km) and located on either side of the Rio Magdalena valley (i.e., Ibague, Casanare, Agua de Dios, Rey Zamuro, and Chaparral) (Table S2). GeneClass2 direct migrant assessment revealed 15 likely first-generation migrants. Ten of these likely migrants were captured in Population Three (Table S3) and the remaining five in Population Two. Migrants were captured at sites Agua de Dios, Casanare, Chaparral, Coello, Piedras, Rey Zamuro, Pipiral, Puerto Quetame, and Rey Zamuro. Identifying first-generation migrants between local collection sites was not possible due to limited sample size from some such sites.

Multiple *t*-tests of environmental characteristics at the respective sampling locations showed no significant differences between the environments of each population in Colombia. Population Three occurred at an overall lower elevation (mean elevation 575.2 m) than Population Two (mean of 807.5 m), a difference which was not significant statistically (t=1.91, df=71.72, p=0.06). There was a positive but non-significant relationship between genetic distance (F_{ST}, G'_{ST}, or Euclidean distance) and geographic distance (km) (Mantel statistic=0.05, p=0.27, Mantel statistic=0.07, p=0.18, and Mantel statistic=0.05, p=0.23, respectively). There was no significant relationship between the elevation of sampling sites and genetic distance (Mantel statistic=0.05, p=0.15). Both females and males showed positive spatial autocorrelation of genotype frequencies up to 165 meters (Figure 6). Females had stronger fine-scale genetic structure than males at short geographic distances. Females had significant fine-scale genetic structure at 360 meters (p=0.001).

Males had significant fine-scale genetic structure at greater distances (>330 meters, p=0.03). These results suggest that *D. rotundus* individuals captured >360 meters apart are unlikely to be related, and that males disperse farther than females. Assessment of differential dispersal by sex for each independent population was not possible due to limited power for Population Three, where only five females were captured.

Discussion

The objective of this study was to conduct a baseline assessment of population genetic structure among *D. rotundus* individuals collected across an elevational gradient in Colombia. Our main goal was to assess the possible implications of these genetic structures and associated geographic patterning and ecological factors on transmission dynamics for RABV in Colombia. We utilized standard molecular genetic methods for assessment of genetic variation at 11 microsatellite loci developed by Piaggio et al. (2008). We then quantified genetic variation and distribution of genetically clustered individuals across the landscape of Colombia, using a comparator group of *D. rotundus* individuals from Mexico. We found that genetic structure was present within our collection of samples from Colombia, with two distinct populations being evident. Limited differences were present between these populations with regard to genetic variance, climate of occupancy, or landscape characteristics. Based upon the data assessed here, we observed a trend suggestive of a difference in elevation between the two inferred *D. rotundus* populations identified in Colombia. Our assessment also confirmed male-biased dispersal for *D. rotundus* individuals sampled for this study [46]. These trends, although not statistically significant, could inform future research on the importance of genetic connectivity upon RABV transmission between *D. rotundus* colonies.

Two distinct populations were apparent within the collection of samples from Colombia. Less genetic variance was present between sampling sites within each inferred population than between individuals within each sampling site, indicating that each cluster of *D. rotundus* colonies in our analysis is genetically diverse (Table 3). Results of previous research on *D. rotundus* have suggested that individuals have limited home ranges (10-20 km) [41,83], and short-range dispersal has been related to slow wave fronts of outbreaks of *D. rotundus*-associated RABV [84]. Given that dynamic, we anticipated greater differentiation between the clusters identified, owing to the relatively large distances between our sampling locations across the landscape and elevational gradient of Colombia (21.6 km - 696.7 km between sites). Furthermore, genetic distance between the two populations based on both the F_{ST} and G'_{ST} metrics of genetic differentiation was modest (Table 3). Allelic richness, a metric of genetic diversity [85], also showed similar genetic diversity within the two Colombian populations. The small number of populations identified, coupled with the limited genetic distance between these two populations indicates that *D. rotundus* colonies in Colombia may be interconnected by migration [44,46,86]. Other research on genetic structure of *D. rotundus* in French Guiana found a greater degree of gene flow at a similar geographic scale to that in our study (i.e., regional) when compared to larger-scale comparisons between North and South America (Huguin et al., 2018). The spatial scale and geographic locations of previous studies may account for the differences identified between our results and among studies done in different locations.

Our estimate of equilibrium rate of migration (m=1.83) showed long-term connection between Colombian populations, and our direct migrant identification assessment identified many first-generation migrants within the sampled generation (n=15 of 86 individuals assessed). Most first-generation migrants (n=10) originated in the eastern population in Colombia (Population

Two), but were captured in the western population (Population Three) (Figure 4). All migrants were captured at low or moderate elevations (<1000 meters) except for one individual captured at sampling site Rey Zamuro. These results indicate that there is both an ecological history of migration between *D. rotundus* populations in Colombia, and current patterns of migration involving individuals moving west toward lower elevations. No significant differences in environment or climate of occupancy were apparent between the two inferred populations. There was also no statistical difference in anthropogenic factors such as agricultural activity or human population density. Greater effective migration rates were inferred between sites surrounding the Rio Magdalena valley, with sites to the east at higher elevations having the most apparent gene flow (Figure 6, Table S2). The two inferred populations were geographically separated by the Andes Mountains to the east of this valley as well (Figure 6). Other studies of *D. rotundus*-associated RABV have found that this species may disperse through low-resistance areas such as valleys [84,87], a finding convergent with our results. As such, our results support the potential role of elevation or topography in shaping *D. rotundus* dispersal.

Previous research also has found low genetic divergence among *D. rotundus* populations over large distances in some regions (i.e., Central America and Pantanal regions of Bolivia), while other regions in the same study had large genetic divergence over short distances (i.e., Atlantic Forests in southern Brazil) [46]. The authors hypothesized that greater genetic divergence may be driven by differences in ecoregion, rather than by distance per se for this species due to its volant nature. These results are consistent with those of our study, as distance among sites did not relate significantly to genetic differentiation. Nevertheless, other studies have found relatively low genetic differentiation across different ecoregions for *D. rotundus* at the leading edge of the species' broader geographic range in Mexico [88]. In contrast, another study in Mexico found a

higher degree of genetic diversity across a larger sample size and geographic area [48]. The lack of consensus among previous studies, and the lack of significant geographic or landscape patterns between populations in this study, reflects uncertainty regarding geographic population genetic patterning in *D. rotundus* across its range.

Results from this study confirm male-biased dispersal for *D. rotundus* [44,46]. Females showed positive spatial autocorrelation up to 165 meters, and males up to 660 meters (Figure 5). Related males were collected at locations much farther apart than females, which echoes results from previous literature [44]. Previous studies have assessed inbreeding coefficients (F_{IS}) by sex and by population to further assess male-biased dispersal [44]. Assessment of F_{IS} by sex and by population was not possible here, however, due to the limited number of females – just five – collected in Population Three. Dispersal of infected *D. rotundus* individuals could facilitate RABV transmission between subpopulations [83,89–91]. A limitation of this study is the lack of RABV prevalence data for the individuals collected. Hence, we are unable to assess the effect of genetic structure of *D. rotundus* in Colombia upon RABV spillover. Our findings of broader interconnection between *D. rotundus* populations in Colombia could help explain how RABV is spread across the country, particularly from eastern locations with higher cattle density to other, less agriculturally dense areas [92]. Our sample size was smaller than those of previous assessments [48,93], though our samples were collected over a narrower time-range. Assessment of a greater sample size across a broader geographic area or more diverse environments may further elucidate the impacts of environmental variation upon population genetic patterning of *D. rotundus* in Colombia. Utilizing only amplified fragment-size analysis for scoring microsatellite markers may have limited our observation of genetic variation as well. Other methods such as microsatellite genotyping by sequencing (SSR-GBS) or whole-genome sequencing for single

nucleotide polymorphisms (SNPs) likely could have shown more detailed patterns of genetic structure [94]. Future research in this system should work to increase the geographic scope of sampling to capture more ecoregions or fine-scale landscape factors that may shape genetic differentiation for *D. rotundus* populations. Future research should also couple genetic assessments with RABV seroprevalence assessment to more directly test hypotheses of RABV transmission driven by dispersal of infected *D. rotundus* individuals.

Conclusions

Our results add to current knowledge of the regional distribution of genetic variation for *D. rotundus*. Our results support previous literature that has hypothesized that topographic features such as valleys may facilitate dispersal and connectivity of *D. rotundus* populations across space. A more detailed assessment of the role of elevation in *D. rotundus* population structure and distribution is needed to fill knowledge gaps identified in this study. A broader understanding of the regional factors that impact *D. rotundus* dispersal could inform efforts to control RABV spillover transmission and would thereby benefit both animal and human health. Broader geographic population genetic patterning of *D. rotundus* has yet to be definitively identified. On a more global scale, by understanding how landscape variability impacts the genetic differentiation of a widely distributed bat disease reservoir, we may be better able to forecast disease emergence in the age of global climate change [95].

Tables and Figures

Table 1: Sample sites for collection of tissue from *Desmodus rotundus* individuals. Sampling sites (i.e. locations of collection) were located across an elevational gradient from low (<500 meters in elevation), to moderate (500-1000 meters in elevation) to high (> 1000 meters in elevation). This elevational gradient was used as a proxy for environmental variation through which we assessed multiple factors as they relate to population genetics of *D. rotundus* in Colombia. Samples for this study were collected in the summers of 2022 and 2023. Five samples were provided by the Humboldt Institute (Bogota, Colombia) and were collected in Colombia between 2019 and 2022. As a comparator, we amplified DNA from six *D. rotundus* individuals collected in western Mexico in 2007 by Piaggio et al. (2008).

Sampling Site	N	Source	Latitude (Decimal Degrees)	Longitude (Decimal Degrees)	Elevation (m)
Agua de Dios	40	This Study, Colombia	4.35107	-74.6516	407.80
Arauca	1	Humbolt Institute, Colombia	6.567921	-70.8962	15.54
Casanare	1	Humbolt Institute, Colombia	5.880638	-71.8929	151.00
Chaparral	9	This Study, Colombia	3.64442	-74.4784	615.00
Coello	7	This Study, Colombia	4.24741	-74.9761	439.20
El Porveni	1	Humbolt Institute, Colombia	9.374642	-75.7619	36.16
Ibague	5	This Study, Colombia	4.57583	-75.3265	2198.90
Medina	1	A. Piaggio, Mexico	4.5084	-73.3499	760.00
Nuevo Leon	2	A. Piaggio, Mexico	25.32615	-100.159	1200.00
Piedras	6	This Study, Colombia	4.44218	-74.9877	619.10
Pipiral	5	This Study, Colombia	4.204709	-73.7138	965.30
Puente Quetame	7	This Study, Colombia	4.30932	-73.8788	1890.00
Puerto Gaitan	1	Humbolt Institute, Colombia	4.312969	-72.0836	207.00
Rey Zamuro	2	This Study, Colombia	3.531883	-73.4025	297.30
Tamaulipas	4	A. Piaggio, Mexico	23.96592	-99.3659	623.00

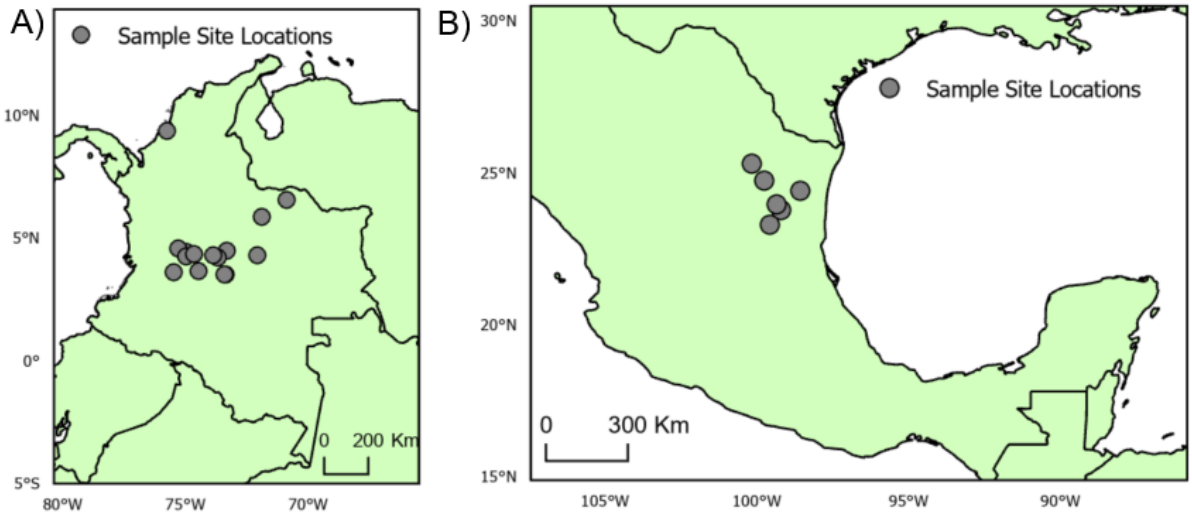

Figure 1. Sample sites for tissue collection. A) Locations of sample sites for *D. rotundus* individuals in Colombia. All sampling sites were at least 20 km from one another. Greatest distance between sampling sites was 669 km. **B) S**ites of collection for *D. rotundus* samples from Mexico provided by A. Piaggio. Geographic coordinates for sampling sites are provided in Table 1.

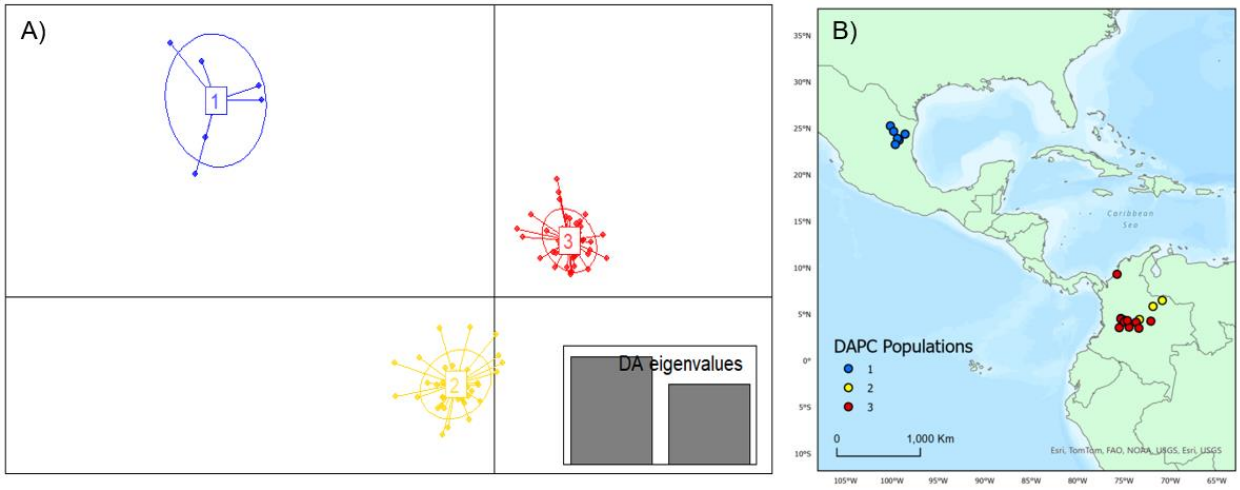

Figure 4. DAPC cluster distribution of genotype data by collection. A) Visual representation of each population cluster identified by DAPC. The axes used are the first two principal components with two discriminant analysis eigenvalues (DA eigenvalues, inset). **B)** Geographic distribution of DAPC populations. The colors of the respective DAPC clusters and geographic locations are the same. Note that only six individuals comprise the first population, which was utilized as a comparator for this study.

Table 2. Descriptive metrics of populations and sampling sites. Populations (Pops) represent clusters identified by DAPC analysis. Sampling sites represent locations of collection. *N* indicates number of individuals collected at each site. We utilized multiple R packages to quantify the mean number of alleles per locus, private alleles per locus (alleles only found in specific populations or subpopulations), allelic richness, observed (H_o) and expected (H_e) heterozygosities, significance of divergence from Hardy-Weinberg equilibrium (HWE), and effective population size (N_e) of each cluster identified by DAPC and for each sampling site. N_e was estimated using the Waples correction (Waples & Do, 2010; Waples et al., 2016) to mitigate downward bias. Inf indicates that N_e was estimated as infinite, likely owing to small sample size and related lack of heterozygotes. There was evidence of divergence from HWE for sampling sites Auga de Dios, Pipiral, and Puente Quetame.

Pops	**Sampling Sites**	***N***	**Mean alleles per locus**		**Private alleles per locus**		**Allele Richness**		***H*o**		***H*e**		**Departure from HWE**		***N*e**	
1	Tamaulipas	4	2.91	3.90	10	24	1.56	4.18	0.55	0.52	0.56	0.66	0.55	0.53	0.3	Inf
	Nuevo Leon	2	2.36		7		1.68		0.55		0.81		0.36		Inf	
2	Agua de Dios	18	6.45	7.36	4	11	1.65	4.91	0.40	0.37	0.66	0.67	**0.001**	0.25	20.8	16.9
	Arauca	1	1.09		1		NA		0.20		NA		0.86		Inf	
	Casanare	1	1.27		0		1.27		0.27		NA		0.81		In.	
	Chaparral	9	4.45		1		1.64		0.47		0.65		0.24		Inf	
	Coello	7	3.09		0		1.67		0.48		0.72		0.49		Inf	
	Medina	1	1.36		0		1.36		0.36		NA		0.75		Inf	
	Pipiral	5	4.18		5		1.73		0.35		0.79		**0.01**		Inf	
3	Agua de Dios	22	6.50	7.09	4	11	1.65	4.49	0.40	0.4	0.66	0.64	**0.01**	0.23	20.8	41.6
	El Porveni	1	1.36		0		1.36		0.36		NA		0.75		Inf	
	Ibague	5	3.55		0		1.64		0.35		0.68		0.36		Inf	
	Piedras	6	3.45		1		1.55		0.33		0.58		0.29		0.8	
	Puente Quetame	7	3.82		2		1.63		0.39		0.65		**0.03**		42.6	
	Puerto Gaitan	1	1.09		1		NA		0.20		NA		0.86		Inf	
	Rey Zamuro	2	2.36		0		1.67		0.41		0.78		0.42		Inf	

Table 3. Analysis of molecular variance between and among collection of *D. rotundus* populations and sampling sites analyzed. Variance and significance values within and between both Colombia populations delineated by DAPC and subpopulation (i.e., sample site locations). Significant variance was present across all strata tested. Most covariance originated from within the samples.

Source	Degrees of Freedom	Sum of Squares	Mean Square	Sigma	% Covariance	ϕ	*p* value
Between populations	2	164.93	82.47	1.28	14.89	0.15	0.01
Between sample sites within populations	20	239.34	11.97	0.43	5.01	0.06	0.01
Between individuals within each sample site	69	640.05	9.28	2.38	27.70	0.35	0.01
Within individuals	92	414.81	4.51	4.51	52.40	0.48	0.01
Total	183	1459.14	7.97	8.61	100	-	-

Table 4. Metrics of genetic distance between populations. F_{ST} (below diagonal) and G'_{ST} (above diagonal) metrics of genetic distance between populations identified by DAPC. Greater genetic distance is signified by large numbers. Largest genetic distance was present between populations one and three. Less genetic distance was present between Colombian populations two and three, indicating greater gene flow between the two populations.

	Population 1	**Population 2**	**Population 3**
Population 1	-	0.78	0.83
Population 2	0.28	-	0.34
Population 3	0.31	0.12	-

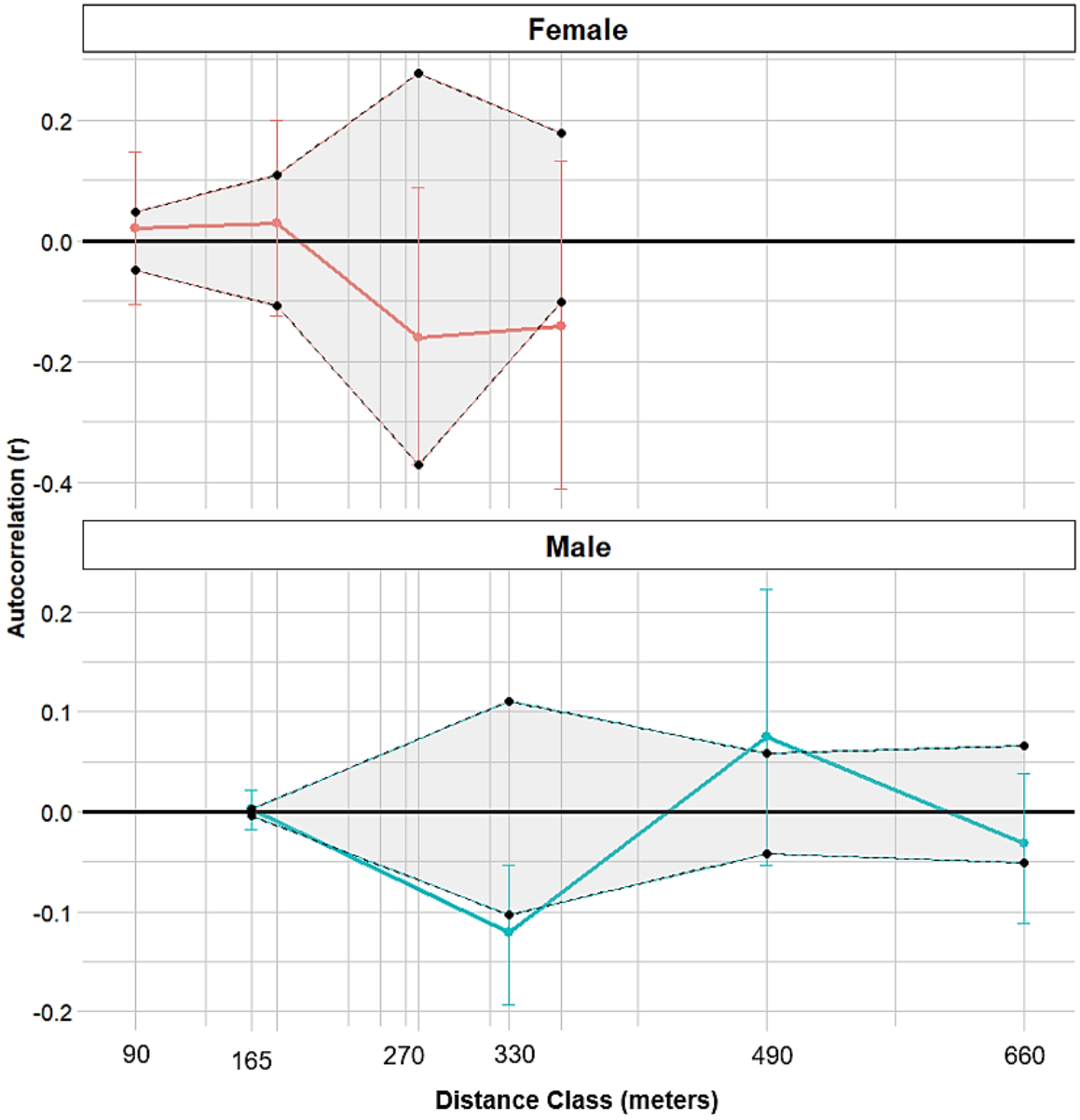

Figure 5. Genetic structure across distance by sex. To assess whether fine-scale genetic structure was evident based on sex, we conducted a one-tailed permutation test to identify autocorrelation coefficients (*r*). We then estimated 95% bootstrap confidence intervals (grey shaded area) around the value for *r* for each sex at different distances classes based on our samples. In this case, if the bootstrap confidence intervals do not overlap zero, then fine-scale genetic structure is present. Both females and males showed positive spatial autocorrelation up to 165 meters.

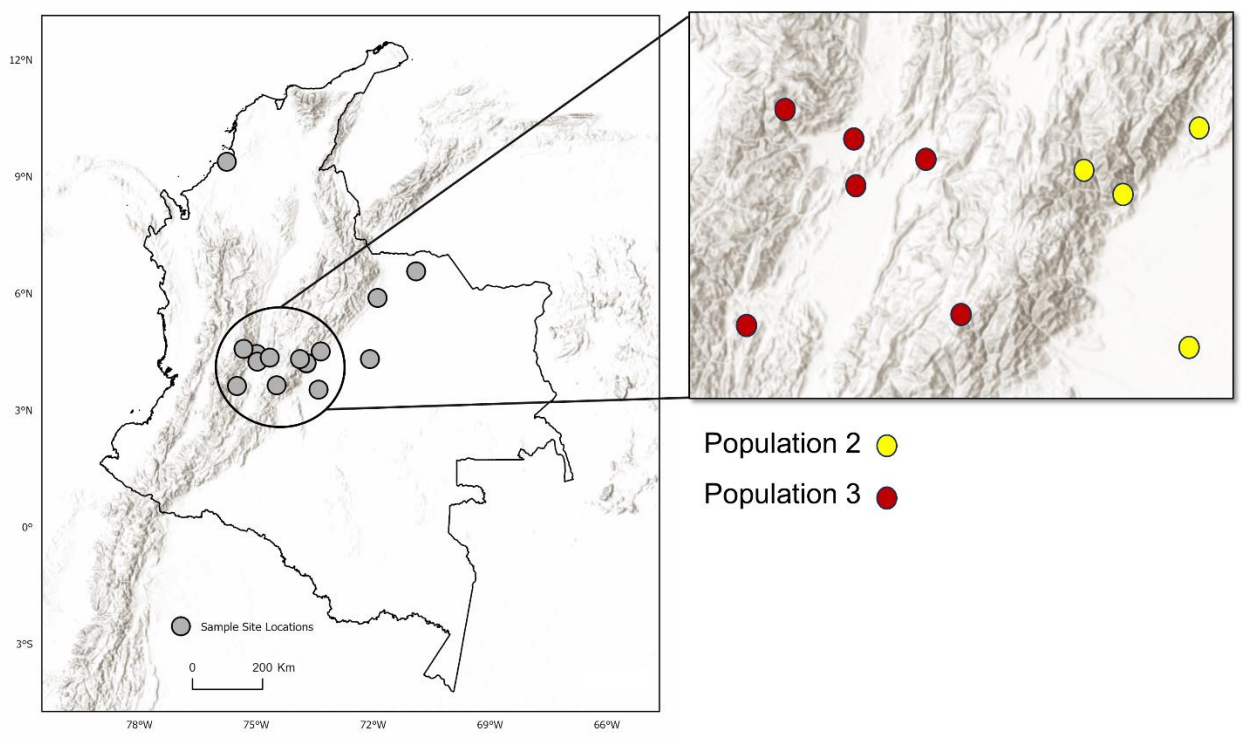

Figure 6. Topographic relief and population distribution. Location of sampling sites across the Andes Mountain range. Inset map shows the Rio Magdalena valley, where higher rates of migration between sampling sites were detected. Partition of DAPC populations Two and Three (inset map on right) are shown as well. Note the topographic pattern of population partitioning from Population Three to Population Two.

Supplementary Information

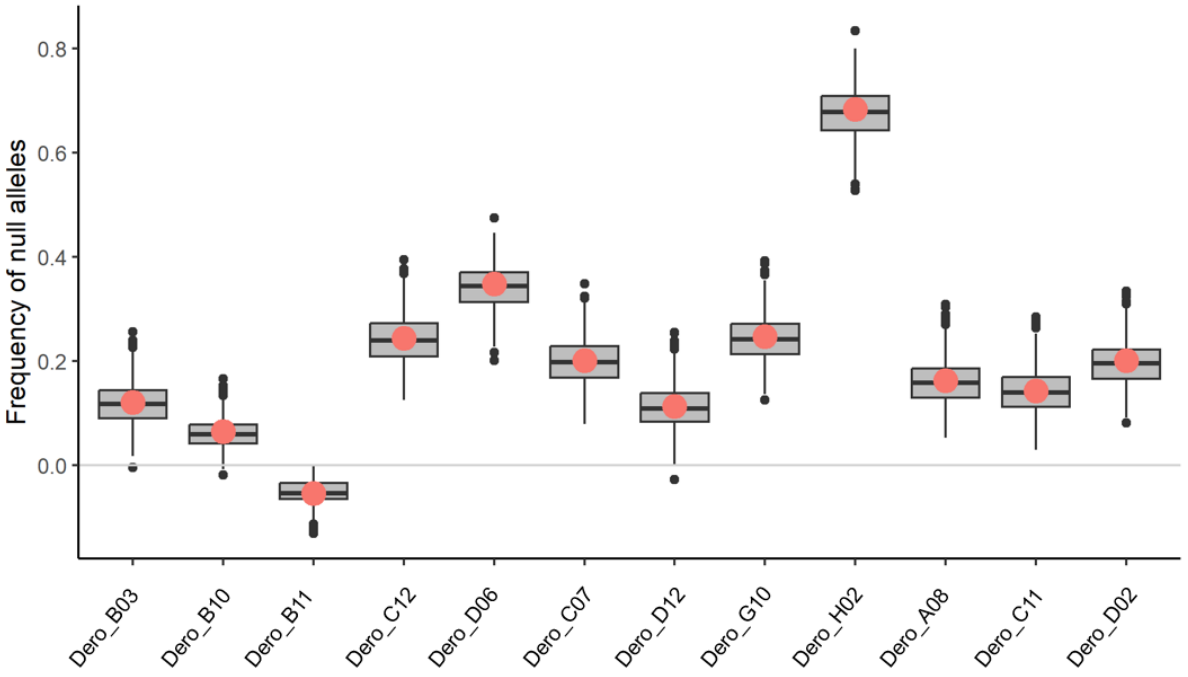

Figure S1. Null Allele Frequency in *Desmodus rotundus* samples from Colombia. Estimated frequencies of null alleles at each of the 12 microsatellite loci for *Desmodus rotundus*. Null allele frequency was estimated using the Brookfield (1996) method in MicroChecker [55]. Loci with null allele frequency >0.5 were eliminated from consideration (i.e., locus *Dero_H02*).

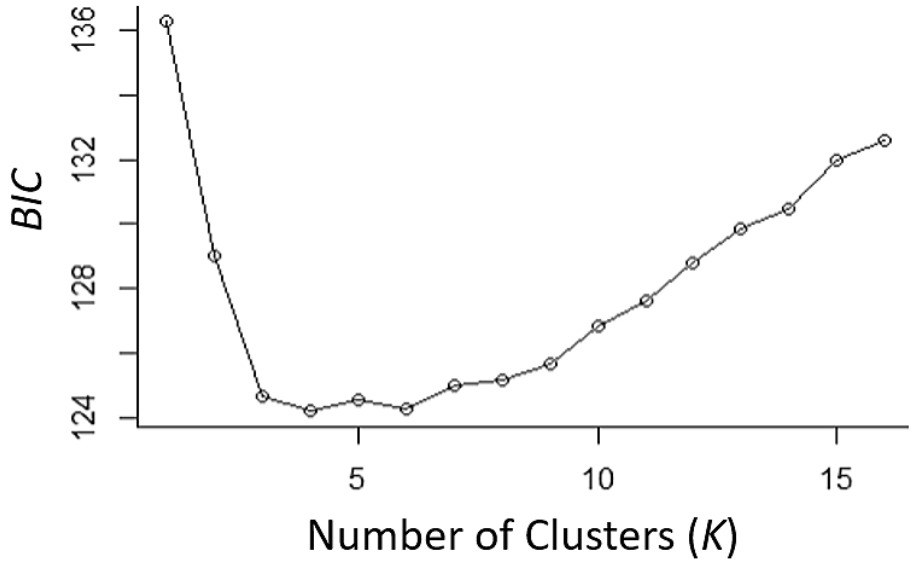

Figure S2. DAPC Cluster analysis of *Desmodus rotundus* genotype data by collection. Bayesian information criterion (*BIC*) model selection criterion for progressive numbers of DAPC clusters (*K*) for identification of the best-supported number of clusters within our samples. We tested one to 15 clusters (three more than the number of sampling sites). Results indicate that three clusters of genetically similar individuals (i.e. populations) are most likely present within the data.

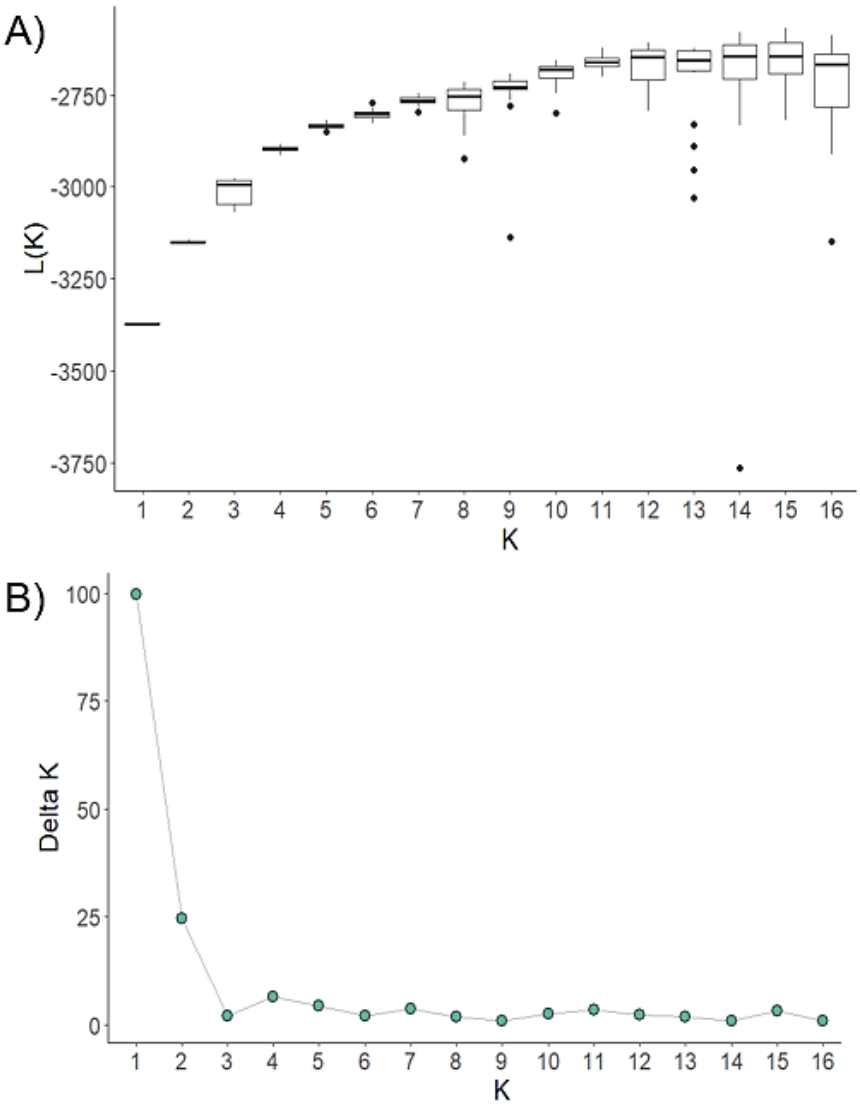

Figure S3. Structure based cluster analysis of *Desmodus rotundus* microsatellite data: Analysis of Structure-based clusters (*K*) [61] conducted using the delta *K* method of Evanno et al. (2005) [96]. **A)** Mean likelihood of each cluster from 20 replicate runs for each value of *K*. **B)** Delta *K* (mean absolute value of average likelihood over 20 runs divided by the standard deviation of mean likelihood) of each progressive number of clusters. Analysis of delta *K* was performed using Structure version 2.3.4 [61].

Table S1. Metrics of genetic distance between sampling sites. F_{ST} and G'_{ST} metrics of genetic distance between each sampling site of *D. rotundus* individuals. Greater genetic distance is signified by large numbers. Sampling sites Nuevo Leon and Tamaulipas were located in Mexico and were used as a comparator for all other sites located in Colombia.

	G'_{ST}															
F_{ST}		Agua de Dios	Arauca	Casanare	Chaparral	Coello	El Porveni	Ibague	Medina	Nuevo Leon	Piedras	Pipiral	Puente Quetame	Puerto Gaitan	Rey Zamuro	Tamaulipas
	Agua de Dios	-	0.73	0.53	0.14	0.06	0.48	0.07	0.54	0.79	0.18	0.29	0.23	0.52	0.06	0.80
	Arauca	0.20	-	0.68	0.71	0.65	0.91	0.72	0.52	0.88	0.82	0.60	0.61	0.94	0.66	0.95
	Casanare	0.11	0.00	-	0.61	0.51	0.88	0.46	0.68	0.88	0.72	0.41	0.53	0.71	0.42	0.93
	Chaparral	0.04	0.21	0.17	-	0.14	0.52	0.18	0.61	0.84	0.34	0.35	0.36	0.62	0.12	0.82
	Coello	0.00	0.13	0.03	0.02	-	0.56	0.04	0.61	0.77	0.34	0.27	0.19	0.63	0.18	0.83
	El Porveni	0.09	0.00	0.00	0.13	0.07	-	0.62	0.81	0.88	0.60	0.59	0.74	0.70	0.59	0.91
	Ibague	0.00	0.16	0.00	0.04	0.00	0.10	-	0.62	0.69	0.29	0.32	0.21	0.64	0.07	0.76
	Medina	0.12	0.00	0.00	0.17	0.10	0.00	0.10	-	0.92	0.70	0.50	0.40	0.85	0.18	0.94
	Nuevo Leon	0.23	0.16	0.18	0.26	0.18	0.16	0.17	0.18	-	0.83	0.72	0.77	0.98	0.82	-0.02
	Piedras	0.05	0.30	0.25	0.12	0.09	0.17	0.08	0.24	0.29	-	0.45	0.43	0.77	0.36	0.84
	Pipiral	0.08	0.04	0.00	0.09	0.01	0.00	0.04	0.00	0.09	0.13	-	0.19	0.48	0.18	0.77
	Puente Quetame	0.07	0.11	0.09	0.11	0.02	0.21	0.04	0.02	0.22	0.15	0.02	-	0.60	0.05	0.80
	Puerto Gaitan	0.13	0.00	0.00	0.19	0.13	0.00	0.13	0.00	0.22	0.28	0.00	0.17	-	0.39	0.93
	Rey Zamuro	0.00	0.00	0.00	0.01	0.00	0.00	0.00	0.00	0.13	0.09	0.00	0.00	0.00	-	0.85
	Tamaulipas	0.29	0.44	0.45	0.31	0.31	0.44	0.28	0.45	0.00	0.36	0.24	0.30	0.44	0.33	-

Table S2: Effective Migration Rate (*m*) between sampling sites. Metrics of effective migration between collection sites in Colombia using both Wright's F_{ST} equation for effective migration (*m*) [73,74]. Effective migration or "equilibrium" migration rates can be interpreted as individuals migrants per generation across ecological time calculated using F_{ST}, which is a summary statistic of genetic differentiation [76,77]. High migration rates (>1 individual per generation) was present between sites surrounding the Rio Magdalena valley.

	Agua de Dios	Arauca	Casanare	Chaparral	Coello	El Porveni	Ibague	Medina	Nuevo Leon	Piedras	Pipiral	Puente Quetame	Puerto Gaitan	Rey Zamuro
Arauca	0.02	-												
Casanare	0.05	0.00	-											
Chaparral	0.15	0.02	0.03	-										
Coello	0.00	0.04	0.18	0.35	-									
El Porveni	0.06	0.00	0.00	0.04	0.08	-								
Ibague	4.02	0.03	2.15	0.15	0.00	0.06	-							
Medina	0.04	0.00	0.00	0.03	0.06	0.00	0.06	-						
Nuevo Leon	0.02	0.03	0.03	0.02	0.03	0.03	0.03	0.03	-					
Piedras	0.12	0.01	0.02	0.05	0.06	0.03	0.07	0.02	0.01	-				
Pipiral	0.07	0.14	0.00	0.06	0.44	0.00	0.13	0.00	0.06	0.04	-			
Puente Quetame	0.08	0.05	0.06	0.05	0.31	0.02	0.15	0.25	0.02	0.03	0.31	-		
Puerto Gaitan	0.04	0.00	0.00	0.03	0.04	0.00	0.04	0.00	0.02	0.02	0.00	0.03	-	
Rey Zamuro	0.00	0.00	0.00	1.16	0.00	0.00	0.00	0.00	0.04	0.06	0.00	0.00	0.00	-
Tamaulipas	0.01	0.01	0.01	0.01	0.01	0.01	0.02	0.01	0.00	0.01	0.02	0.01	0.01	0.01

Table S3: First-generation migration probability between populations. Migrant identification was conducted in GeneClass 2.0 [75]. This software identifies likely first-generation migrants (shown in red) and the likelihood that these migrants originated from other sampled populations [75]. Lowest metrics of -log(*L*) indicate the most likely population of origin (shown in green). 15 first-generation migrants were identified.

***D. rotundus* Sample**	**Population of Collection**	**-log (*L*_home / *L*_max)**	**Probability**	**-log(*L*) Pop1**	**-log(*L*) Pop2**	**-log(*L*) Pop3**
W6_100303_1	1	0.000	0.50	10.869	28.749	28.344
W6_100303_144	1	0.000	0.5000	9.766	23.146	22.740
W6_100303_22	1	0.000	0.5000	13.310	35.329	34.737
W6_100303_61	1	0.000	0.5000	11.035	28.865	28.147
W6_100303_82	1	0.000	0.5000	14.541	27.551	27.994
W6_100303_94	1	0.000	0.5000	16.306	28.759	27.445
1_110	2	1.019	0.0573	19.061	7.362	6.343
108148_133	2	0.000	0.6674	25.699	9.002	9.217
118166_140	2	0.000	0.6550	36.079	13.820	14.378
119167_134	2	0.000	0.6538	33.334	15.159	15.476
120168_136	2	0.839	0.1232	34.113	15.163	14.324
186226_11	2	1.086	0.0941	29.299	12.460	11.374
187227_81	2	0.360	0.2318	34.539	14.760	14.401
2_128	2	3.048	0.0031	32.743	16.441	13.392
201241_39	2	0.000	0.6574	34.238	13.720	14.845
2034_112	2	0.000	0.6523	31.635	12.740	12.839
211251_103	2	0.000	0.6594	31.715	10.850	11.451
218258_82	2	0.891	0.1161	32.937	16.427	15.536
219259_97	2	0.000	0.6521	31.908	11.732	12.247
2337_138	2	1.459	0.0545	31.760	12.737	11.278
2784_55	2	0.618	0.1618	35.097	14.300	13.682
3_123	2	2.066	0.0204	34.289	14.109	12.044
3964_113	2	1.327	0.0684	35.222	13.084	11.757
4269_108	2	2.851	0.0048	30.380	13.947	11.096
4467_130	2	0.765	0.1439	33.812	15.052	14.287
4467_22	2	1.220	0.0787	29.253	13.266	12.045
5475_72	2	0.000	0.6590	32.651	11.905	13.636
5578_104	2	0.230	0.2531	33.362	15.115	14.885
5682_57	2	0.638	0.1632	29.444	14.284	13.647
6086_87	2	0.259	0.2512	28.146	10.580	10.321
6187_120	2	0.909	0.1132	33.766	13.492	12.583
6490_73	2	2.363	0.0141	26.141	14.772	12.408

6490_86	2	0.000	0.6570	25.266	10.469	11.193
6798_84	2	0.000	0.6567	31.192	9.818	9.911
9_137	2	0.403	0.2150	34.635	10.957	10.554
H2_114	2	1.651	0.0441	36.732	14.291	12.640
H33_116	2	0.000	0.6600	34.113	12.315	12.912
H9_115	2	0.000	0.6568	36.033	15.004	15.323
Pipi3_205	2	0.000	0.6506	30.919	17.244	18.888
Pipi4_148	2	0.247	0.2248	35.523	19.241	18.994
Pipi4_206	2	0.000	0.6538	36.079	19.780	20.692
Queta1_198	2	0.112	0.2725	34.079	17.641	17.529
Queta2_199	2	0.000	0.6527	33.556	12.351	13.369
Queta3_200	2	0.672	0.1591	34.778	12.119	11.446
Queta4_201	2	0.000	0.6541	33.125	17.473	19.273
Queta5_202	2	0.000	0.6551	32.077	15.909	17.122
Queta6_203	2	0.000	0.6524	32.952	15.666	17.312
RZ2_208	2	0.000	0.6588	29.980	13.689	14.655
1065_3	3	1.035	0.0645	30.016	10.553	11.588
116164_101	3	0.596	0.1293	35.018	12.791	13.387
118166_135	3	0.000	0.6326	31.760	12.922	12.206
119164_119	3	1.975	0.0146	34.158	19.473	21.448
185225_109	3	0.456	0.1547	33.493	11.790	12.246
187227_63	3	0.000	0.6334	31.204	13.002	12.220
190230_62	3	0.066	0.2432	34.033	12.799	12.865
200240_40	3	0.225	0.2071	30.937	13.307	13.532
206246_34	3	2.592	0.0052	35.602	13.433	16.024
209249_121	3	0.920	0.0860	32.079	10.215	11.134
2135_98	3	0.529	0.1481	32.635	11.772	12.301
220260_65	3	0.000	0.6289	32.431	13.488	12.761
2381_17	3	0.000	0.6319	34.635	16.412	14.162
2541_4	3	0.000	0.6309	30.266	16.129	13.806
289229_49	3	0.595	0.1262	31.176	12.667	13.262
3553_68	3	0.000	0.6304	27.891	14.677	13.680
3656_131	3	0.000	0.6354	34.845	13.260	12.211
3656_71	3	0.000	0.6342	35.715	12.656	11.466
3758_105	3	0.000	0.6311	31.061	18.318	17.281
4_124	3	0.000	0.6324	31.192	12.325	11.967
4370_102	3	0.481	0.1489	29.459	11.460	11.942
4467_74	3	0.910	0.0874	33.556	13.122	14.032
4571_111	3	0.000	0.6338	29.459	16.534	13.835
4980_24	3	0.232	0.2089	28.901	14.020	14.251
5_126	3	0.000	0.6327	31.569	17.346	16.437
5373_106	3	0.926	0.0848	25.600	11.490	12.416
5475_132	3	1.421	0.0393	29.459	11.179	12.600

5885_67	3	0.000	0.6302	34.334	14.656	13.579
6_125	3	0.389	0.1746	34.095	12.209	12.597
6389_91	3	0.358	0.1877	37.431	12.700	13.058
6591_99	3	1.197	0.0600	33.715	14.134	15.331
6595_129	3	0.000	0.6351	31.378	10.967	10.863
6894_107	3	2.655	0.0026	36.635	16.990	19.645
7_139	3	0.491	0.1507	34.493	13.250	13.741
77125_78	3	1.281	0.0480	31.697	13.254	14.535
79_100	3	0.000	0.6334	31.414	12.526	12.460
8_127	3	0.000	0.6297	32.255	12.435	12.315
85133_122	3	2.141	0.0101	35.511	14.640	16.781
H37_117	3	0.404	0.1609	29.186	14.142	14.546
H58_118	3	0.000	0.6358	32.937	14.329	14.110
Pipi1_146	3	1.186	0.0456	26.194	15.105	16.291
Pipi3_147	3	1.443	0.0332	36.192	21.190	22.634
Queta7_204	3	2.889	0.0015	31.386	16.719	19.608
RZ1_207	3	1.412	0.0320	31.812	12.745	14.157

References

1. García-Morales R, Badano EI, Moreno CE. Response of neotropical bat assemblages to human land use. Conserv Biol. 2013;27: 1096–1106. doi:10.1111/cobi.12099

2. Becker DJ, Nachtmann C, Argibay HD, Botto G, Escalera-Zamudio M, Carrera JE, et al. Leukocyte profiles Rrflect geographic range limits in a widespread Neotropical bat. Integr Comp Biol. 2019;59: 1176–1189. doi:10.1093/icb/icz007

3. Keesing F, Ostfeld RS. Impacts of biodiversity and biodiversity loss on zoonotic diseases. Proc Natl Acad Sci U S A. 2021;118: e2023540118. doi:10.1073/PNAS.2023540118

4. Piret J, Boivin G. Pandemics throughout history. Front Microbiol. 2021;11: e631736. doi:10.3389/fmicb.2020.631736

5. Koch LK, Cunze S, Kochmann J, Klimpel S. Bats as putative Zaire ebolavirus reservoir hosts and their habitat suitability in Africa. Sci Rep. 2020;10: e14268. doi:10.1038/s41598-020-71226-0

6. Nahar N, Asaduzzaman M, Mandal UK, Rimi NA, Gurley ES, Rahman M, et al. Hunting bats for human consumption in Bangladesh. Ecohealth. 2020;17: 139–151. doi:10.1007/s10393-020-01468-x

7. Epstein JH, Anthony SJ, Islam A, Marm Kilpatrick A, Khan SA, Balkey MD, et al. Nipah virus dynamics in bats and implications for spillover to humans. Proc Natl Acad Sci U S A. 2020;117: 29190–29201. doi:10.1073/pnas.2000429117

8. Christou L. The global burden of bacterial and viral zoonotic infections. Clin Microbiol Infect. 2011;17: 326–330. doi:10.1111/j.1469-0691.2010.03441.x

9. Wang J, Pan Y fei, Yang L fen, Yang W hong, Lv K, Luo C ming, et al. Individual bat virome analysis reveals co-infection and spillover among bats and virus zoonotic potential. Nat Commun. 2023;14. doi:10.1038/s41467-023-39835-1

10. Shereen MA, Khan S, Kazmi A, Bashir N, Siddique R. COVID-19 infection: Origin, transmission, and characteristics of human coronaviruses. J Adv Res. 2020;24: 91–98. doi:10.1016/j.jare.2020.03.005

11. Plowright RK, Parrish CR, McCallum H, Hudson PJ, Ko AI, Graham AL, et al. Pathways to zoonotic spillover. Nat Rev Microbiol. 2017;15: 502–510. doi:10.1038/nrmicro.2017.45

12. Venkatesan P. Avian influenza spillover into mammals. The Lancet Microbe. 2023;4: e492. doi:10.1016/s2666-5247(23)00173-8

13. Han HJ, Wen H ling, Zhou CM, Chen FF, Luo LM, Liu J wei, et al. Bats as reservoirs of severe emerging infectious diseases. Virus Res. 2015;205: 2–6. doi:10.1016/j.virusres.2015.05.006

14. Gibb R, Redding DW, Chin KQ, Donnelly CA, Blackburn TM, Newbold T, et al. Zoonotic host diversity increases in human-dominated ecosystems. Nature. 2020;584: 398–402. doi:10.1038/s41586-020-2562-8

15. Letko M, Seifert SN, Olival KJ, Plowright RK, Munster VJ. Bat-borne virus diversity,

spillover and emergence. Nat Rev Microbiol. 2020;18: 461–471. doi:10.1038/s41579-020-0394-z

16. Plowright RK, Eby P, Hudson PJ, Smith IL, Westcott D, Bryden WL, et al. Ecological dynamics of emerging bat virus spillover. Proc R Soc B Biol Sci. 2014;282. doi:10.1098/rspb.2014.2124

17. Plowright RK, Peel AJ, Streicker DG, Gilbert AT, McCallum H, Wood J, et al. Transmission or within-host dynamics driving pulses of zoonotic viruses in reservoir–host populations. PLoS Negl Trop Dis. 2016;10: 1–21. doi:10.1371/journal.pntd.0004796

18. Subudhi S, Rapin N, Misra V. Immune system modulation and viral persistence in bats: Understanding viral spillover. Viruses. 2019;11. doi:10.3390/v11020192

19. Plowright RK, Foley P, Field HE, Dobson AP, Foley JE, Eby P, et al. Urban habituation, ecological connectivity and epidemic dampening: The emergence of hendra virus from flying foxes (*Pteropus spp*.). Proc R Soc B Biol Sci. 2011;278: 3703–3712. doi:10.1098/rspb.2011.0522

20. Perez-Gonzalez J, Carranza J, Martinez R, Benitez-Medina JM. Host genetic diversity and infectious diseases. Focus on wild boar, red deer and tuberculosis. Animals. 2021;11: e1630. doi: 10.3390/ani11061630

21. Baucom RS, Estill JC, Cruzan MB. The effect of deforestation on the genetic diversity and structure in *Acer saccharum* (Marsh): Evidence for the loss and restructuring of genetic variation in a natural system. 2005; 39–50. doi:10.1007/s10592-004-7718-9

22. Guegan J, Ayouba A, Cappelle J, De Thoisy B. Forests and emerging infectious diseases: unleashing the beast within. Environ Res Lett. 2020; 083007. doi: 10.1088/1748-9326/ab8dd7

23. Ellwanger JH, Fearnside PM, Ziliotto M, Valverde-villegas JM, Beatriz ANA, Veiga GDA, et al. Synthesizing the connections between environmental disturbances and zoonotic spillover. 2022. doi:10.1590/0001-3765202220211530

24. Betts MG, Wolf C, Ripple WJ, Phalan B, Millers KA, Duarte A, et al. Global forest loss disproportionately erodes biodiversity in intact landscapes. Nature. 2017;547: 441–444. doi:10.1038/nature23285

25. Carlson KB, Wcisel DJ, Ackerman HD, Romanet J, Christiansen EF, Niemuth JN, et al. Transcriptome annotation reveals minimal immunogenetic diversity among Wyoming toads , *Anaxyrus baxteri*. Conserv Genet. 2022;23: 669–681. doi: 10.1007/s10592-022-01444-8

26. Kim DH, Sexton JO, Townshend JR. Accelerated deforestation in the humid tropics from the 1990s to the 2000s. Geophys Res Lett. 2015;42: 3495–3501. doi:10.1002/2014GL062777

27. Jones KE, Patel NG, Levy MA, Storeygard A, Balk D, Gittleman JL, et al. Global trends in emerging infectious diseases. Nature. 2008;451: 990–993. doi:10.1038/nature06536

28. Messina JP, Brady OJ, Golding N, Kraemer MUG, Wint GRW, Ray SE, et al. The current and future global distribution and population at risk of dengue. Nat Microbiol. 2019;4:

1508–1515. doi:10.1038/s41564-019-0476-8

29. Hansen G, Cramer W. Global distribution of observed climate change impacts. Nat Clim Chang. 2015;5: 182–185. doi:10.1038/nclimate2529

30. Bathiany S, Dakos V, Scheffer M, Lenton TM. Climate models predict increasing temperature variability in poor countries. Sci Adv. 2018;4: e5809. doi:10.1126/sciadv.aar5809

31. Pörtner, H.O. D.C. Roberts, M. Tignor, E.S. Poloczanska, K. Mintenbeck, A. Alegría, M. Craig, S. Langsdorf, S. Löschke, V. Möller, A. Okem BR. Sixth Assessment Report (AR6) of the IPCC: Summary for policymakers. H.-O. Pörtner DCR, E.S. Poloczanska, K. Mintenbeck MT, A. Alegría, M. Craig, S. Langsdorf, S. Löschke, V. Möller AO, editors. Managing the Risks of Extreme Events and Disasters to Advance Climate Change Adaptation: Special Report of the Intergovernmental Panel on Climate Change. 2022. doi:10.1017/CBO9781139177245.003

32. Anderson A, Shwiff S, Gebhardt K, Ramírez AJ, Shwiff S, Kohler D, et al. Economic evaluation of vampire bat (*Desmodus rotundus*) rabies prevention in Mexico. Transbound Emerg Dis. 2014;61: 140–146. doi:10.1111/tbed.12007

33. Velasco-Villa A, Mauldin MR, Shi M, Escobar LE, Gallardo-Romero NF, Damon I, et al. The history of rabies in the Western Hemisphere. Antiviral Res. 2017;146: 221–232. doi:10.1016/j.antiviral.2017.03.013

34. Barquez, R., Perez, S., Miller, B. & Diaz M. *Desmodus rotundus*. In: The IUCN Red List of Threatened Species. 2015 [cited 25 Jan 2021]. Available: https://dx.doi.org/10.2305/IUCN.UK.2015-4.RLTS.T6510A21979045.en.

35. Stoner-Duncan B, Streicker DG, Tedeschi CM. Vampire bats and rabies: Toward an ecological solution to a public health problem. PLoS Neglected Trop Dis. 2014;8: e2867. doi:10.1371/journal.pntd.0002867

36. Meske M, Fanelli A, Rocha F, Awada L, Soto PC, Mapitse N, et al. Evolution of rabies in south america and inter-species dynamics (2009–2018). Trop Med Infect Dis. 2021;6: 2–18. doi:10.3390/tropicalmed6020098

37. Mara MTO, Wikelski M, Dechmann DKN. 50 years of bat tracking: device attachment and future directions. Methods Ecol Evol. 2014;5: 311–319. doi:10.1111/2041-210X.12172

38. Schorr A, Robert A, Laura E, Paul M. Estimating sample size for landscape-scale mark-recapture studies of North American migratory tree bats. Acta Chiropterologica. 2014;16: 231–239. doi:10.3161/150811014X683426

39. Clerici N, Armenteras D, Kareiva P, Botero R. Deforestation in Colombian protected areas increased during post-conflict periods. Sci Rep. 2020;10: e4971. doi:10.1038/s41598-020-61861-y

40. McNab BK. Energetics and the distribution of vampires. J Mammal. 1973;54: 131–144. doi:10.2307/1378876

41. Trajano E. Movements of cave bats in southeastern Brazil, with emphasis on the population

ecology of the Common Vampire Bat, *Desmodus rotundus* (Chiroptera). Biotropica. 1996;28: 121. doi:10.2307/2388777

42. Zeppelini CG, Azeredo LMM, Lopez LCS. Bats like dimmer lights: lunar phobia as a luminosity threshold phenomenon on Neotropical bats (Mammalia: Chiroptera). Acta Ethol. 2019;22: 125–128. doi:10.1007/s10211-019-00314-w

43. Sikes RS. 2016 Guidelines of the American Society of Mammalogists for the use of wild mammals in research and education. J Mammal. 2016;97: 663–688. doi:10.1093/jmammal/gyw078

44. Streicker DG, Winternitzc JC, Satterfield DA, Condori-Condori RE, Broos A, Tello C, et al. Host-pathogen evolutionary signatures reveal dynamics and future invasions of vampire bat rabies. Proc Natl Acad Sci. 2016;113: 10926–10931. doi:10.1073/pnas.1606587113

45. Piaggio AJ, Johnson JJ, Perkins SL. Development of polymorphic microsatellite loci for the common vampire bat, *Desmodus rotundus* (Chiroptera: Phylostomidae). Mol Ecol Resour. 2008;8: 440–442. doi:10.1111/j.1471-8286.2007.01986.x

46. Martins FM, Templeton AR, Pavan AC, Kohlbach BC, Morgante JS. Phylogeography of the common vampire bat (*Desmodus rotundus*): Marked population structure, Neotropical Pleistocene vicariance and incongruence between nuclear and mtDNA markers. BMC Evol Biol. 2009;9: 1–13. doi:10.1186/1471-2148-9-294

47. Promega. GoTaq PCR Core System Protocol. Madison: Promega Corporation; 2019.

48. Romero-nava C, León-paniagua L, Ortega J. Microsatellites loci reveal heterozygosis and population structure in vampire bats (*Desmodus rotundus*) (Chiroptera : Phyllostomidae) of Mexico. Rev Biol Trop. 2014;62: 659–669.

49. Covarrubias-pazaran G, Diaz-garcia L, Schlautman B, Salazar W, Zalapa J. Fragman: an R package for fragment analysis. BMC Genet. 2016;17: 1–8. doi:10.1186/s12863-016-0365-6

50. The R Institute. R version 4.1.0. In: R Intitute, Vienna. 2021 [cited 21 May 2022]. Available: https://cran.r-project.org/bin/windows/base/old/4.1.0/

51. SoftGenetics. GeneMarker Version 2.6.3. 2018 [cited 12 Apr 2024]. Available: https://softgenetics.com/products/genemarker/

52. Adamack AT, Gruber B. PopGenReport: simplifying basic population genetic analyses in R. Methods Ecol Evol. 2014;5: 384–387. doi:10.1111/2041-210X.12158

53. Campagne P, Smouse PE, Varouchas G, Silvain JF, Leru B. Comparing the van Oosterhout and Chybicki-Burczyk methods of estimating null allele frequencies for inbred populations. Mol Ecol Resour. 2012;12: 975–982. doi:10.1111/1755-0998.12015

54. Brookfield JFY. A simple new method for estimating null allele frequency from heterozygote deficiency. Mol Ecol. 1996;5: 453–455. doi:10.1111/j.1365-294X.1996.tb00336.x

55. Van Oosterhout C, Hutchinson WF, Wills DPM, Shipley P. MICRO-CHECKER: Software

for identifying and correcting genotyping errors in microsatellite data. Mol Ecol Notes. 2004;4: 535–538. doi:10.1111/j.1471-8286.2004.00684.x

56. Van Oosterhout C, Weetman D, Hutchinson WF. Estimation and adjustment of microsatellite null alleles in nonequilibrium populations. Mol Ecol Notes. 2006;6: 255–256. doi:10.1111/j.1471-8286.2005.01082.x

57. The Earth and Life Systems Alliance. Micro-Checker Version 2.2.3. Mol Ecol Notes. 2023;4: 535–538. doi:10.1111/j.1471-8286.2004.00684.x

58. Jombart T, Devillard S, Balloux F. Discriminant analysis of principal components: A new method for the analysis of genetically structured populations. BMC Genet. 2010;11. doi:10.1186/1471-2156-11-94

59. Desvars-Larrive A, Hammed A, Hodroge A, Berny P, Benoît E, Lattard V, et al. Population genetics and genotyping as tools for planning rat management programmes. J Pest Sci (2004). 2019;92: 691–705. doi:10.1007/s10340-018-1043-4

60. Jombart T. A tutorial for Discriminant Analysis of Principal Components (DAPC) using adegenet 1.3-4. 2012; 1–43.

61. Pritchard JK, Stephens M, Donnelly P. Inference of population structure using multilocus genotype data. Genetics. 2000;155: 945–959. doi:10.1093/genetics/155.2.945

62. Kamvar ZN, Tabima JF, Gŕunwald NJ. Poppr: An R package for genetic analysis of populations with clonal, partially clonal, and/or sexual reproduction. PeerJ. 2014;2: e281. doi:10.7717/peerj.281

63. Jerome A, Archer E, Hardy O, Goudet MJ. Package 'hierfstat' CRAN. 2022; 4–37.

64. Mijangos JL, Gruber B, Berry O, Pacioni C, Georges A. dartR v2: An accessible genetic analysis platform for conservation, ecology and agriculture. Methods Ecol Evol. 2022;13: 2150–2158. doi:10.1111/2041-210X.13918

65. Weir BS, Cockerham CC. Estimating *F*-statistics for the analysis of population structure. Evolution (N Y). 1984;38: 1358. doi:10.2307/2408641

66. Do C, Waples RS, Peel D, Macbeth GM, Tillett BJ, Ovenden JR. NeEstimator v2: Re-implementation of software for the estimation of contemporary effective population size (Ne) from genetic data. Mol Ecol Resour. 2014;14: 209–214. doi:10.1111/1755-0998.12157

67. Waples RS, Do C. Linkage disequilibrium estimates of contemporary Ne using highly variable genetic markers: A largely untapped resource for applied conservation and evolution. Evol Appl. 2010;3: 244–262. doi:10.1111/j.1752-4571.2009.00104.x

68. Waples RK, Larson WA, Waples RS. Estimating contemporary effective population size in non-model species using linkage disequilibrium across thousands of loci. Heredity. 2016;117: 233–240. doi:10.1038/hdy.2016.60

69. Yang RC. Estimating hierarchical F-statistics. Evolution. 1998;52: 950–956. doi:10.1111/j.1558-5646.1998.tb01824.x

70. Hedrick PW. A standardized genetic differentiation measure. Evolution. 2005;59: 1633–

1638. doi:10.1111/j.0014-3820.2005.tb01814.x

71. Mantel N. The detection of disease clustering and generalized regression approach. Cancer Res. 1967;27: 209–220. doi:10.1021/j150334a020

72. Banks SC, Peakall R. Genetic spatial autocorrelation can readily detect sex-biased dispersal. Mol Ecol. 2012;21: 2092–2105. doi:10.1111/j.1365-294X.2012.05485.x

73. Wright S. The genetical structure of populations. Ann Eugen. 1951;15: 323–354.

74. Zhivotovsky LA. Relationships Between Wright's F_{ST} and F_{IS} Statistics in a Context of Wahlund Effect. Am Genet Assoc. 2015;2: 306–309. doi:10.1093/jhered/esv019

75. Piry S, Alapetite A, Cornuet JM, Paetkau D, Baudouin L, Estoup A. GENECLASS2: A software for genetic assignment and first-generation migrant detection. J Hered. 2004;95: 536–539. doi:10.1093/jhered/esh074

76. Yamamichi M, Innan H. Estimating the migration rate from genetic variation data. Heredity. 2012;108: 362–363. doi:10.1038/hdy.2011.83

77. Wang J, Whitlock MC. Estimating effective population size and migration rates from genetic samples over space and time. Genetics. 2003;163: 429–446. doi: 10.1093/genetics/163.1.429

78. NASA Earth Data. United States Socioeconomic Data and Applications Center (SEDAC). In: Earth Observing System Data and Information System. 2022 [cited 17 Aug 2023]. Available: https://sedac.ciesin.columbia.edu/

79. Food and Agriculture Organization of the United Nations. Gridded Livestock of the World Database. 2022 [cited 1 Jun 2023]. Available: https://data.apps.fao.org/catalog/dataset/glw

80. Hengl T. WorldGrids archived layers at 1 km to 20 km spatial resolution. 2018 [cited 8 Jul 2022]. doi:10.5281/ZENODO.1637816

81. Petit RJ, Mousadik AEL, Pons O. Identifying populations for conservation on the basis of genetic markers. Conserv Biol. 1998;12: 844–855. doi:10.1046/j.1523-1739.1998.96489.x

82. Szpiech ZA, Rosenberg NA. On the size distribution of private microsatellite alleles. Theor Popul Biol. 2011;80: 100–113. doi:10.1007/978-3-319-25826-3_1

83. Streicker DG, Recuenco S, Valderrama W, Benavides JG, Vargas I, Pacheco V, et al. Ecological and anthropogenic drivers of rabies exposure in vampire bats: Implications for transmission and control. Proc R Soc B Biol Sci. 2012;279: 3384–3392. doi:10.1098/rspb.2012.0538

84. Benavides JA, Valderrama W, Streicker DG. Spatial expansions and travelling waves of rabies in vampire bats. Proc R Soc B. 2016;283: 20160328. doi:10.1098/rspb.2016.0328

85. Foulley JL, Ollivier L. Estimating allelic richness and its diversity. Livest Sci. 2006;101: 150–158. doi:10.1016/j.livprodsci.2005.10.021

86. Streicker DG, Lemey P, Velasco-Villa AA, Rupprecht CE. Rates of viral evolution are linked to host geography in bat rabies. PLoS Pathog. 2012;8: e1002720.

doi:10.1371/journal.ppat.1002720

87. Streicker DG, Allgeier JE. Foraging choices of vampire bats in diverse landscapes: potential implications for land-use change and disease transmission. J Appl Ecol. 2016. doi:10.1111/1365-2664.12690

88. Piaggio AJ, Russell AL, Osorio IA, Jiménez Ramírez A, Fischer JW, Neuwald JL, et al. Genetic demography at the leading edge of the distribution of a rabies virus vector. Ecol Evol. 2017;7: 5343–5351. doi:10.1002/ece3.3087

89. Becker DJ, Simmons NB, Broos A, Bergner LM, Meza DK, Fenton MB, et al. Temporal patterns of vampire bat rabies and host connectivity in Belize. Transbound Emerg Dis. 2021;68: 870–879. doi:10.1111/tbed.13754

90. Bakker KM, Rocke TE, Osorio JE, Abbott RC, Tello C, Carrera JE, et al. Fluorescent biomarkers demonstrate prospects for spreadable vaccines to control disease transmission in wild bats. Nat Ecol Evol. 2019;3: 1697–1704. doi:10.1038/s41559-019-1032-x

91. Horta MA, Ledesma LA, Moura WC, Lemos ERS. From dogs to bats: Concerns regarding vampire bat-borne rabies in Brazil. PLoS Negl Trop Dis. 2022;16: 6–10. doi:10.1371/journal.pntd.0010160

92. Rojas-sereno ZE, Streicker DG, Medina-Rodriguez AT, Benavides JA. Drivers of spatial expansions of vampire bat rabies in Colombia. Viruses. 2022;14. doi:10.3390/v14112318

93. Piaggio AJ, Russell AL, Osorio IA, Jiménez Ramírez A, Fischer JW, Neuwald JL, et al. Genetic demography at the leading edge of the distribution of a rabies virus vector. Ecol Evol. 2017;7: 5343–5351. doi:10.1002/ece3.3087

94. Tibihika PD, Curto M, Dornstauder E, Silvia S, Alemayehu E, Waidbacher H, et al. Application of microsatellite genotyping by sequencing (SSR-GBS) to measure genetic diversity of the East African Oreochromis niloticus. Conserv Genet. 2019;20: 357–372. doi:10.1007/s10592-018-1136-x

95. Kerth G. Long-term field studies in bat research: importance for basic and applied research questions in animal behavior. Behav Ecol Sociobiol. 2022;76. doi:10.1007/s00265-022-03180-y

96. Evanno G, Regnaut S, Goudet J. Detecting the number of clusters of individuals using the software STRUCTURE: A simulation study. Mol Ecol. 2005;14: 2611–2620. doi:10.1111/j.1365-294X.2005.02553.x

CHAPTER 2: Drivers of rabies virus spillover risk distribution from bats to livestock in Colombia

Previously submitted to PLOS Neglected Tropical Disease on November 9th, 2024 under the title "Drivers of rabies virus spillover risk distribution from bats to livestock in Colombia"

Abstract

Rabies is an acute and progressive viral zoonotic disease of the nervous system widely affecting domestic animals in Latin America. Bat-borne rabies virus (RABV) has significant negative impacts on the livestock industry via animal mortality. Nevertheless, the landscape factors that facilitate or limit rabies virus spillover transmission from bats to livestock remain elusive. To determine how different abiotic and biotic factors modulate rabies spillover from bats to livestock, we assessed the role of different landscape variables on the occurrence of rabies virus spillover from *Desmodus rotundus* to livestock in Colombia. Using ecological niche modeling as an analytical framework, we analyzed ecological and epidemiological data of rabies in Colombia as a study case. Anthropogenic variables including livestock and human density were consistently selected as strong predictors of rabies virus spillover from bats to livestock. Cattle density had the highest average relative contribution (i.e., percent contribution to final MaxEnt model) (64.7%) of any variable. We also found improvement of rabies spillover risk estimates when sampling bias in the form of cattle density was used in the modeling process. High risk for RABV spillover (0.75-0.98) was consistently predicted in the departments of Cordoba, Sucre, Bolivar, Magdalena, Cesar, and Arauca. Our modeling effort revealed that variable selection and use of bias surface have tractable impacts on the final estimates of spillover risk. Our results indicate that, rather than environmental variables alone, human activity may ultimately drive RABV spillover risk. Ecological niche models revealed a wide distribution of RABV spillover risk in Colombia and

provide important information about landscape conditions linked to transmission risk and areas where livestock vaccination should be prioritized.

Introduction

Rabies is an acute and progressive disease of the central nervous system caused by the rabies virus (RABV) (Rhabdoviridae, Genus *Lyssavirus*). Rabies is one of the oldest recorded infectious diseases to affect humans in history [1]. Rabies has been classified as a neglected disease in several countries, despite over a century of eradication efforts and effective pre- and post-exposure vaccination efforts [2–4]. When untreated, the rabies fatality rate is almost 100% in most mammals. There are ~60,000 recorded human deaths due to rabies annually, mainly in Asia and Africa in areas where vaccination is limited [1,5]. In the Americas, where bats are key reservoirs [1,5,8], rabies has precipitous impacts upon non-human mammals such as livestock [6–8]. In Latin America, the common vampire bat (*Desmodus rotundus)* [9] is considered to be the main wildlife species responsible for transmitting RABV to other species [8,10–12]. *Desmodus rotundus* is one of three sanguivorous (i.e., blood-feeding) species, and as a result can transmit RABV to their prey during normal feeding behavior [13]. *Diaemus youngi* (i.e., white-winged vampire bat) and *Diphylla ecaudata* (i.e., hairy-legged vampire bat) are also blood-feeding species present in Latin America, though they are more rare and primarily feed upon wild and domestic birds [14–16].

Vampire bat-borne RABV outbreaks in humans and livestock regularly occur in tropical and subtropical regions of Latin America were *D. rotundus* and livestock co-occur [17], with clinical cases in humans normally following outbreaks in livestock [8].Thousands of cattle are lost to RABV in Latin America annually [4,8,18], and billions of US dollars are used for rabies prevention and control measures [19,20]. Rabies disease has been reported to cause at least US$8.6 billion in

economic losses in impacted areas due to lost income and productivity [21]. Furthermore, recent years have even shown an increase in RABV livestock cases in Latin American countries [8,11,12,22,23], in concurrence with a range expansion of *D. rotundus* into novel areas in North America [24–26]. As such, there is a pressing need to understand factors at the local level that explain RABV spillover from bats to livestock.

It has been hypothesized that abiotic factors, such as temperature, may limit the distribution of *D. rotundus*, and thereby shape the geographic distribution of RABV spillover [27–30]. Alternately, biotic factors, such as changes in vegetation primary productivity or increase in prey density may have increased the incidence of RABV [30–32]. A combination of both abiotic and biotic factors at the landscape level, such as geomorphology and landscape type, shape *D. rotundus* roosting and feeding behaviors [33,34]. Previous modeling efforts to reconstruct the distribution of both *D. rotundus* and RABV have been biased to small study areas [34] and use of abiotic (climate) variables only [26,28,30]. Hence, there is a need for a more comprehensive, country-level analysis of factors that shape bat-borne RABV spillover to livestock at the landscape level [35]. Colombia is a diverse country located at the apex of South America, and houses a wide variety of ecosystems and biodiversity [36]. Colombia is also home to an expansive agricultural industry [37,38]. Recent reports from the Instituto Colombiano Agropecuario (ICA) have identified 638,941 farms across the country, with over 29 million cattle [38]. While rabies pre- and post-exposure vaccination is available for both humans and many animal species in Colombia, RABV spillover incidence in livestock persists, with 25 outbreaks reported in 2023, mainly in cattle [39–41]. We therefore chose Colombia as the study area due to its environmental heterogeneity, expansive livestock industry, and robust surveillance system for RABV in livestock. We conducted an ecological niche modeling study to reconstruct the distribution of RABV spillover locations in

Colombia using abiotic and biotic environmental variables. Environmental variables included climatological, landscape, and anthropogenic data.

Methods

We collected geographic locations of RABV spillover to livestock data from 2014 to 2019 from ICA [38] via the Epidemiological Information and Surveillance System in Colombia [41]. RABV spillover data included locations of farms with confirmed rabies deaths in livestock (e.g., cattle, pigs, goats, or horses), year of confirmed rabies deaths, and annual number of unique locations with confirmed rabies deaths hereafter referred to as outbreak of locations or simply "outbreaks". We then used the locations of farms with spillover (i.e., outbreaks, n=896) as occurrence data for our modeling effort. We resampled the locations of RABV spillover occurrences to one per pixel of the study extent (11.72° N, 3.80° S, 77.37° W, 67.67° S) to reduce sampling bias [42]. We used data from all uncorrelated predictor variables to build an environmental background where outliers were identified in environmental space [43]. Values of each predictor variable were first extracted for the spillover location to create a cloud of data points representing the entire distribution of RABV spillover events in environmental space [43]. We then developed a principal component analysis (PCA) of the predictor variables to obtain three principal component axes which summarized 53.2% of the variance of the data. Within the three-dimensional environmental space created by the PCA axes, we used an ellipsoid calculated using Mahalanobis distance (i.e., distance between each point in environmental space) and a precision factor of one to identify environmental outliers (i.e., those points which fell outside of the ellipsoid) from the cloud of extracted values, which were removed from consideration during model calibration. The remaining 541 filtered

occurrences were randomly split into 70% training and 30% testing subsets from the thinned dataset for each model calibration and evaluation run.

We compared the effects of different predictor variables to identify the combination providing the best model performance. Predictor variables were both grouped and ungrouped based upon their characteristics (i.e., climate, landscape, or anthropogenic) (Table 1). We selected a wide array of predictor variables important to both reservoir host ecology, as well as variables suspected to be related to RABV spillover [33,40,44–46]. These included anthropogenic variables such as human population density, night time light, human poverty index data, and agricultural influences in the form of cattle, chicken, goat, buffalo, horse, duck, and pig density, combined-livestock density, and changes to livestock density across the last 50 years [47]. We also assessed 19 different climate variables derived from remotely sensed temperature and precipitation data [48], and an array of landscape factors including reservoir host (i.e., *D. rotundus*) density, vegetation phenology (i.e., Enhanced Vegetation Index (EVI)), continuous land cover data (Top of Atmosphere (TOA) spectral variance MERIS data), and elevation [49,50]. Anthropogenic variables were collected from the NASA Socioeconomic Data and Applications Center (SEDAC) [51] and the Gridded Livestock of the World Database [47]. Climatic variables were collected from WorldClim bioclimatic database [48]. Landscape variables were collected from the WorldGrids Archived database [49]. *Desmodus rotundus* density was calculated using a kernel density analysis of *D. rotundus* historical records from Colombia [52] and then output to a raster format in ArcGIS Pro software (Version 2.5) [53].

All predictor variables were collected or resampled to 1 km resolution with the World Geodetic System 1984 (WGS84) reference system and cropped to a rectangular study area that encompassed continental Colombia (11.72° N, 3.80° S, 77.37° W, 67.67° S) in R (Version 4.1.0).

Pixels within the study area that fell within the Pacific Ocean or Caribbean Sea were classified as "no data", and removed from consideration during the model calibration process. Predictor variables from each characteristic group (i.e., climate, landscape, and anthropogenic) were compared using a Pearson Correlation coefficient analysis [43], where variables with a correlation coefficient greater than 0.5 were classified as highly correlated and removed. Variables that were removed from further consideration included night time light, goat, buffalo, horse, duck, and pig density, combined-livestock density, changes to livestock density across the last 50 years, and 15 of the 19 climate variables. We then compared all remaining predictor variables regardless of characteristic, and removed correlated variables from the "All Uncorrelated Variables" predictor variable group (Table 1). We created suites of all possible combinations of each predictor variable set (Table 1), by removing and replacing each variable (i.e., by jackknifing) and then removing redundant combinations. The best combination of variables for each predictor variable model run/experiment was selected during the calibration and evaluation process.

Model calibration, evaluation, and projection was done using MaxEnt [54] version 3.4.4 in R statistical software version 4.1.0 using the *kuenm* package [55]. MaxEnt is a presence-background comparison-based ecological niche modelling algorithm frequently used in scientific literature [56–58], which does not require true absence locations. MaxEnt has built in parameterizations (e.g., regularization multiplier and feature classes), which can be altered and evaluated to identify the best potential combination of these parameters in terms of the resultant model's predictive capacity [59]. The regularization multiplier defines how precisely the output distribution is fitted, penalizing model over-fit and is set to one as a default value within the software [60]. Feature classes within MaxEnt are used as a mathematical transformation of the original predictor variables, which allows for more complex relationships to be identified [60]. To

elucidate the impact of regularization multipliers and feature classes within MaxEnt on the outcome of each predictor variable experiment, we tested a suite of regularization multipliers above and below default (i.e., 0.01, 0.1, 0.5, 1, 2, 5, and 10), and all possible combinations of the available continuous feature classes (i.e., linear, product, quadratic, threshold, and hinge). The *kuenm* package allows for a systematic comparison between different predictor variables sets, regularization multipliers, and feature classes, and thus permits a systematic and holistic comparison between different iterations of the desired model. Furthermore, MaxEnt allows the incorporation of bias surfaces, which manipulate the background sampling effort within the algorithm. This is accomplished via a density raster which represents relative sampling effort, thereby accounting for possible sampling bias [61]. We tested the use of cattle density [47] or road accessibility [49] surfaces as possible drivers of sampling bias, as we assumed that both of these factors potentially shape the surveillance of RABV spillover in Colombia. Parameters for each predictor variable experiment/model run were tested in terms of model fit and prediction (Table 2).

After creating all possible interactions of candidate models for each experiment, we used the function *kuenm_ceval*, which evaluates model performance based upon statistical significance using partial area under the receiver operating characteristic curve (pROC), omission rate (E=0.05) [62], and model complexity Akaike values (AICc) [55]. pROC and omission rates were calculated based on models created with training data only, whereas AICc values are calculated for models created with both training and testing data [56]. pROC values were utilized to isolate statistically significant models, which also met the omission rate criteria (E=0.05, 500 iterations, p<0.05) [55]. These models resembling robust predictive performance were used to compare across predictor variable combinations with an analysis of variance and post-hoc Fisher's least significance

difference (LSD) test. We also recorded and reported the regularization multiplier and feature classes most frequently present in statistically significant models which met the omission rate criteria. We used *kuenm_eval* to select best models based on our user-set criteria with the lowest AICc, which were then used to project each final model from each experiment to the geographic extent of Colombia. Model parameterizations (i.e., variable combination, regularization, features classes) with more than one best model were averaged using the logistic continuous model outputs from MaxEnt (Table 2). Logistic continuous model outputs from MaxEnt were also used to delineate and quantify suitability or similarity of model outputs to areas of known spillover risk (i.e., locations of known spillover used as occurrence data for model calibration) [59]. The MaxEnt suitability index, which ranges from zero to one, can therefore be interpreted as suitability for RABV spillover risk or similarity to areas of known RABV spillover risk. In other words, the higher the value of MaxEnt suitability index, the higher the RABV spillover risk of that given area. High risk was quantified as any value above 0.75, moderate risk was classified as any value between 0.25 and 0.50, and low risk was classified as any value below 0.25. We then recorded the total area of the study extent reported as "suitable" (fractional predicted area) of each best model using two threshold values: (i) minimum training presences threshold and (ii) a 10^{th} percentile training presence threshold [63] as the absolute lowest value of suitability for RABV spillover risk. We also created an ensemble map of model agreement by summing all final model raster outputs from each predictor variable experiments. This map permitted us visualize where models agreed regarding RABV spillover risk geographically.

Results

Each RABV model parameterization and predictor variable experiment generated statistically significant predictions of independent localities with spillover reports (Table 2). As such, any single suite of predictor variables tested in this study could ostensibly be used to generate acceptable maps of RABV spillover risk, at least based on statistical significance. Models calibrated using only climate variables had lowest errors in terms of omission rates and models calibrated using anthropogenic variables only had the lowest complexity in terms of AICc values (Figure 1). Models calibrated with grouped variables with cattle density as a bias surface had higher stability in the form of the lowest amount of variance in both omission rates and AICc (Figure 2). AICc was significantly different in models with cattle density as a bias surface per a post hoc LSD analysis (std = 139.4, df = 5664, r = 87, $p < 0.001$). Using road accessibility as a bias surface did not improve model performance (Figure 1).

Anthropogenic variables such as livestock density, human population density, and poverty index provided the best predictive performance (Table 2). Cattle density had the highest average relative contribution (i.e., percent contribution to final MaxEnt model) (64.7%) when the variable was not used as bias surface. Of the remaining anthropogenic variables, chicken density had the highest relative contribution (40%) to RABV spillover distribution, followed by human population density (10.6%), and poverty index (1.3%). In contrast to poverty index and cattle density, there was a negative association between chicken density and human population density and the continuous log suitability for RABV suitability (Figure 3). The bulk of RABV spillover risk occurred when chicken density was less than 5000 individuals per km^2 and where poverty index was greater than 70 (Figure 3).

For climate-only models, precipitation seasonality had the highest percent contribution (44.5%) followed by annual precipitation (39.4%), minimum temperature of the coldest month

(8.4%), and isothermality (7.7%). Using only landscape variables resulted in continuous land cover data having the highest percent contribution (40.5%), followed by Enhanced Vegetation Index (EVI) standard deviation (34.3%), and elevation (25.2%). The only variable not present in any final model was *D. rotundus* density. For experiments with predictor variables grouped by their characteristics (i.e., climate, landscape, or anthropogenic), anthropogenic variables were consistently selected as the best set of predictor variables with and without sample bias correction. Climate-only models and models using cattle density as a bias surface had the smallest difference in fractional predicted area (i.e., area predicted to be at risk) between minimum training presence and 10^{th} percentile training presence (Table 2). The lack of change in fractional predicted area indicates that climate models and models with bias file correction had the most consistent predictions regardless of the threshold used to classify areas suitable for RABV spillover. Anthropogenic variables (i.e., chicken density and human population density) consistently explained the likelihood of spillover to a greater extent than climate or landscape alone.

Spatial clusters of RABV transmission risk were predicted in the northern most portions of Colombia and the lowland areas to the east of the Andes Mountain range (Figure 4). Northern portions of Colombia and lowland areas east of the Andes fall within the Caribbean, Andean, and Orinoquia regions of Colombia, where higher numbers of RABV spillover outbreaks have been reported previously [64,65]. High RABV spillover risk (0.75-0.98 MaxEnt suitability index) was consistently predicted in the departments of Cordoba, Sucre, Bolivar, Magdalena, Cesar, and Arauca (Figure 4). There was low (0.25-0 MaxEnt suitability index) predicted RABV spillover risk in the Amazonian and Pacific regions (Figure 4). Though the patterns of projected suitability for RABV spillover were consistent between models, the magnitude of spillover suitability risk in certain areas differed (Figure 4 and Figure 5). The total area predicted to have moderate or

moderately-high suitability (0.5-0.75 MaxEnt suitability index) was larger (30.6% of the total area) in the model that used cattle density as a bias surface (Figure 4). Consistency in the areas predicted as at-risk for RABV spillover was present in northern portions of the country, as well as more lowland regions to the east of the Andes (i.e., more agreement between models) (Figure 5).

Discussion

We compared the efficacy and role of different predictor variables in explaining the spatial risk of RABV spillover to livestock in Colombia. While all predictor variable experiments/model runs generated statistically significant results, there were differences present in the performance and projection of each modeling experiment. Anthropogenic variables more accurately explained the geography of RABV spillover than climatic and landscape variables alone. These results could indicate that spatial epidemiology models using anthropogenic variables may be useful to refine RABV transmission risk estimates. Climate-only models demonstrated lowest omission rates, suggesting overall predictive power at the cost of losing spatial detail by predicting large areas of risk. For a zoonotic pathogen of high lethality (~100%) such as RABV, omission rates may be of more priority than commission rates, which can be interpreted as overestimation of risk instead of underestimation of it. Using climate variables only in ecological niche modeling is a common practice, though recent literature has highlighted the importance of including biotic variables for more accurate prediction of biodiversity distributions [45]. Our results indicate that the use of only climate variables or only landscape variables, as is common in spatial epidemiology, may be inaccurate for predicting zoonotic spillover risk.

Cattle density was an important variable in predicting areas with RABV spillover risk, as cattle comprise the majority of RABV cases in livestock in Colombia [38,40]. The importance of this variable echoes results of previous research in Colombia, which found that number of cattle was correlated with changes in RABV spillover expansion [64]. Chicken density also proved to be an informative variable, especially when cattle density was used as a bias surface rather than as a predictor variable. The likelihood of chicken density directly driving RABV spillover risk, however, is unlikely due to its limited relationship to the epidemiology of RABV [66]. In fact, there was a negative association between suitability for RABV spillover and chicken density (Figure 3). That is, risk of RABV spillover to livestock is greater in areas where chickens are scarce, such as in subsistence farming or backyard chicken farming. Chickens are not considered to be a preferred prey species for *D. rotundus*, and are not susceptible to RABV [66], but their density can be a proxy of socioeconomic conditions in rural Colombia. Chicken density could also function as a proxy for landscape perturbation, human presence, or subsistence agriculture [46] which could impact RABV spillover risk. Low chicken density is linked to poverty, food insecurity, and income disparity, contrasting with more-developed areas with industrial poultry production [67,68]. Rural poverty, food insecurity, and income disparity are linked to RABV spillover risk [69]. In summary, the relationship between high RABV spillover risk and low chicken density in Colombia likely reflects the presence of small villages, such as those in rural settlements which may be more likely to experience *D. rotundus* predation.

We also identified differences in the magnitude of RABV spillover risk projection when sampling bias was included in the models. We assumed that the cattle industry was a driver of RABV surveillance in Colombia and thus considered the density of cattle as source of sampling bias. Estimates of RABV spillover risk created using cattle density as bias surface identified larger

proportional areas of risk, with lower redundancy with areas of known spillover (Figure 4). Mitigating sampling bias in this way revealed that areas of Colombia at risk for RABV spillover were more generalized (Figure 4). As such, RABV spillover risk may be more widespread than previously recognized. For example, lowland areas in central portions of the country were identified as having equal RABV spillover risk to more northern areas of the country where cattle density is higher. Another recent study assessing RABV spillover risk found that there was no relationship between RABV prevalence and increased cattle density as was previously hypothesized [70], which could support our findings. Nevertheless, a shift in the distribution of cattle density could influence a spatial shift in the incidence and distribution of RABV spillover. Overall, our study demonstrates that the decision to use a variable as a predictor or as a sampling bias surface has a strong effect on the final risk estimates. Modelers should consider the biological meaning of the data when deciding whether a variable can or should be used as a predictor or a proxy of bias predictor.

The spatial risk of RABV spillover identified here is temporally static and does not account for bat dispersal potential and waves of disease spread. Fine-scale studies of *D. rotundus* movement are still needed to better quantify how bat-population connectivity and dispersal may affect RABV dynamics [71]. It has been hypothesized that colony or roost level factors, such as seasonal reproduction or dispersal, may influence RABV spillover frequency [24,72–74]. Alternatively, livestock could be acting as a source of infection for bat colonies, thus perpetuating circulation of RABV within the wildlife reservoir. An exploration of RABV seroprevalence in *D. rotundus* colonies in Colombia across gradients of livestock density or landscape perturbation may help refine the patterns of spillover risk identified in this study.

Conclusions

The results of this study suggest that anthropogenic factors, notably livestock density, are more informative for anticipating RABV spillover risk than environmental or climatic data. From an analytical perspective, our results highlight the importance of predictor variable selection (e.g., combinations of predictor variables and control of sampling bias) in spillover risk estimations. In a more applied context, our modeling efforts show that human agricultural practices may ultimately drive RABV spillover risk, rather than environmental variables alone. Future research on RABV spillover should further explore the impacts of anthropogenic factors on RABV spillover at the local level, such as socioeconomic conditions and individual human behaviors (e.g., animal management practices). Ecological niche models revealed a wide distribution of RABV spillover risk in Colombia. This study provides important information about conditions linked to transmission risk, and reveals hotspots of RABV risk where livestock vaccination should be prioritized.

Tables and Figures

Predictor Variable Sets	***Variable Names***	***Units***	***Original Spatial Resolution***	***Sources***
Abiotic Climate Variables	Isothermality (Bio3)	*°C*	*30 Arc Seconds*	*WorldClim Bioclimatic Variables of the World Dataset* [48]
	Minimum Temperature of the Coldest Month (Bio6)	*°C*	*30 Arc Seconds*	
	Annual Precipitation (Bio12)	*mm*	*30 Arc Seconds*	
	Precipitation Seasonality (Bio15)	*mm*	*30 Arc Seconds*	
Biotic Anthropogenic Variables	Cattle Density	*Individuals per km^2*	*5 Arc Minutes*	*Gridded Livestock of the World database* [47]
	Chicken Density			
	Human Population Density	*Individuals per km^2*	*5 Arc Minutes*	*WorldGrids Archived Database* [49]
	Poverty Index	*Index value (1-100)*	*1 km^2*	*Gridded Relative Deprivation Index* [75]
Abiotic and Biotic Landscape Variables	Elevation	*Meters*	*30 Arc Seconds*	*WorldGrids Archived Database* [49]
	Enhanced Vegetation Index (EVI) Standard Deviation	*Index value (0-1)*	*1 km^2*	
	Continuous Land Cover	*TOA Reflectance*	*30 Arc Seconds*	Derived from *Desmodus rotundus Occurrence Database* [52]
	Desmodus rotundus density	*Individuals per km^2*	*1 km^2*	
All Uncorrelated Variables	Minimum Temperature of the Coldest Month (Bio6)	*°C*	*30 Arc Seconds*	*WorldClim Bioclimatic Variables of the World Dataset* [48]
	Annual Precipitation (Bio12)	*mm*	*30 Arc Seconds*	
	Enhanced Vegetation Index (EVI) Standard Deviation	*Index Value (0-1)*	*1 km^2*	*WorldGrids Archived Database* [49]
	Continuous Land Cover	*TOA Reflectance*	*30 Arc Seconds*	Derived from *Desmodus rotundus Occurrence Database* [52]
	Desmodus rotundus density	*Individuals per km^2*	*1 km^2*	
	Poverty Index	*Index value (1-100)*	*1 km^2*	*Gridded Relative Deprivation Index* [75]

Table 1: Variable type summary. List and experiment names of each background environmental variables used in each modeling experiment. Predictor variables were grouped based on their abiotic, biotic, and anthropogenic characteristics. Variables with Pearson Correlation coefficient greater than 0.5 were not grouped together in their respective experimental subsets, and were removed from the "All Uncorrelated Variables" group.

Predictor Variable Set Experiments (Model Runs)	***Significant Candidate Models (p<0.05, E<0.05)***	***N Final Models Selected by MaxEnt***	***Final Model(s) Parameters***	***Final Model Predictor Variables***	***Fractional Predicted Area (minimum training presence)***	***Fractional Predicted Area (10^{th} percentile training presence)***
All Variables, Ungrouped	3167	1	RM-1 FC- lqp	All variables but Poverty Index	0.95	0.35
Climate Only	680	1	RM-5 FC-pth	Isothermality (Bio3) Minimum Temperature of the Coldest Month (Bio6) Annual Precipitation (Bio12) Precipitation Seasonality (Bio15)	0.99	0.66
Anthropogenic Only	649	2	RM-2 FC-lt,lqt	Cattle Density Chicken Density Human Population Density Poverty Index	0.98	0.47
Landscape Only	632	1	RM-1 FC-lpt	Elevation Enhanced Vegetation Index Standard Deviation Continuous Land Cover	0.98	0.62
Grouped Variables	172	2	RM-2 FC-lt,lqt	Cattle Density Chicken Density Human Population Density Poverty Index	0.98	0.47
Grouped, Corrected with Accessibility	284	2	RM-5 FC-t,pt	Cattle Density Chicken Density Human Population Density Poverty Index	0.94	0.35
Grouped, Corrected with Cattle Density	87	2	RM-5 FC-lt, lpt	Chicken Density Human Population Density Poverty Index	0.98	0.59

Table 2: Final models summary. Summary of significant models (those which fit Omission Rate and AICc criteria) and final models selected by MaxEnt. Final models selected by MaxEnt are identified by the algorithm using pROC, omission rate, and AICc. Regularization multipliers of final selected models (RM) and feature classes (FC) of final selected models. Feature class options were l-linear, p-product, q-quadratic, t-threshold, and h-hinge. Both RM and FCs are user set parameterizations, for which we tested a suite of options during the model calibration phase.

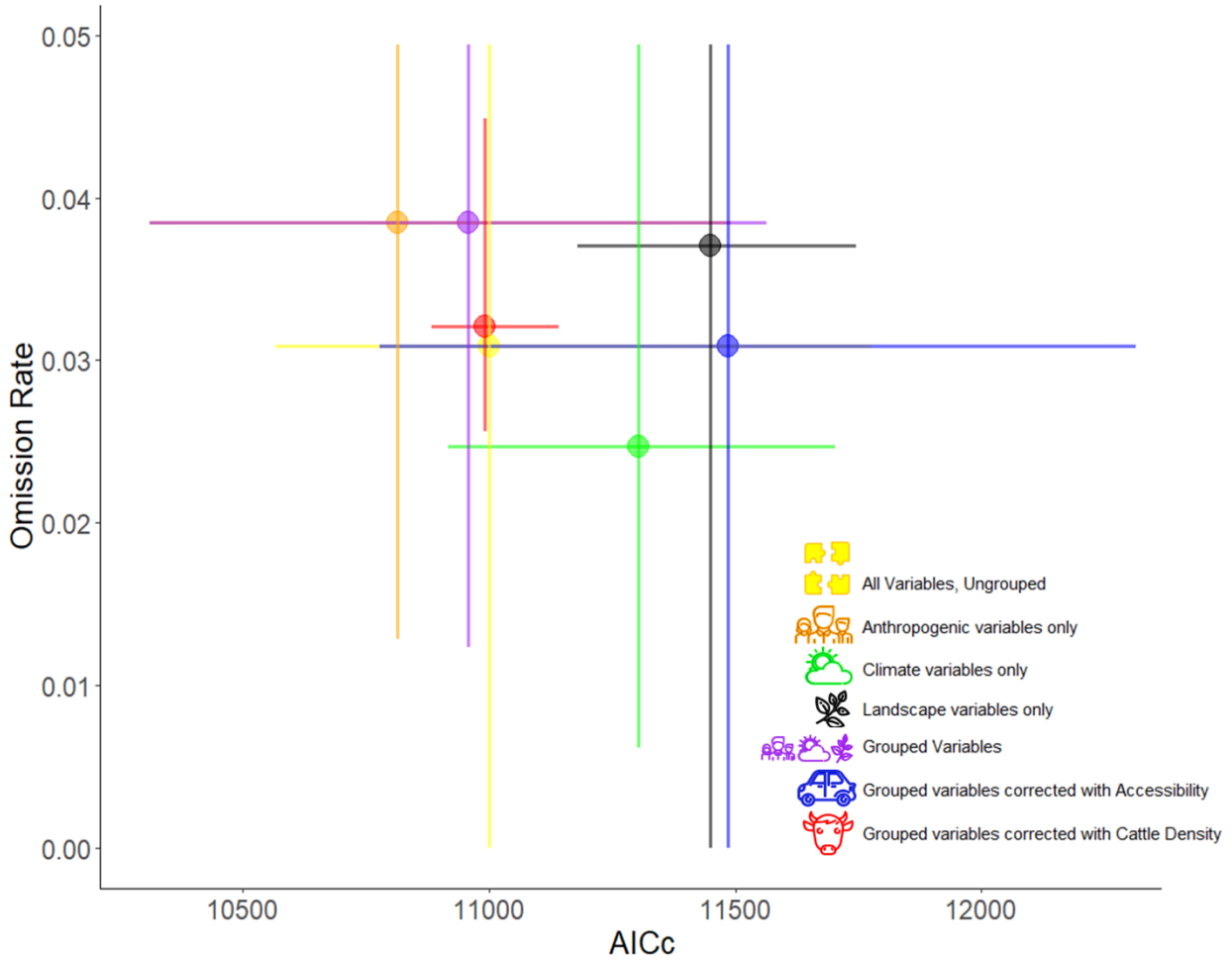

Figure 1: Model run experiment performance. Model performance in terms of omission rate and AICc for each set of predictor variable experiments. Predictor variables for each experiment are shown as: all variables (yellow), climate only (green), landscape only (black), anthropogenic only (orange), grouped variables (purple), and grouped variables with bias surface correction (red and blue). Point in the middle of each model experiment run indicated average omission rate and AICc of each corresponding predictor variable experiment/model run. Models calibrated using only climate variables had the overall lowest omission rates (green). Models calibrated with anthropogenic variables which used cattle density as a bias file, however, had the lowest variance in both omission rates and AICc (red).

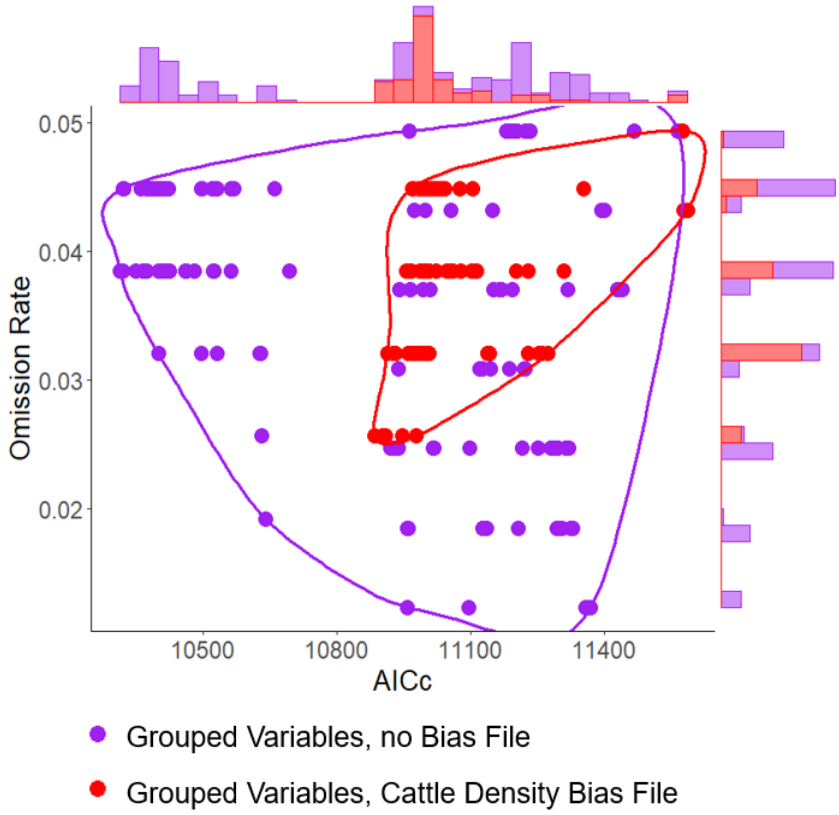

Figure 2: Bias file impact on model performance. The overall reduction in model performance uncertainty between models without sampling bias correction (purple), and models which accounted for sampling bias (red) highlights the importance of accounting for sampling bias in ecological niche modeling. While models without bias correction were better-performing (i.e., low omission rate and AICc of purple points), model performance was more precise when bias was taken into account (red points). Sampling bias was corrected using cattle density data from Gridded Livestock of the World database [47]. Models which accounted for sampling bias using cattle density (red) had lower variance in both omission rates (sd= 0.006 vs 0.0110) and AICc (sd=139 vs 395), with the differences in AICc being statistically significant per post-hoc LSD analysis (p<0.001).

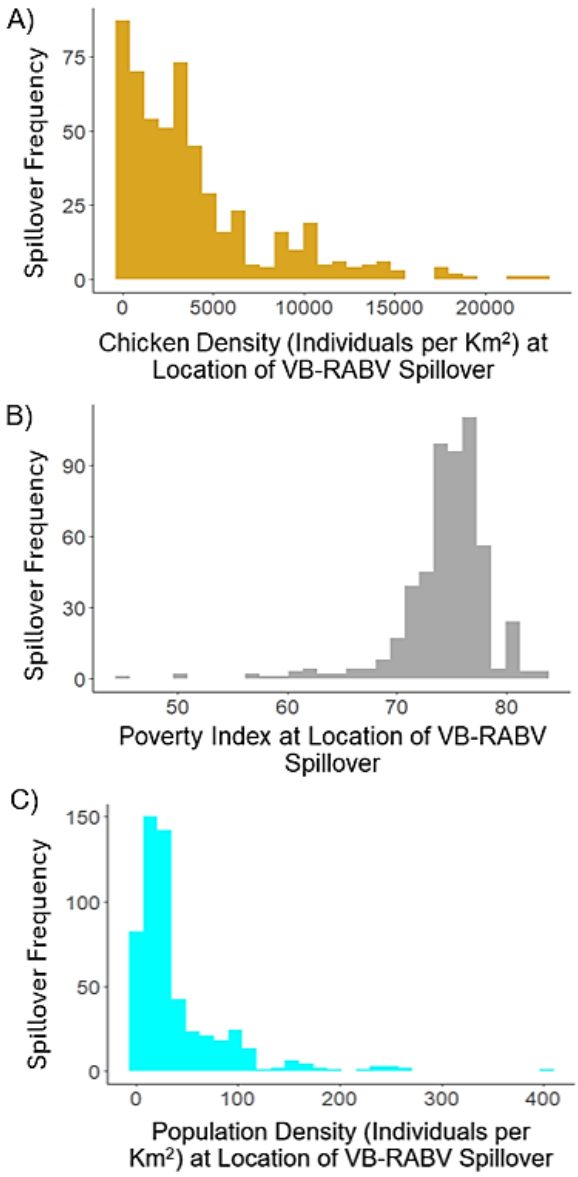

Figure 3: Anthropogenic Predictor Variable Relationships to RABV. **A)** Histogram of chicken density (number of individual chickens per square kilometer) at locations of RABV spillover used as training and testing data. Note the negative relationship between chicken density and RABV spillover locations. **B)** Histogram of poverty index at locations of RABV spillover used as training locations. Note the positive association between poverty index and RABV spillover locations. **C)** Histogram of human population density (number of individuals per km^2) at locations of RABV spillover used as training locations. Note the negative association between human population density and RABV locations. These results indicate that RABV spillover risk is higher when chicken density is low, poverty index is high, and human population density is low. The majority of RABV spillover occurred in locations with fewer than 5000 chickens per km^2, human density was less than 100 per km^2, and where poverty index was greater than 70.

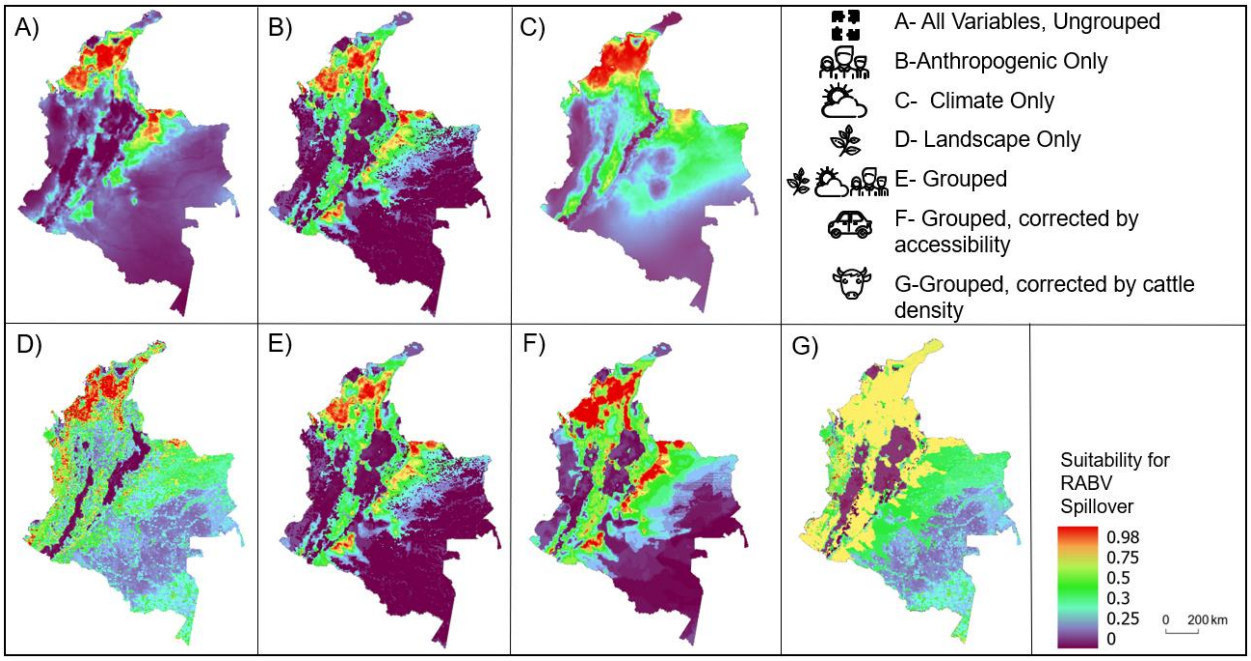

Figure 4: Risk maps. Geographic projection of each final model by predictor variable model experiment. Similarity of projected pixel to presence locations (i.e., suitability for RABV spillover) is shown from low (purple) to high (red). Maps correspond to predictor variable groups used including: **A)** all uncorrelated variables, **B)** anthropogenic variables only, **C)** climate variables only, **D)** landscape variables only, **E)** all variables grouped by characteristics, **F)** all variables grouped by characteristic and with accessibility as a bias surface, and **G)** all variables grouped by characteristic and with cattle density as a bias surface. Predictor variable sets are broken down in Table 2. Note the differences between model outputs when cattle density data are used as a predictor variable vs as a sampling bias correction file (G). The total area predicted to have moderately or moderately-high suitability (yellow) was much larger (30.6% of the total area) when sampling bias was accounted for in panel G. High suitability for RABV spillover (red) was localized to northern portions of the country when only climate variables were used (C) than when anthropogenic (B) or landscape (D) variables were used.

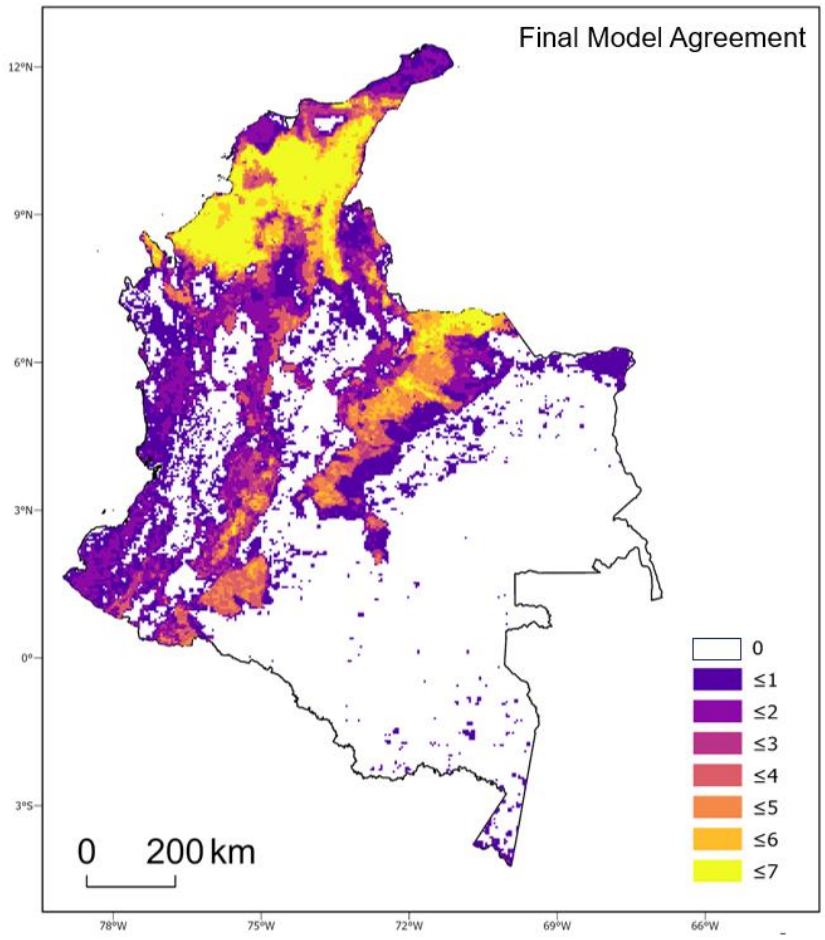

Figure 5: Model Agreement Ensemble (sum). Ensemble of all final models from each predictor variable experiment. Each map was added together to create this map, which is a representation of model agreement. High agreement between experiments (yellow) indicates areas where more models agreed that there was elevated RABV spillover risk. Low agreement (purple) indicates areas where fewer final models agreed that there was RABV spillover risk.

References

1. Rupprecht CE, Hanlon CA, Hemachudha T. Rabies re-examined. Lancet Infect Dis. 2002;2: 327–343. doi:10.1016/s1473-3099(02)00287-6

2. Bourhy H, Dautry-Varsat A, Hotez PJ, Salomon J. Rabies, still neglected after 125 years of vaccination. PLoS Negl Trop Dis. 2010;4: 4–6. doi:10.1371/journal.pntd.0000839

3. Vigilato MAN, Clavijo A, Knobl T, Silva HMT, Cosivi O, Schneider MC, et al. Progress towards eliminating canine rabies: Policies and perspectives from Latin America and the Caribbean. Philos Trans R Soc B Biol Sci. 2013;368: 20120143. doi:10.1098/rstb.2012.0143

4. Freire de Carvalho M, Vigilato MAN, Pompei JA, Rocha F, Vokaty A, Molina-Flores B, et al. Rabies in the Americas: 1998-2014. PLoS Negl Trop Dis. 2018;12: e0006271. doi:10.1371/journal.pntd.0006271

5. World Health Organization. Rabies. In: WHO. 2020 [cited 24 Feb 2021]. Available: https://www.who.int/news-room/fact-sheets/detail/rabies

6. Kotait I, Gonçalves C. Manual Técnico MAPA - Controle da raiva dos herbívoros. Manual Técnico 2009. Brasília: Ministério da Agricultura, Pecuária e Abastecimento; 2009. pp. 7–124.

7. Acha PN, Malaga-Alba A. Economic losses due to *Desmodus rotundus*. In: Greenhall AM, Schmidt U, editors. Natural History of Vampire Bats. Boca Raton: CRC Press; 1968. pp. 207–214.

8. Meske M, Fanelli A, Rocha F, Awada L, Soto PC, Mapitse N, et al. Evolution of rabies in south america and inter-species dynamics (2009–2018). Trop Med Infect Dis. 2021;6: 2–18. doi:10.3390/tropicalmed6020098

9. Geoffrey E. Sur les Phyllostomes et les Megadermes, deux Genres de la famille des Chauve-souris. In: Dufour G, editor. Annales du Museum d'histoire. d'Ocagne; 1810. pp. 181–182.

10. Lee DN, Papeş M, Van Den Bussche RA. Present and potential future distribution of common vampire bats in the Americas and the associated risk to cattle. PLoS One. 2012;7: e42466. doi:10.1371/journal.pone.0042466

11. Vigilato MAN, Cosivi O, Knöbl T, Clavijo A, Silva HMT. Rabies update for Latin America and the Caribbean. Emerg Infect Dis. 2013;19: 678–679. doi:10.3201/eid1904.121482

12. VERA (Vigilancia Epidemiológica de la Rabia en las Américas). Organización Panamericana de la Salud Organización Mundial de la Salud Boletín. 2020. pp. 8–27.

13. Páez A, Polo L, Heredia D, Nuñez C, Rodriguez M, Agudelo C, et al. Brote de rabia humana transmitida por gato en el municipio de Santander de Quilichao, Colombia, 2008. Rev Salud Pública. 2009;11: 931–943. doi:10.1590/S0124-00642009000600009

14. Uieda W, Buck S, Sazima I. Feeding behavior of the vampire bats *Diaemus youngi* and *Diphylla ecaudata* on smaller birds in captivity. J Brazilian Assoc Adv Sci. 1992;44: 410–412.

15. Ito F, Bernard E, Torres RA. What is for dinner? First report of human blood in the diet of the hairy-legged vampire bat *Diphylla ecaudata*. Acta Chiropterologica. 2016;18: 509–515. doi:10.3161/15081109ACC2016.18.2.017

16. Sazima I, Uieda W. Feeding behavior of the white-winged vampire bat, *Diaemus youngi*, on poultry. J Ma. 1980;61: 102–104.

17. Stoner-Duncan B, Streicker DG, Tedeschi CM. Vampire bats and rabies: Toward an ecological solution to a public health problem. PLoS Neglected Trop Dis. 2014;8: e2867. doi:10.1371/journal.pntd.0002867

18. PAHO/PANAFTOSA. SIRVERA. In: Sistema de Información Regional para la Vigilancia Epidemiológica de la Rabia (SIRVERA). 2019 [cited 20 Feb 2020]. Available: https://sirvera.panaftosa.org.br/

19. Cleaveland S, Hampson K. Rabies elimination research: Juxtaposing optimism, pragmatism and realism. Proc R Soc B. 2017;284: 20171880. doi:10.1098/rspb.2017.1880

20. Benavides JA, Rojas Paniagua E, Hampson K, Valderrama W, Streicker DG. Quantifying the burden of vampire bat rabies in Peruvian livestock. PLoS Negl Trop Dis. 2017;11: 1–17. doi:10.1371/journal.pntd.0006105

21. Brunker K, Mollentze N. Rabies Virus. Trends Microbiol. 2018;26: 886–887. doi:10.1016/j.tim.2018.07.001

22. Escobar LE, Peterson AT, Favi M, Yung V, Medina-Vogel G. Bat-borne rabies in Latin America. Rev Inst Med Trop Sao Paulo. 2015;57: 63–72. doi:10.1590/S0036-46652015000100009

23. Raynor B, Díaz EW, Shinnick J, Zegarra E, Monroy Y, Mena C, et al. The impact of the COVID-19 pandemic on rabies reemergence in Latin America: The case of Arequipa, Peru. PLoS Negl Trop Dis. 2021;15: e0009414. doi:10.1371/journal.pntd.0009414

24. Benavides JA, Valderrama W, Streicker DG. Spatial expansions and travelling waves of rabies in vampire bats. Proc R Soc B. 2016;283: 20160328. doi:10.1098/rspb.2016.0328

25. Streicker DG, Recuenco S, Valderrama W, Benavides JG, Vargas I, Pacheco V, et al. Ecological and anthropogenic drivers of rabies exposure in vampire bats: Implications for transmission and control. Proc R Soc B Biol Sci. 2012;279: 3384–3392. doi:10.1098/rspb.2012.0538

26. Van de Vuurst P, Qiao H, Soler-Tovar D, Escobar LE. Climate change linked to vampire bat expansion and rabies virus spillover. Ecography. 2023; e06714. doi:10.1111/ecog.06714

27. Zarza H, Martínez-Meyer E, Suzán G, Ceballos G. Geographic distribution of *Desmodus rotundus* in Mexico under current and future climate change scenarios: Implications for bovine paralytic rabies infection. Vet México OA. 2017;4: 1–16. doi:10.21753/vmoa.4.3.390

28. Hayes MA, Piaggio AJ. Assessing the potential impacts of a changing climate on the distribution of a rabies virus vector. PLoS One. 2018;13: e0192887. doi:10.1371/journal.pone.0192887

29. Piaggio AJ, Russell AL, Osorio IA, Jiménez Ramírez A, Fischer JW, Neuwald JL, et al. Genetic demography at the leading edge of the distribution of a rabies virus vector. Ecol Evol. 2017;7: 5343–5351. doi:10.1002/ece3.3087

30. Milena J, Neves M, Belo VS, Maria C, Catita S, Beatriz F, et al. Modeling of human rabies cases in Brazil in different future global warming scenarios. Int J Environ Res Public Health. 2024;21: 2–15. doi:10.3390/ijerph21020212

31. Streicker DG, Recuenco S, Valderrama W, Gomez Benavides J, Vargas I, Pacheco V, et al. Ecological and anthropogenic drivers of rabies exposure in vampire bats: Implications for transmission and control. Proc R Soc B. 2012;279: 3384–92. doi:10.1098/rspb.2012.0538

32. De Andrade FAG, Gomes MN, Uieda W, Begot AL, Ramos ODS, Fernandes MEB. Geographical analysis for detecting high-risk areas for bovine/human rabies transmitted by the common hematophagous bat in the Amazon region, Brazil. PLoS One. 2016;11: 1–15. doi:10.1371/journal.pone.0157332

33. Rocha F, Ulloa-Stanojlovic FM, Rabaquim VCV, Fadil P, Pompei JC, Brandão PE, et al. Relations between topography, feeding sites, and foraging behavior of the vampire bat, *Desmodus rotundus*. J Mammal. 2020;101: 164–171. doi:10.1093/jmammal/gyz177

34. Rocha F, Dias RA. The common vampire bat *Desmodus rotundus* (Chiroptera: Phyllostomidae) and the transmission of the rabies virus to livestock: A contact network approach and recommendations for surveillance and control. Prev Vet Med. 2020;174: e104809. doi:10.1016/j.prevetmed.2019.104809

35. Benavides JA, Valderrama W, Recuenco S, Uieda W, Suzán G, Avila-Flores R, et al. Defining new pathways to manage the ongoing emergence of bat rabies in Latin America. Viruses. 2020;8: 1002. doi:10.3390/v12091002

36. Jiménez G, Echeverry D, Baptiste MP, Isaacs-Cubides P, García L, Noguera E, et al. Estado y tendencias de la biodiversidad continental de Colombia. Biodiversidad. Instituto de Investigación de Recursos Biológicos Alexander von Humboldt; 2023. pp. 3–50.

37. Tapasco J, LeCoq JF, Ruden A, Rivas JS, Ortiz J. The livestock sector in Colombia: toward a program to facilitate large-scale adoption of mitigation and adaptation practices. Front Sustain Food Syst. 2019;3. doi:10.3389/fsufs.2019.00061

38. ICA. Censos Bovinos. In: Instituto Colombiano Agropecuario. 2020 [cited 1 Dec 2023]. Available: https://www.ica.gov.co/areas/pecuaria/servicios/epidemiologia-veterinaria/censos-2016/censo-2019

39. ICA. No Resolución 00383 de 2015. Bogotá, Colombia; 2015. p. 20. Available: https://www.ica.gov.co/normatividad/normas-ica/resoluciones-oficinas-nacionales

40. Bonilla-Aldana DK, Jimenez-Diaz SD, Barboza JJ, Rodriguez-Morales AJ. Mapping the spatiotemporal distribution of bovine rabies in Colombia, 2005–2019. Trop Med Infect Dis. 2022;7. doi:10.3390/TROPICALMED7120406

41. ICA. Sanidad Animal 2016. Dirección Tecnica de Vigilancia Epidemiológica. Subgerencia de Protección Animal. Instituto Colombiano Agropecuario. Boletines Epidemiológicos Dirección Tecnica de Vigilancia Epidemiológica Subgerencia de Protección Animal Intituto

Colombiano Agropecuario. Bogotá, Colombia: Produmedios; 2019. pp. 5–100.

42. Haining R. Spatial Autocorrelation. Wright JD, editor. Int Encycl Soc Behav Sci Second Ed. Second Edi. 2015;23: 105–110. doi:10.1016/B978-0-08-097086-8.72056-3

43. Peterson AT, Soberón J, Pearson RG, Anderson RP, Martínez-Meyer E, Nakamura M, et al. Ecological Niches and Geographic Distributions. Horn SAL and HS, editor. Ecological Niches and Geographic Distributions (MPB-49). Princeton, New Jersery: Princeton University Press; 2011. doi:10.23943/princeton/9780691136868.001.0001

44. Mantovan KB, Menozzi BD, Paiz LM, Sev P, Brand PE, Langoni H. Geographic distribution of common vampire bat *Desmodus rotundus* (Chiroptera : Phyllostomidae) shelters : Implications for the spread of rabies virus to cattle in Southeastern Brazil. Pathogens. 2022;11.

45. Magalhães AR, Codeço CT, Svenning JC, Escobar LE, Van de Vuurst P, Guncalves-Souza T. Neglected tropical diseases risk correlates with poverty and early ecosystem destruction. Infect Dis Poverty. 2023;12: 1–15. doi:10.1186/s40249-023-01084-1

46. Jones C, Vicente-Santos A, Clennon JA, Gillespie TR. Deforestation and bovine rabies outbreaks in Costa Rica, 1985–2020. Emerg Infect Dis. 2024;30: 1039–1042. doi:10.3201/eid3005.230927

47. Food and Agriculture Organization of the United Nations. Gridded Livestock of the World Database. 2022 [cited 1 Jun 2023]. Available: https://data.apps.fao.org/catalog/dataset/glw

48. Fick SE, Hijmans RJ. WorldClim 2: new 1-km spatial resolution climate surfaces for global land areas. Int J Climatol. 2017;37: 4302–4315. doi:10.1002/joc.5086

49. Hengl T. WorldGrids archived layers at 1 km to 20 km spatial resolution. 2018 [cited 8 Jul 2022]. doi:10.5281/ZENODO.1637816

50. Clevers J, Bartholomeus H, Mücher S, Wit A De. Land cover classification with the Medium Resolution Imaging Spectrometer (MERIS). EARSeL eProceedings. 2004;3: 354–362. doi: edepot.wur.nl/139566

51. NASA Earth Data. United States Socioeconomic Data and Applications Center (SEDAC). In: Earth Observing System Data and Information System. 2022 [cited 17 Aug 2023]. Available: https://sedac.ciesin.columbia.edu/

52. Van de Vuurst P, Diaz MM, Rodriguez-San Pedro A, Allendes JL, Brown N, Gutierrez JD, et al. A database of common vampire bat reports. Sci Data. 2021;9: e41597. doi:10.1038/s41597-022-01140-9

53. ESRI. ArcGIS Pro (Version 2.5). ESRI Inc.; 2019. Available: https://www.esri.com/en-us/arcgis/products/arcgis-pro/overview

54. Phillips SJ, Dudík M, Schapire RE. Maxent software for modeling species niches and distributions Version 3.4.1. 2019 [cited 24 May 2021]. Available: http://biodiversityinformatics.amnh.org/open_source/maxent/

55. Cobos ME, Townsend Peterson A, Barve N, Osorio-Olvera L. Kuenm: An R package for

detailed development of ecological niche models using Maxent. PeerJ. 2019;7: e6281. doi:10.7717/peerj.6281

56. Warren DL, Seifert SN. Ecological niche modeling in Maxent: The importance of model complexity and the performance of model selection criteria. Ecol Appl. 2011;21: 335–342. doi:10.1890/10-1171.1

57. Mesgaran MB, Cousens RD, Webber BL. Here be dragons: A tool for quantifying novelty due to covariate range and correlation change when projecting species distribution models. Divers Distrib. 2014;20: 1147–1159. doi:10.1111/ddi.12209

58. Graham CH, Hijmans RJ. A comparison of methods for mapping species ranges and species richness. Glob Ecol Biogeogr. 2006;15: 578–587. doi:10.1111/j.1466-822x.2006.00257.x

59. Morales NS, Fernández IC, Baca-González V. MaxEnt's parameter configuration and small samples: Are we paying attention to recommendations? A systematic review. PeerJ. 2017;5: e3093. doi:10.7717/peerj.3093

60. Merow C, Smith MJ, Silander JA. A practical guide to MaxEnt for modeling species' distributions: What it does, and why inputs and settings matter. Ecography. 2013;36: 1058–1069. doi:10.1111/j.1600-0587.2013.07872.x

61. Kramer-Schadt S, Niedballa J, Pilgrim JD, Schröder B, Lindenborn J, Reinfelder V, et al. The importance of correcting for sampling bias in MaxEnt species distribution models. Divers Distrib. 2013;19: 1366–1379. doi:10.1111/ddi.12096

62. Peterson AT, Papeş M, Soberón J. Rethinking receiver operating characteristic analysis applications in ecological niche modeling. Ecol Modell. 2008;213: 63–72. doi:10.1016/j.ecolmodel.2007.11.008

63. Peterson AT, Soberón J, Pearson RG, Anderson RP, Martínez-Meyer E, Nakamura M, et al. Ecological Niches and Geographic Distributions. Princeton: Princeton University Press; 2011. pp. 51–96.

64. Rojas-sereno ZE, Streicker DG, Medina-Rodriguez AT, Benavides JA. Drivers of spatial expansions of vampire bat rabies in Colombia. Viruses. 2022;14. doi:10.3390/v14112318

65. Sa´nchez-Cuervo AM, Aide TM, Clark ML, Etter A. Land cover change in Colombia : Surprising forest recovery trends between 2001 and 2010. PLoS One. 2012;7: e43943. doi:10.1371/journal.pone.0043943

66. Brown N, Escobar LE. A review of the diet of the common vampire bat (*Desmodus rotundus*) in the context of anthropogenic change. Mamm Biol. 2023;103: 433–453. doi:10.1007/s42991-023-00358-3

67. Wong JT, Bruyn J De, Bagnol B, Grieve H, Li M, Pym R, et al. Small-scale poultry and food security in resource-poor settings: A review. Glob Food Sec. 2017;15: In Press. doi:10.1016/j.gfs.2017.04.003

68. Gilbert M, Conchedda G, Boeckel TP Van, Cinardi G, Linard C, Nicolas G, et al. Income disparities and the global distribution of intensively farmed chicken and pigs. PLoS One. 2015;10: e0133381. doi:10.1371/journal.pone.0133381

69. Roess A, Robertson K, Recuenco S. Historical Disparities in Health: Rabies Surveillance, Risk Factors and Prevention. In: Rupprecht CE, editor. History of Rabies in the Americas: From the Pre-Columbian to the Present, Volume 1. Springer; 2023. pp. 261–280.

70. Meza DK, Mollentze N, Broos A, Tello C, Valderrama W, Recuenco S, et al. Ecological determinants of rabies virus dynamics in vampire bats and spillover to livestock. Proc R Soc B. 2022;289: e20220860. doi:10.1098/rspb.2022.0860

71. Becker DJ, Simmons NB, Broos A, Bergner LM, Meza DK, Fenton MB, et al. Temporal patterns of vampire bat rabies and host connectivity in Belize. Transbound Emerg Dis. 2021;68: 870–879. doi:10.1111/tbed.13754

72. Streicker DG, Winternitzc JC, Satterfield DA, Condori-Condori RE, Broos A, Tello C, et al. Host-pathogen evolutionary signatures reveal dynamics and future invasions of vampire bat rabies. Proc Natl Acad Sci. 2016;113: 10926–10931. doi:10.1073/pnas.1606587113

73. Streicker DG, Fallas González SL, Luconi G, Barrientos RG, Leon B. Phylodynamics reveals extinction–recolonization dynamics underpin apparently endemic vampire bat rabies in Costa Rica. Proc R Soc B Biol Sci. 2019;286. doi:10.1098/rspb.2019.1527

74. Delpietro HA, Russo RG. Ecological and epidemiologic aspects of the attacks by vampire bats and paralytic rabies in Argentina and analysis of the proposals carried out for their control. Rev Sci Tech. 1996;15: 971–984. doi:10.20506/rst.15.3.964

75. Center for International Earth Science Information Network (CIESIN). Global Gridded Relative Deprivation Index (GRDI), Version 1. In: NASA Socioeconomic Data and Applications Center (SEDAC). 2022 [cited 27 Jan 2024]. Available: https://doi.org/10.7927/xwf1-k532.

CHAPTER 3: Vampire bats, emerging disease, and future climate change

Previously submitted to Scientific Reports on October 16th, 2024 under the title "Vampire bats, emerging disease, and future climate change"

Abstract

Interactions among humans, livestock, and wildlife within disturbed ecosystems, including those impacted by climate change, can facilitate pathogen spillover transmission and increase disease emergence. The study of future climate change impacts on the distribution of free-ranging bats is therefore relevant for forecasting disease emergence. This study used current and future climate data and historic occurrence locations of the vampire bat species *Desmodus rotundus*, a reservoir of the rabies virus, to conduct a comprehensive comparison of different climate change projections, carbon emission scenarios, and global circulation models (GCMs) on final model outputs. Model results revealed that, although climatic scenarios and GCMs used have an influence on model outputs, there was a consistent signal of predicted range expansion across the future climates analyzed. Areas suitable for *D. rotundus* range expansion include the southern United States and south-central portions of Argentina and Chile. Certain areas in the Amazon rainforest, which currently rests at the geographic center of *D. rotundus'* range, may become climatically unsuitable for this species in the context of niche conservatism. While the impacts of rabies virus transmitted by *D. rotundus* on livestock are well known, an expansion of *D. rotundus* into novel areas may impact hitherto unaffected mammalian species and livestock with unexpected consequences. Some areas in the Americas may therefore benefit from an assessment of their preparedness to deal with a *D. rotundus* range expansion.

Introduction

Climate change is a global driver of ecosystem degradation, which has been found to have chain effects and unexpected impacts on ecosystem health [1–5]. Greenhouse gases trap heat which would usually radiate from Earth toward space, causing surface air temperature and subsurface ocean temperatures to rise over time [2,6,7]. Changes in global temperature, precipitation seasonality, and weather patterns have been well documented as a result of climate change, all of which can impact ecosystem stability [7–11]. The Intergovernmental Panel on Climate Change (IPCC) has predicted that climate change will amplify negative health impacts across the globe [1,7]. Ecosystem degradation linked to climate change can also alter the spatial distribution of many wildlife species [12,13]. Models of species' responses to climate change have predicted that various species will experience latitudinal and altitudinal shifts in their distributions [14–17]. Distributional shifts may facilitate the creation of novel species assemblages [15,16,18]. Distributional shifts also may result in increases in pathogen transmission to novel hosts [19]. Climate change can therefore be a driver of disease emergence [19]. Pathogen spillover, or the transmission of a pathogen from one species to another, has been linked to some of the most lethal zoonotic diseases which impact humans [20]. Distributional shifts and poor wildlife health driven by climate change can increase risks of pathogen spillover from wildlife to humans via their disruption of multiple biological processes [21]. More specifically, spillover from wildlife to livestock has been shown to have negative animal and human health impacts, as well as considerable economic losses [20,22].

Bats can tolerate infection by viruses that are highly pathogenic to livestock and humans [23,24]. Examples of high-impact spillover-derived zoonotic diseases which are transmitted by bats include Nipah virus encephalitis, severe acute respiratory syndrome (SARS), and rabies [25–27]. Currently, we lack a comprehensive understanding of how anthropogenic climate change may

influence the ecology, climate suitability, and potential geographic distribution of bat disease reservoirs in general. Furthermore, climate change impacts on health are not evenly distributed geographically [28], with some areas in the tropics being among those most impacted by emerging infectious diseases due to ecosystem degradation and climate change [11,28,29]. Low-income countries in the tropics are at even greater risk of bat-borne emerging diseases, as increased socioeconomic risk factors compound with climate change impacts in these regions [31]. The study of future climate change impacts to the distribution of bats is critically important to predict and mitigate the impacts of disease emergence, but research on this tropic has been poor [32].

In Latin America, rabies virus (RABV) is a well-documented and impactful bat-borne pathogen [27,33]. Thousands of cattle are lost to bat-borne rabies in Latin America annually [34–36], and billions of United States (US) dollars are forfeited annually for rabies prevention and control measures [37]. Rabies is almost 100% fatal for infected individuals, with rabies killing ~60,000 people a year, mainly in Africa and Asia where it is principally transmitted by dogs [34,37,28]. Rabies has been reported to cause at least US$8.6 billion in economic losses in impacted areas due to loss of working hours of humans and death of their livestock [38]. The common vampire bat, *Desmodus rotundus*, is a common and widespread bat occurring across Latin America [39]. *Desmodus rotundus* feeds upon the blood of a variety of prey types including wildlife, livestock, pets, and humans [27]. During feeding, *D. rotundus* can transmit RABV to their prey [40], thus acting as a wildlife reservoir and known host for the virus. Vampire bat-borne RABV (VB-RABV) outbreaks in humans and livestock regularly occur in tropical and subtropical regions [41], where risks of human infection have been directly correlated with risks of outbreaks in livestock [35].

In the last 120 years, *D. rotundus* has expanded its range northward towards the continental United States due to climate change [42,43]. Furthermore, Benavides *et al.* (2016) documented an expansion of the geographic distribution of VB-RABV outbreaks in livestock in Peru, with a concurrent shift of *D. rotundus* populations to higher elevations. The expansion of *D. rotundus* and associated VB-RABV into southern portions of South America has also been linked to changes in the landscape and climate [44,45]. As such, there is sufficient evidence to suggest that future climate change may continue to change the distribution of *D. rotundus* and, as a result, the likelihood of VB-RABV spillover. To assess the ramifications of different climate change scenarios on the potential future distribution of *D. rotundus*, we evaluated future climate change effects on the likely distribution of this RABV reservoir.

Methods

We utilized ecological niche modeling-based methods to forecast suitability of future climates for *D. rotundus* across multiple future-climate scenarios in the Americas. We used MaxEnt [46], which functions by comparing the environmental conditions of occurrence locations with those of selected background locations from the available environmental space where the species could potentially occur (i.e., environmental "similarity" between field observations and study area) (Equation 1) [46–48]. MaxEnt is a frequently utilized presence-background modeling platform successfully utilized in previous assessments of *D. rotundus*' distribution [42,43,49]. MaxEnt does not require true absence data for its calibration, and therefore more logically abides by the available occurrence locations data for this species. In its most basic form, the analytical framework of MaxEnt can be described as:

$$Similarity * \left(z(x_i)\right) = \mathrm{Q}(x_i)\exp\left(z(x_i)\lambda\right) / \sum_i^n \exp\left(z(x_i)\lambda\right) \quad (1)$$

where Z is a vector of background environmental variables at location X_i , λ is a vector of regression coefficients and Q is the prior probability density of Z at a known presence location [50–52]. Equation 1 is adapted from Merow et al. 2013.

Occurrence location filtering

We collected occurrence locations of *D. rotundus* from an extensive database specific to this species from across Latin America from 1901-2023 [53]. We isolated all occurrence locations from this database with associated location data (i.e., geographic coordinates or locality description) using the *dplyr* package in R statistical software version 4.1.0 resulting in 74.6% geolocated records (n=29174 of 39118 available records) [54]. To address possible sample selection bias and spatial autocorrelation within the occurrence locations data, we filtered the *D. rotundus* occurrence locations to one per pixel of the study area (Figure 1). Pixels were delineated based on the background environmental variables used for model calibration (see below) at 2.5-arc-minute (~5 km) resolution. To resample the occurrence locations to one per pixel, we created a blank raster mask of the same spatial scale and resolution as the background environmental variables for which each pixel was assigned a pixel index value for its corresponding location within the study area (i.e., Latin America). We then removed all but one occurrence location for each pixel index value within the study area (n=5788). As the current estimates of *D. rotundus* climate suitability were to be calibrated using current climate estimates averaged across 30 years (1970-2000), occurrence locations that were redundant by location (i.e., duplicate coordinates) were not retained, even if they were collected in different years. This approach allowed us to mitigate any overrepresentation of certain climatic conditions due to greater sampling effort.

The remaining occurrence locations were then matched with the corresponding values of the background environmental variables (i.e., climate) from the WorldClim database [55] at 2.5-arc-minute resolution (~5 km). WorldClim provides 19 different global metrics of climate, both for current climates and for a variety of different future periods and emission scenarios [55]. Current climate data from WorldClim are averaged from the years 1970-2000 [55], which were used as the closest approximation of the available historical occurrence location data. We used the *raster* package [56] in R to extract the value of each WorldClim variable for current climates at the location of each occurrence location. We used these values to create a cloud of data points representing the species' historic distribution in environmental space (E-space) [57]. We then developed a principal component analysis of the background environmental variables (i.e., current climate) extracted at each occurrence location to obtain principal component axes summarizing variance of the climatic data at location of known occurrence. Principal components one, two, and three (summarizing 80.4% of the background environmental variable data variance) were then used as axes to plot the occurrence locations in environmental space. We then calculated the Mahalanobis distances between each occurrence location in E-space. These distances were used to fit a minimum-volume ellipsoids to with all occurrence locations in E-space with permutations taking one point out in each iteration. A Chi-squared test was used to identify which occurrence locations fell outside of the ellipsoid. Occurrence locations significantly outside the bulk of ellipsoids (n=269 or 4.6% of the occurrence locations) were identified as environmental outliers (i.e., occurrence locations which do not represent the "typical" climate tolerances of *D. rotundus*) and were removed (following methods of Qiao et al. 2024). After filtering in geographic and environmental space, the remaining 5519 occurrence locations were randomly split into 50% training and 50% testing subsets for model calibration and evaluation.

Ecological Niche Modeling

Ecological niche model calibration, evaluation, and projection was completed in R using the *kuenm* package [58]. While 19 different metrics of climate are available within the WorldClim database, some of these variables are correlated. To reduce background environmental variable redundancy, we used a Pearson Correlation coefficient analysis [57] of all 19 variables to eliminate highly correlated variables (i.e., $\rho \geq 0.5$, n=12). The remaining seven climate variables were evaluated based on their known importance to the ecology of *D. rotundus*. As such, three variables (mean diurnal temperature range, maximum temperature of the warmest month, and precipitation of the dryest quarter) were eliminated from consideration. Four final variables were used as background environmental variables which included: precipitation seasonality (standard deviation of monthly precipitation estimation as a percentage of annual mean precipitation) (kg m^{-2}), annual precipitation (kg m^{-2}), minimum temperature of the coldest month (°C), and isothermality (mean diurnal temperature range divided by annual temperature range) (°C). We then restricted the background environmental variables to a specific calibration area [57]. A calibration area comprises a smaller sub-portion of the study area that the species of interest has access to, and is used to calibrate the model [57]. To create this calibration area we used ArcGIS Pro version 2.5 software [59] to create a 200 kilometer buffer around each occurrence location, which is ten times the species' home range [60,61] and encompasses any amount of long range dispersal that the species may have performed in current climates [44,62]. This buffer was exported as a shape file and used to crop the background environmental variables to the calibration area. By limiting the calibration area in this way, areas that the species may not have access to due to dispersal limitations are eliminated from consideration during the calibration process, thus making the comparison between presence and background more accurate [57].

The *kuenm* package allowed us to create candidate models with multiple parameterizations and feature class assumptions in MaxEnt [63]. More specifically, feature classes are functions derived from background environmental variables to minimize model overfitting, and regularization multipliers are parameters which impose penalties on models for over-complexity [52,64]. We tested a suite of regularization parameters that modulate model fit to the data (i.e., 0.1, 0.2,0.5,1,2, and 5) and all possible combinations of five feature classes that dictate the assumed species responses to the environmental variables (linear=l, quadratic=q, product=p, threshold=t, and hinge=h). After redundant model combinations were removed, the remaining 434 candidate models were evaluated based on omission rates (E=0.05) [65] and model complexity (*AICc*) [58].

The final ecological niche model selected by the evaluation process was then projected to the geographic extent of the study area (the Americas) and to multiple future climate change scenarios across six Global Circulation Models (GCMs) [66-68]. These GCMs included the Australian Community Climate and Earth System Simulator (ACCESS-CM2), the Beijing Climate Center Climate System Model (BCC-CSM2-HR), the UK Earth System Model (UKESM1-0-LL), the Europe wide consortium climate model (EC-Earth3-Veg-LR), the National Institute for Environmental Studies of the University of Tokyo model (MIROC6), and the Max Planck Institute for Meteorology Model (MPI-ESM1-2-LR) (Table 1). These six models were chosen to capture GCM-projected climate variability as available in the most recent iteration of NEX-GDDP CMIP6 GCMs [66–68]. These six models also capture equilibrium climate sensitivity (ECS) and transient climate response (TCR) variance from high to low [67] (Table 1). Both ECS and TCR are standard metrics of climate model sensitivity related to increased CO_2 concentrations [67].

We also projected the final ecological niche model across four possible future shared socio-economic pathways (SSPs one, two, three, and five), which capture variation in the magnitude or

severity of climate change based on possible future global greenhouse gas emissions and future population growth and development trajectories [69,70]. Each GCM and SSP was used as a reference climate to project the final ecological niche model across three different time periods, including 2020-2040, 2041-2060, and 2061-2080). This combination of GCMs, SSPs, and time periods allowed us to develop a comprehensive assessment of likely *D. rotundus* distributions in a variety of possible future climates, and captures variation as a proxy of uncertainty in the species' future distribution (Figure 2).

The continuous MaxEnt model outputs were interpreted as a numeric representation of the similarity of the projected location to the bulk of locations with known occurrences of *D. rotundus* (i.e., the training data) from the calibration area [48,50]. These values can also be theoretically interpreted as a metric of how "suitable" each location is for *D. rotundus* occurrence relative to the background environmental variables (i.e., in this case, climate).

Models in MaxEnt can be projected using free extrapolation, limited extrapolation, or no extrapolation to predict suitability in environments outside values from the known occurrence locations [58,71]. Extrapolation, in this case, would allow features to extend beyond the ranges of the training data, thereby predicting future occurrence into new climatic conditions which do not currently exist and may be outside of the climatic tolerances of *D. rotundus* [50]. In other words, projecting MaxEnt models with free or limited extrapolation would assume that the species has physiological tolerances beyond the tolerances observed under current climates. Alternatively, model projection using extrapolation assumes that the species would evolve fast enough to adapt to novel climates [72]. Thus, model extrapolation violates ecological niche conservatism, which postulates that species are expected to retain climate tolerances under rapid climate change [72]. As such, within the *kuenm* package we chose to project our model to future climates without

extrapolation, thus limiting the uncertainty of our projection into future time periods [58]. The strict model transferences without extrapolation allowed us to make inferences and conclusions from a comparatively conservative representation of projected future suitability for *D. rotundus*.

Post Projection Analysis

After model projection, we utilized *kuenm* post-projection processing functions to identify areas of strict extrapolation risk via a mobility-oriented parity (MOP) analysis for all four SSPs for the 2080 time period. A MOP analysis identifies areas with the most dissimilar climate conditions from the background environmental variables in the calibration data (i.e., where one or more covariate variables are outside ranges present in the training data). This analysis allowed us to identify areas where extrapolation could impact the certainty of future suitability projections. We summarized these results by summing all four MOP rasters into one map across all SSPs to visualize geographic areas with strict extrapolation risk, regardless of projected climate-change severity.

The projected continuous suitability maps created during model projections were ensembled for each time period and SSP by adding them using the *raster* package in R version 4.1.0 [56]. The model ensemble allowed us to identify how the magnitude of climate change may impact the potential distribution of *D. rotundus* across time, regardless of GCM. We also used these GCM ensembles to assess changes in suitability for *D. rotundus* across time periods (Figure 2).

Additionally, we quantified the directions and magnitudes of any *D. rotundus* distributional changes projected by using a minimum training presences threshold to isolate areas suitable for *D. rotundus* based on the final ecological niche model. This minimum training presence value was used as a threshold to reclassify the continuous projected maps into binary maps. Model binarization was based upon the assumption that the least suitable location at which the species is

known to have occurred is the minimum suitability value for the species [73]. The resulting binary maps were used to assess how the distribution of projected suitability for *D. rotundus* may change across time (Figure 2).

We used the *raster* package [56] to quantify the total suitable area in km^2 from each binary map by SSP. We then isolated the 100 highest (most northern) and lowest (most southern) latitudes predicted by the projected range models by time-period, which allowed us to assess whether or not the projected suitable range for *D. rotundus* may vary latitudinally based on time period or SSP. We also identified the 100 highest projected suitable elevations from each binary map by GCM and averaged across SSP to determine the extent to which *D. rotundus*' potential range varied in elevation. Elevation data were collected from the WorldClim database at ~5 km spatial resolution in agreement with the climate data [55]. We used multiple regressions and two-way analysis of variance to assess trends in distributional ranges across the periods.

Results

Of all 434 candidate ecological niche models, 304 performed better than random in terms of prediction of independent, testing data, and had omission rates lower than our exclusion threshold (E=0.05). Final ecological niche model parameterizations and performance metrics were obtained from the model evaluation process. The most well-performing model selected during the evaluation process had a regularization multiplier of 0.1 and used the linear, product, and threshold feature classes. Other well-preforming models that were not selected had the same regularization multiplier (0.1), but had different combinations of feature classes. The average area under the receiver operating characteristic curve (AUC) of the final ecological niche model was 1.11, the omission rate was 0.048, and the overall AICc was 153639.9 (Delta AICc=0, Weighted AICc=0.5).

Minimum temperature of the coldest month had the highest variable contribution (32.7%), followed by precipitation seasonality (32.6%), annual precipitation (18.5%), and isothermality (16.1%). Based on the projection of this model, we found that *D. rotundus* is likely to extend its range both northward and southward of current range estimates in the next 20-80 years (Figure 3 and 4). GCMs which had lower sensitivity values of ECS had higher rates of variance in our distributional projections, specifically for our northern latitudinal analysis (Figure 6). The Max Planck Institute model (MPI) and the Europe wide consortium model (EVeg) in particular had wider variance in the most northern projected suitable latitudes for all SSPs (Figure 6).

Based on the average ensemble of all GCMs, a multiple linear regression model (Maximum Latitude ~ Period + SSP) showed that northern expansion was significant, but modest, across all SSPs (p<0.01, Adjusted R^2=0.1, Standard Error=3.48) (Figure 5). Northern suitability peaked during the 2020-2040 period under the best-case scenario for sustainable development (SSP1). By 2080, northern expansion of suitability for *D. rotundus* was approximately two degrees of latitude (over 200 km) higher in the worst-case scenario of future climate (SSP 5). Southern expansion beyond current estimates of suitable range for *D. rotundus* existed across all SSPs, but was not significant per a multiple linear regression analysis (Minimum Latitude ~ Period + SSP) (p=0.98, Adjusted R^2=0.04, Standard Error=0.13).

In terms of total suitable area, a linear model of all SSP across all GCMs (i.e., Total Suitable Area ~ period) showed a significant increase in total suitable area (p=0.028, Standard Error=276.9, R^2=0.43) from current projections to the 2080 time period. Nevertheless, there was no significant change in total suitable area for *D. rotundus* across the projected time periods when SSP was included as a predictor (Total Suitable Area ~ Period + SSP) (p=0.15, Adjusted R^2=0.22, Standard Error=24770) (Figure 5). Increases in total suitable area were maintained in later periods (2060

and 2080) of best-case scenarios (SSPs 1 and 2). In later periods of future projected climate there was a decrease in total suitable area in the worst-case scenarios (SSPs 3 and 5) (Figure 5). The distribution of suitable area for each scenario and time period was not consistent across the Americas. We found that certain areas in the Amazon, which currently rests at the geographic center of *D. rotundus'* range [39], may become unsuitable under more extreme climate change scenarios such as SSP 3 and SSP 5 (Figure 5). In these scenarios, the Amazon is expected to become drier and precipitation seasonality is expected to become more unstable [74,75]. In contrast, some areas that are currently unsuitable for *D. rotundus* occurrence are projected to gain climate suitability, including the southern United States, western Mexico, and central Argentina (Figure 5). Per the MOP analysis, areas with strict extrapolation risk in the GCMs corresponded with many of the areas projected to lose suitability (Figure 4). The MOP strict extrapolation was located in the Amazon rainforest and in some areas of Central America (Figure 7). As such, projections of future suitability for *D. rotundus* in these geographic regions may be more uncertain. We found no identifiable relationship between average suitable elevations for *D. rotundus* and time period or SSP (two-way ANOVA, p=0.27). There was an increase of only 30 meters of average maximum elevation of suitability from current projections in the SSP 5 climate.

Discussion

This study aimed to assess the possible impacts of predicted future climate on the distribution of a bat that serves as a disease reservoir. *Desmodus rotundus* causes significant socioeconomic damage in its current range, and could possibly cause that same damage in new areas that are not prepared for a range expansion by this species. We used current and future climate data and historic occurrence locations of the rabies reservoir *D. rotundus* in MaxEnt to reconstruct the distribution

of this species under different climate change scenarios. We conducted a comprehensive comparison of the methodological implications of different climate change projections, carbon emission scenarios, and GCMs. We identified the potential for *D. rotundus* to expand its distribution into novel areas both north and south of current estimates. Our models revealed certain areas that may lose or gain climate suitability for *D. rotundus* under different emission scenarios (SSPs). This study provides evidence of a potential northward range-shift for *D. rotundus* due to climate change.

Of the climate variables used as background environmental variables, minimum temperature of the coldest month and precipitation seasonality had the highest contribution in the final model. These results echo those of previous modeling efforts [76,77], which found minimum temperatures and seasonality to be major drivers of *D. rotundus* distribution. Results of previous research have suggested that *D. rotundus* may be poorly adapted to survival at lower temperatures [78], as it is assumed that the species cannot effectively thermoregulate in colder climates due to its diet of only blood [79,80]. Nevertheless, a substantial degree of variation in the individual thermal tolerances has been observed among *D. rotundus* individuals [81]. The importance of precipitation seasonality in the ecological niche model could derive from the high annual precipitation across tropical and sub-tropical belts of the Americas [39], [82]. For instance, some of the highest precipitation seasonality indices can be found in the Amazon rainforest [74,82], which currently rests at the geographic center of *D. rotundus*' range. Dry or desert areas have also been identified as barriers to dispersal for *D. rotundus*, especially at the northern extent of its range in Mexico [42]. These currently unsuitable areas could become suitable for *D. rotundus* occurrence and thus no longer act as barriers to the species' dispersal under variations in rain patterns due to climate change.

Climate suitability for *D. rotundus* was predicted to be lost in central portions of the Amazon basin. The Amazon basin is projected to experience compounding climate stressors and decreases in climate stability [74,75]. The final ecological niche model predicted *D. rotundus* range expansion into novel areas such as western Mexico, the southern United States, and central Argentina. These regions of possible expansion may benefit from an assessment of their current preparedness to deal with a natural invasion of *D. rotundus* and the associated VB-RABV they may carry. Preparedness (e.g., vaccination stocks and campaign strategies) against VB-RABV prevention is especially important for areas with high livestock densities.

Areas of projected suitability gain in central Argentina and western Mexico have higher livestock densities (>100 head of livestock per square kilometer) than areas of projected loss such as the Amazon (<10 head of livestock per square kilometer) [83]. Loss of suitable area in our projections also corresponded to areas of known low human population density in countries such as Brazil, where densities are as low as <1 person per square kilometer [84]. Areas of gain in suitability such as western Mexico and the southern US, in contrast, have population densities >25 people per square kilometer, even in rural areas [84]. As such, large areas predicted to become climatically suitable for *D. rotundus* may host higher vulnerability to VB-RABV than current hotspots of *D. rotundus* suitability (Figure 3 and 4) [83–85]. Greater conflict between *D. rotundus* and humans in these regions may drive greater persecution for this and other bat species via culling, which has not been proven to decrease spillover rates for RABV [45,86]. A climate change-driven range shift for *D. rotundus* may therefore exacerbate human-wildlife conflicts involving bats.

Our analyses were conducted across an ensemble of six GCMs to capture a summary of current climate change projections. We found variation between the magnitude of climate suitability change for *D. rotundus* between the GCMs utilized (Figure 6). For instance, latitudinal

variation in *D. rotundus* ranges was influenced by the GCM used. While almost all models predicted northern expansion, some GCMs suggested higher (i.e., farther norther) expansion. For example, Eveg and MPI are GCMs with low sensitivity to increased CO_2 concentrations and highest rates of variation in *D. rotundus* predicted ranges (Figure 6). One possible explanation for this variance is that GCMs are calibrated with differing metrics and effects of Earth system functions [67,70,87]. For example, the MPI and EVeg models have relatively low values of aerosol forcing [67], which could contribute to the uncertainty observed. Furthermore, ECS values for each GCM can be impacted by factors such as cloud feedback and cloud-aerosol interactions, which was identified in many GCMs between CMIP5 and CMIP6 [67]. These factors can increase the range and value of ECS, which could have affected the projection of our model through the GCMs [67,70]. Ultimately, our results indicate that the variation between GCM sensitivity and associated variance in projections should be taken into account when conducting ecological niche modeling under future climate change scenarios. In the absence of such regard, models predicting future species distributions using a single GCM could generate incomplete or misleading estimates of likely species ranges.

We chose to use non-extrapolated projections of our model to future scenarios to generate strict model transferences without prediction in novel climates [58,71,88]. Model transference without extrapolation is a conservative approach that does not assume fast evolutionary adaptation of species to climate change [72,89]. Furthermore, the use of only abiotic climate variables as background environmental variables in our model innately limits the forecasting ability of our future projections of *D. rotundus* distribution at the local level. Nevertheless, the uncertainty present in future land-use projections can heavily impact future climate-change projections of temperature and precipitation, which are strongly influenced by urban and agricultural land-use

changes [90]. As such, we concluded that the inclusion of future landscape or land-use projections may have added more error than was useful for designing general VB-RABV risk mitigation strategies. Future research could explore the possibility of *D. rotundus* adaptation to novel climates under different climate change scenarios, which could refine distributional estimations.

Conclusions

We found that the rabies reservoir *D. rotundus* could extend its range in the next 20-80 years into novel areas due to changes in climate. Future range expansion for *D. rotundus* includes the southern United States and south-central portions of Argentina and Chile. While certain areas may gain climate suitability in the higher latitudes of *D. rotundus* range, we found areas in the Amazon rainforest may become unsuitable for this species in the future. Nevertheless, any loss of suitable area for *D. rotundus* may be offset by gains of suitability in areas that are currently acting as climatological barriers to dispersal for *D. rotundus* in the United States and Argentina. Successful dispersal to new areas, however, would be limited by availability of resources, including cattle densities [77,83]. We recommend preventive and educational programs be designed in areas predicted to be vulnerable to a *D. rotundus* range expansion. A likely range expansion is expected to result in increased human-wildlife conflict due to novel human and livestock populations exposed to *D. rotundus* invasion.

Tables and Figures

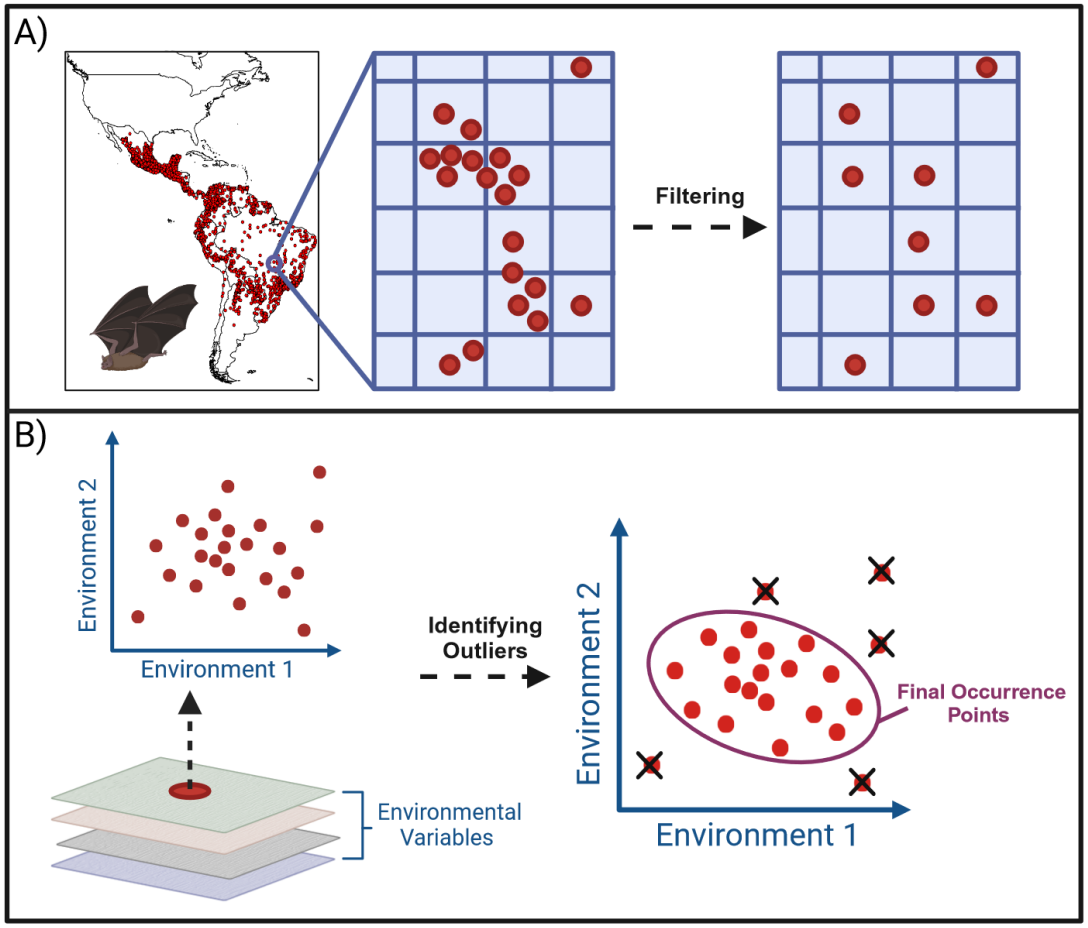

Figure 1: Occurrence Location Filtering. A) Geographic Space: Filtering of *Desmodus rotundus* occurrence locations from 1900-2023 [53] in geographic space. Occurrence locations were resampled to yield one data point per pixel (2.5 arc-minute or ~5 km resolution) of the study area to reduce the overrepresentation of certain environmental conditions. **B) Environmental Space:** Values of background environmental variables averaged from years 1970-2000 were extracted from the location of geographically filtered occurrence locations. These data were then used to create an environmental space [57] where we calculated the distance between occurrence locations using Mahalanobis distance. Using a chi-squared test, we identified environmental outliers via drawing an ellipsoid, where occurrence location which fell outside the ellipsoid (n=269 or 4.6% of the occurrence locations) were excluded from final occurrence locations used for our modeling effort.

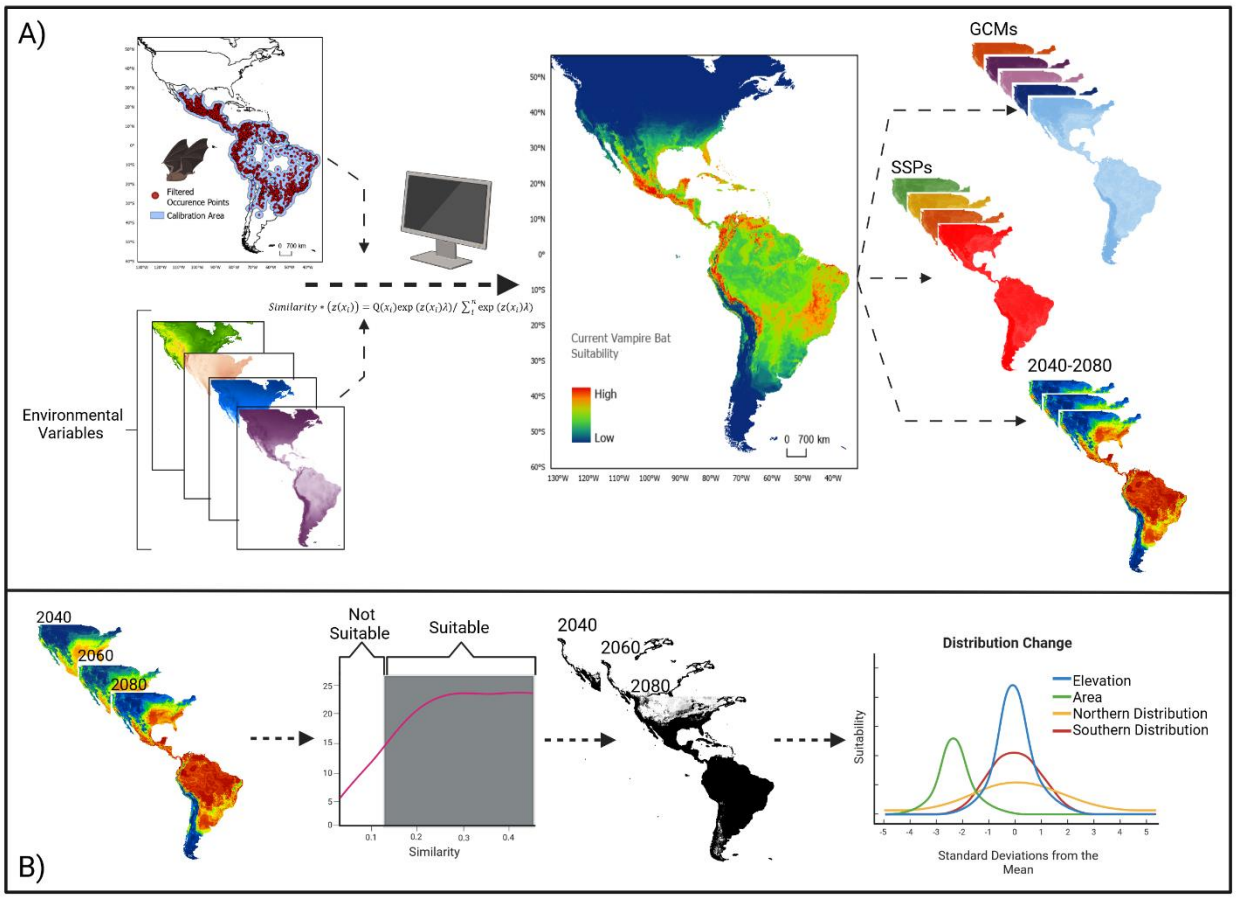

Figure 2: Model Calibration and Pattern Analysis. A) Model calibration: We used filtered occurrence locations and environmental variables from the WorldClim database [55], with a calibration area of 200km^2 (ten times species home range) [60,61] around the occurrence locations to calibrate MaxEnt models. The best model was used to estimate current suitability for *Desmodus rotundus*. We then projected suitability to future climate change projections across six global circulation models (GCMs), four possible future shared socio-economic pathways (SSPs one, two, three, and five), and three time periods (2040, 2060, and 2080). **B) Potential future distributions:** We used a minimum training presences threshold to isolate areas with suitable climates for *D. rotundus* based on results of our model's projections. We used this threshold to create binary rasters of future scenarios to explore possible changes in maximum and minimum latitude of projected occurrence (i.e., range shift north or south), total area (km^2) predicted as suitable for occurrence, and maximum projected elevation (i.e., range shift up mountain ranges into previously temperate areas).

Global Circulation Model Name	Abbreviation	ECS	TCR
Australian Community Climate and Earth System Simulator	ACC	4.7	2.1
Beijing Climate Center Climate System Model	BCC	3	1.7
Europe Wide Consortium Climate Model	EVeg	4.3	2.6
National Institute for Environmental Studies, University of Tokyo Model	MIROC	2.6	1.6
Max Planck Institute for Meteorology, Germany Model	MPI	3	1.8
United Kingdom Earth System Model	UK	5.3	2.8

Table 1: Global Circulation Model Sensitivity. Equilibrium climate sensitivity (ECS) and transient climate response (TCR) metrics from each associated Earth system Global Circulation model (GCM) as reported in Meehl et al. (2020) [67]. Both ECS and TCR are standard metrics of climate model sensitivity related to increased CO_2 concentrations. These six models were chosen to capture GCM-projected climate variability as available in the most recent iteration of NEX-GDDP CMIP6 GCMs [66–68]. These six models also capture ECS and TCR variance from high to low [67].

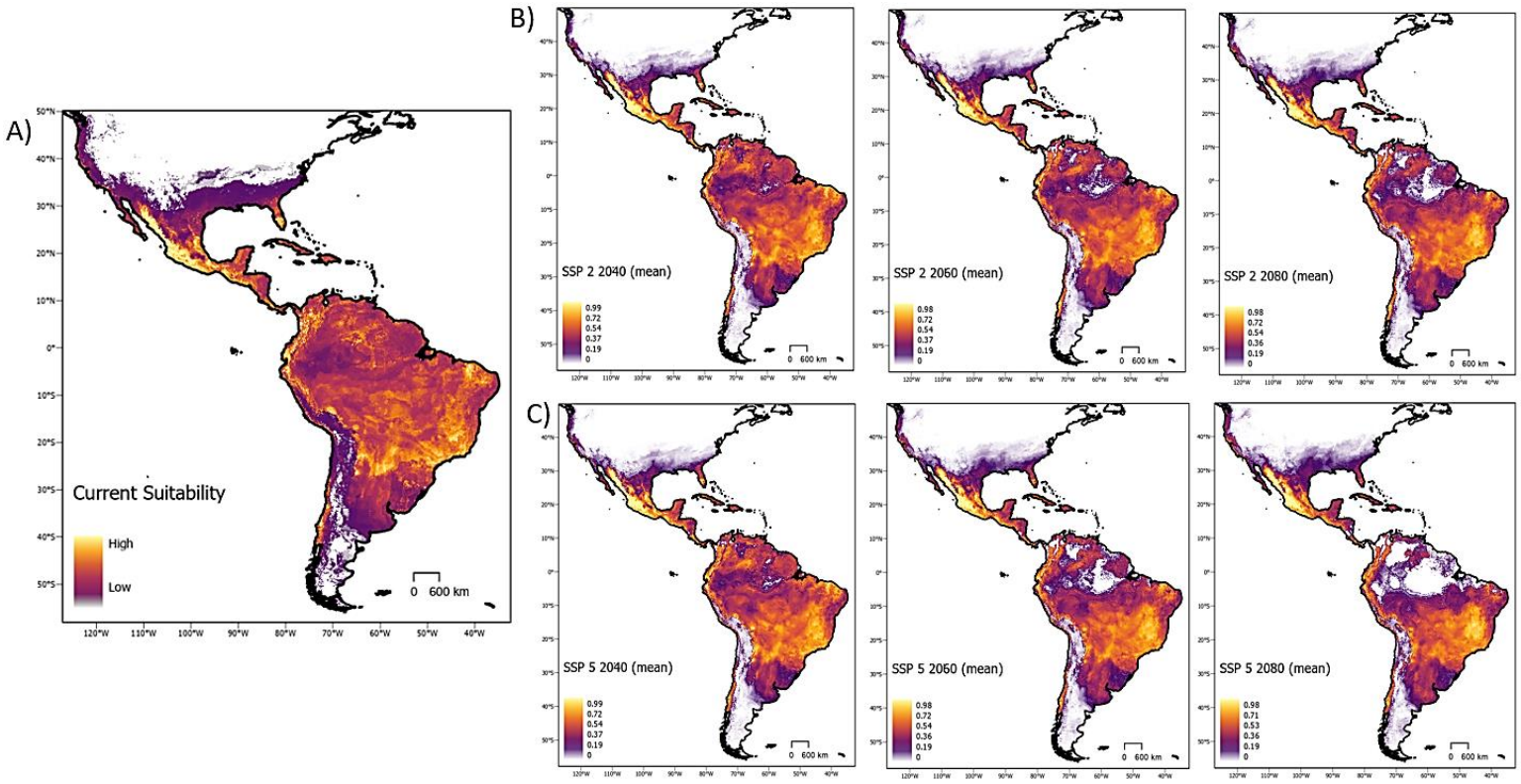

Figure 3: Suitability Projections. A) Continuous log output of projected suitability from best MaxEnt model for current conditions and averaged across all six GCMs for future scenarios. **B)** SSP two (upper panel), and **C)** SSP five (lower panel) are shown as the most likely best case (SSP 2) and worst case (SSP 5) scenarios. Current suitability is shown for no suitability (below minimum training presence) (white), low suitability (purple), and high suitability (yellow). Suitability is show from low (purple) to high (yellow) for future scenarios in panels at right. Note the loss of suitable area in central portions of the Amazon rainforest in both 2060 and 2080 projections. SSP five, which anticipates greater changes to precipitation seasonality, had much more extreme changes to *D. rotundus* potential future distribution when compared to current estimates. Suitability for the species extended both northward and southward of current estimates.

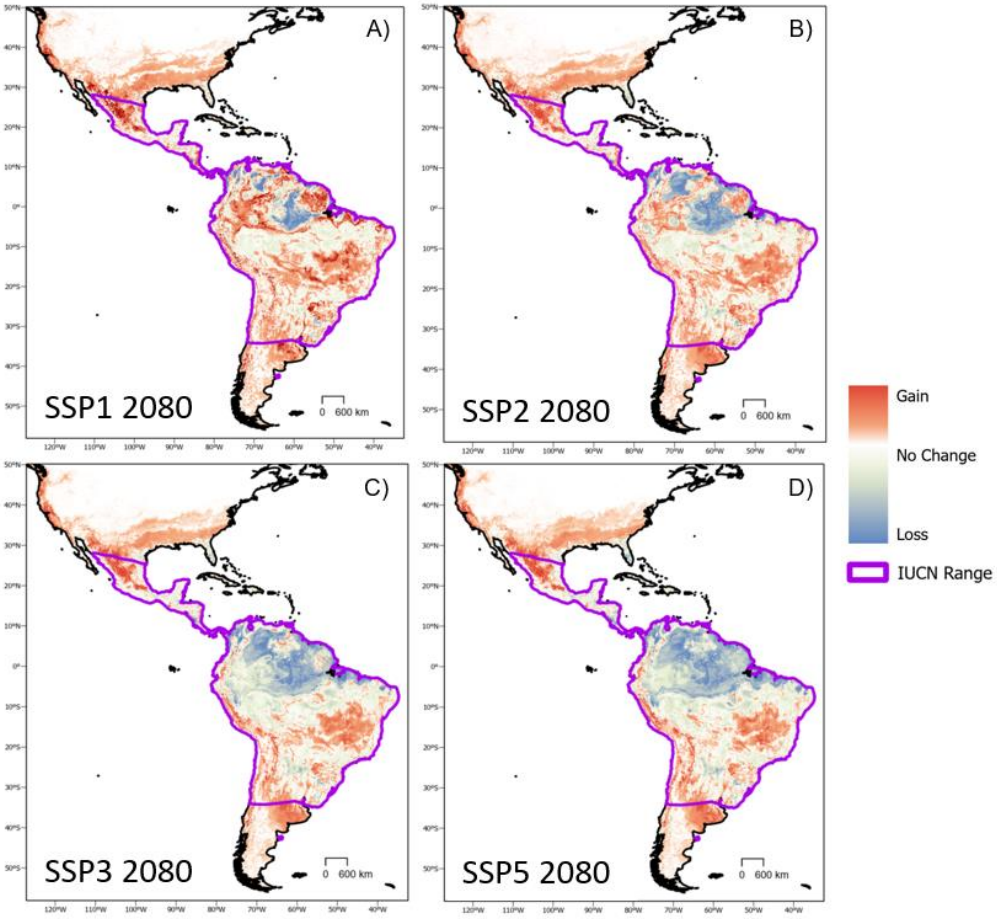

Figure 4: Change in Future Suitability. Continuous comparison of projected future suitability from the most distant future (2080) averaged across all GCMs to current estimates. Different shared socioeconomic pathways (climate change scenarios) are shown in panels **A)** SSP1, **B)** SSP2, **C)** SSP3, and **D)** SSP4. Areas with increase suitability are shown in red, areas with a loss of suitability are shown in blue. The current International Union for Conservation of Nature (IUCN) range for *D. rotundus* is shown in purple [39]. As future scenarios increase in their climate change impact, the loss of suitable area for *D. rotundus* in the central Amazon becomes more widespread. Increases in suitability under all SSPs are shown in western portions of Mexico, southern portions of the United States, and central portions of Argentina. Gains in suitability extended both northward and southward of current estimates.

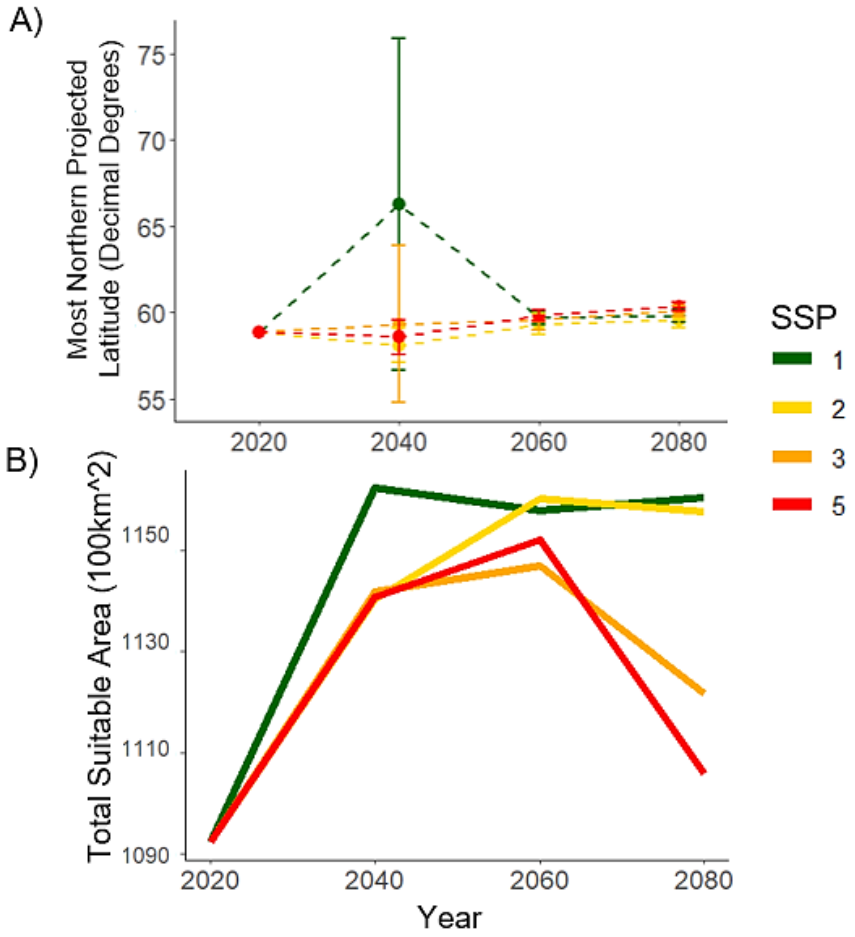

Figure 5: Projected Suitability Changes for *Desmodus rotundus*. A) Averaged most northern predicted range (i.e., maximum latitudes predicted) and from binarized outputs of suitability for *D. rotundus* across all six GCMs. Error bars represent standard error. Each individual SSP showed increases in most-northern suitable latitude. There was a significant increase in most-northern projected suitable latitude for *D. rotundus* across all SSPs (p=0.001, standard error=3.48, R^2=0.1). **B)** Total suitable area identified from binarized outputs of suitable area for *D. rotundus* across all six GCMs. After including SSP as a random effect, there was a significant increase in total suitable area (p=0.028, Standard Error=276.9, R^2=0.43) for *D. rotundus'* range across all projections. There were notable bell-curve patterns in total suitable area for SSPs three and five (i.e., worst-case scenarios).

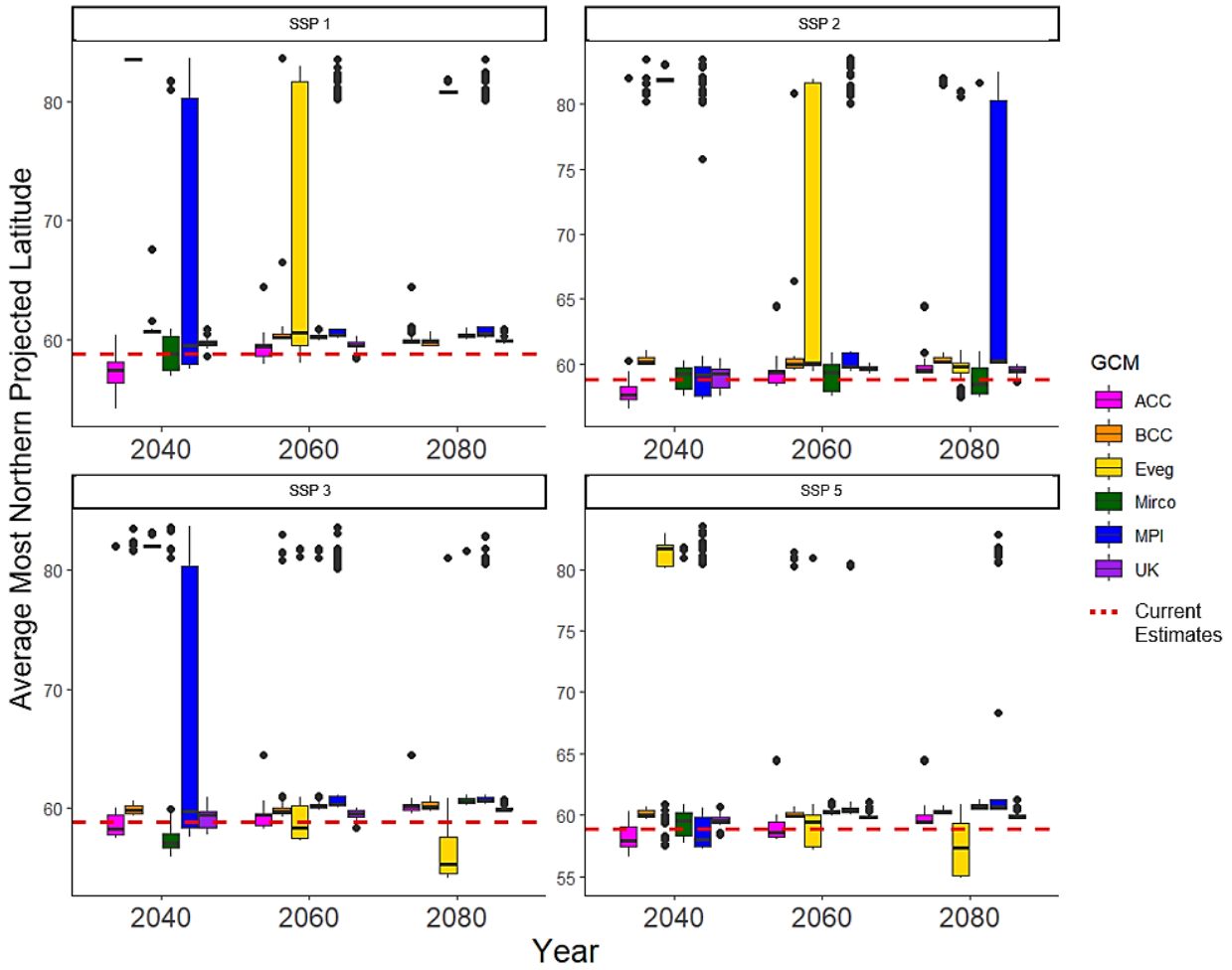

Figure 6: Global Circulation Model Variability. Variation in most northern (i.e., maximum) projected suitable latitude for *D. rotundus* for each GCM across all four SSPs is shown across all three time periods. Current estimates of the most northern suitable latitude for *D. rotundus* are shown by a dashed red line. GCMS included: Australian Community Climate and Earth System Simulator (ACC, pink); the Beijing Climate Center Climate System Model (BCC, orange); the Europe wide consortium climate model (Eveg, yellow), the National Institute for Environmental Studies, University of Tokyo model (Mirco, green); the Max Planck Institute for Meteorology, Germany model (MPI, blue); and the U.K. Earth System Model (UK, purple). While almost all future projections are above current estimates, some GCMs had higher rates or variation in their estimation than others. The Europe wide consortium climate model (Eveg, yellow) and the Max Planck Institute for Meteorology, Germany model (MPI, blue), which both have low sensitivity to increased CO_2 concentrations, had the highest rates of variation in their projections. GCMs are calibrated with differing metrics and effects of Earth system functions such as aerosol forcing [67,70,87]. For example, the MPI and EVeg models have relatively low values of aerosol forcing [67], which could contribute to the uncertainty we observed.

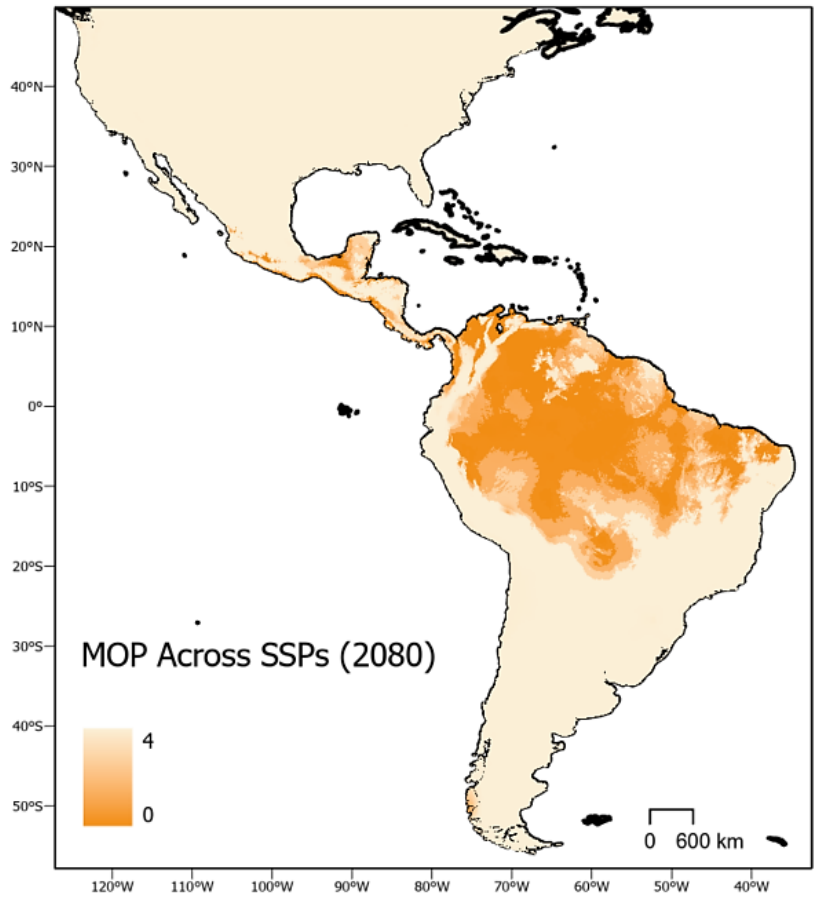

Figure 7: Geographic Patterns of Strict Extrapolation Risk. Post projection analysis of Mobility-Oriented Parity (MOP) for all four Shared Socioeconomic Pathways (SSPs one, two, three, and five) for the 2080 time period. An MOP analysis identifies areas with the most dissimilar climate conditions from the background environmental variables in the calibration data (i.e., where one or more covariate variables are outside ranges present in the training data). Areas with strict extrapolative are represented by zero values. Values above zero represent levels of similarity between the calibration area and the projected study areas across all SSPs (i.e., future scenarios). Areas with strict extrapolation risk are mainly located in the Amazon rainforest and in some areas of Central America.

References

1. IPCC. Climate change 2014 impacts, adaptation, and vulnerability Part B: Regional aspects: Working group ii contribution to the fifth assessment report of the intergovernmental panel on climate change. Barros VR, Field CB, Dokken DJ, Mastrandrea MD, Mach KJ, Chatterjee M, et al., editors. Working Group II Contribution to the Fifth Assessment Report of the Intergovernmental Panel on Climate Change. New York, NY: Cambridge University Press; 2014. doi:10.1017/CBO9781107415386

2. IPCC. Climate Change 2013 The Physical Science Basis. Stocker TF, Qin D, Plattner G-K, Tignor MMB, Allen SK, Boschung J, et al., editors. Working Group I Contribution to the Fifth Assessment Report of the Intergovernmental Panel on Climate Change. New York, NY: Cambridge University Press; 2013. doi:10.1017/CBO9781107415324

3. Iannella M, Masciulli U, Cerasoli F, Musciano M Di, Biondi M. Assessing future shifts in habitat suitability and connectivity to old-growth forests to support the conservation of the endangered giant noctule. PeerJ. 2022;10: e14446. doi:10.7717/peerj.14446

4. Mardani A, Streimikiene D, Cavallaro F, Loganathan N, Khoshnoudi M. Science of the Total Environment Carbon dioxide (CO_2) emissions and economic growth : A systematic review of two decades of research from 1995 to 2017. Sci Tota. 2019;649: 31–49. doi:10.1016/j.scitotenv.2018.08.229

5. Marvel K, Cook BI, Bonfils CJW, Durach PJ, Smerdon JE, Williams AP. Twentieth-century hydroclimate changes consistent with human influence. Nature. 2019;569: 59–65. doi:10.1038/s41586-019-1149-8

6. Lean JL. Cycles and trends in solar irradiance and climate. Sol Energy. 2010;44: 111–122. doi:10.1002/wcc.018

7. IPCC. Climate Change 2014 Part A: Global and Sectoral Aspects. Field CB, Barros VR, Dokken DJ, Mach KJ, Mastrandrea MD, Chatterjee TEBM, et al., editors. Climate Change 2014: Impacts, Adaptation, and Vulnerability. Part A: Global and Sectoral Aspects. Contribution of Working Group II to the Fifth Assessment Report of the Intergovernmental Panel on Climate Change. New York, NY: Cambridge University Press; 2014.

8. Caminade C, McIntyre KM, Jones AE. Impact of recent and future climate change on vector-borne diseases. Ann N Y Acad Sci. 2019;1436: 157–173. doi:10.1111/nyas.13950

9. Watts N, Amann M, Arnell N, Ayeb-Karlsson S, Belesova K, Boykoff M, et al. The 2019 report of The Lancet Countdown on health and climate change: ensuring that the health of a child born today is not defined by a changing climate. Lancet. 2019;394: 1836–1878. doi:10.1016/S0140-6736(19)32596-6

10. Whitmee S, Haines A, Beyrer C, Boltz F, Capon AG, De Souza Dias BF, et al. Safeguarding human health in the Anthropocene epoch: Report of the Rockefeller Foundation-Lancet Commission on planetary health. Lancet. 2015;386: 1973–2028. doi:10.1016/S0140-6736(15)60901-1

11. Hansen G, Cramer W. Global distribution of observed climate change impacts. Nat Clim Chang. 2015;5: 182–185. doi:10.1038/nclimate2529

12. García-Morales R, Badano EI, Moreno CE. Response of Neotropical Bat Assemblages to Human Land Use. Conserv Biol. 2013;27: 1096–1106. doi:10.1111/cobi.12099

13. Becker DJ, Nachtmann C, Argibay HD, Botto G, Escalera-Zamudio M, Carrera JE, et al. Leukocyte profiles reflect geographic range limits in a widespread Neotropical bat. Integr Comp Biol. 2019;59: 1176–1189. doi:10.1093/icb/icz007

14. Burrows MT, Schoeman DS, Richardson AJ, Molinos JG, Hoffmann A, Buckley LB, et al. Geographical limits to species-range shifts are suggested by climate velocity. Nature. 2014;507: 492–499. doi:10.1038/nature12976

15. Chen I, Hill JK, Ohlemüller R, Roy DB, Thomas CD. Rapid range shifts of species of climate warming. Science. 2011;333: 1024–1027.

16. Siraj AS, Santos-Vega M, Bouma MJ, Yadeta D, Carrascal DR, Pascual M. Altitudinal changes in Malaria incidence in highlands of Ethiopia and Colombia. Science. 2014;343: 1154–1159. doi:10.1126/science.1244325

17. Price SJ, Leung WTM, Owen CJ, Puschendorf R, Sergeant C, Cunningham AA, et al. Effects of historic and projected climate change on the range and impacts of an emerging wildlife disease. Glob Chang Biol. 2019;25: 2648–2660. doi:10.1111/gcb.14651

18. Parrish CR, Holmes EC, Morens DM, Park E, Burke DS, Calisher CH, et al. Cross-species virus transmission and the emergence of new epidemic diseases. Microbiol Mol Biol Rev. 2008;72: 457–470. doi:10.1128/MMBR.00004-08

19. Carlson CJ, Albery GF, Merow C, Trisos CH, Zipfel CM, Eskew EA, et al. Climate change increases cross-species viral transmission risk. Nature. 2022;607: 555–561. doi:10.1038/s41586-022-04788-w

20. Piret J, Boivin G. Pandemics throughout history. Front Microbiol. 2021;11: e631736. doi:10.3389/fmicb.2020.631736

21. Keesing F, Ostfeld RS. Impacts of biodiversity and biodiversity loss on zoonotic diseases. Proc Natl Acad Sci U S A. 2021;118: e2023540118. doi:10.1073/PNAS.2023540118

22. Han HJ, Wen H ling, Zhou CM, Chen FF, Luo LM, Liu J wei, et al. Bats as reservoirs of severe emerging infectious diseases. Virus Res. 2015;205: 2–6. doi:10.1016/j.virusres.2015.05.006

23. Irving AT, Ahn M, Goh G, Anderson DE, Wang LF. Lessons from the host defences of bats, a unique viral reservoir. Nature. 2021;589: 363–370. doi:10.1038/s41586-020-03128-0

24. Letko M, Seifert SN, Olival KJ, Plowright RK, Munster VJ. Bat-borne virus diversity, spillover and emergence. Nat Rev Microbiol. 2020;18: 461–471. doi:10.1038/s41579-020-0394-z

25. Pernet O, Schneider BS, Beaty SM, Lebreton M, Yun TE, Park A, et al. Evidence for henipavirus spillover into human populations in Africa. Nat Commun. 2014;5: e6342. doi:10.1038/ncomms6342

26. Li H, Mendelsohn E, Zong C, Zhang W, Hagan E, Wang N, et al. Human-animal interactions and bat coronavirus spillover potential among rural residents in Southern China. Biosaf Heal. 2019;1: 84–90. doi:10.1016/j.bsheal.2019.10.004

27. Velasco-Villa A, Mauldin MR, Mang Shi, Escobar LE, Gallardo-Romero NF, Damona I, et al. The history of rabies in the Western Hemisphere. Antiviral Res. 2017;146: 221–232. doi:10.1016/j.antiviral.2017.03.013.

28. Jones KE, Patel NG, Levy MA, Storeygard A, Balk D, Gittleman JL, et al. Global trends in emerging infectious diseases. Nature. 2008;451: 990–993. doi:10.1038/nature06536

29. Messina JP, Brady OJ, Golding N, Kraemer MUG, Wint GRW, Ray SE, et al. The current and future global distribution and population at risk of dengue. Nat Microbiol. 2019;4: 1508–1515. doi:10.1038/s41564-019-0476-8

30. Bathiany S, Dakos V, Scheffer M, Lenton TM. Climate models predict increasing temperature variability in poor countries. Sci Adv. 2018;4: e5809. doi:10.1126/sciadv.aar5809

31. Pörtner, H.O., D.C. Roberts, M. Tignor, E.S. Poloczanska, K. Mintenbeck, A. Alegría, M. Craig, S. Langsdorf, S. Löschke, V. Möller, A. Okem BR. Summary for policymakers. H.-O. Pörtner DCR, E.S. Poloczanska, K. Mintenbeck MT, A. Alegría, M. Craig, S. Langsdorf, S. Löschke, V. Möller AO, editors. Managing the Risks of Extreme Events and Disasters to Advance Climate Change Adaptation: Special Report of the Intergovernmental Panel on Climate Change. 2022. doi:10.1017/CBO9781139177245.003

32. Van de Vuurst P, Escobar LE. Climate change and infectious disease: A review of evidence and research trends. Infect Dis Poverty. 2023;12: 1–10. doi:10.1186/s40249-023-01102-2

33. Anderson A, Shwiff S, Gebhardt K, Ramírez AJ, Shwiff S, Kohler D, et al. Economic evaluation of vampire bat (*Desmodus rotundus*) rabies prevention in Mexico. Transbound Emerg Dis. 2014;61: 140–146. doi:10.1111/tbed.12007

34. Freire de Carvalho M, Vigilato MAN, Pompei JA, Rocha F, Vokaty A, Molina-Flores B, et al. Rabies in the Americas: 1998-2014. PLoS Negl Trop Dis. 2018;12: e0006271. doi:10.1371/journal.pntd.0006271

35. Meske M, Fanelli A, Rocha F, Awada L, Soto PC, Mapitse N, et al. Evolution of rabies in south america and inter-species dynamics (2009–2018). Trop Med Infect Dis. 2021;6: 2–18. doi:10.3390/tropicalmed6020098

36. PAHO/PANAFTOSA. SIRVERA. In: Sistema de Información Regional para la Vigilancia Epidemiológica de la Rabia (SIRVERA). 2019 [cited 20 Feb 2020]. Available: https://sirvera.panaftosa.org.br/

37. Cleaveland S, Hampson K. Rabies elimination research: Juxtaposing optimism, pragmatism and realism. Proc R Soc B. 2017;284: 20171880. doi:10.1098/rspb.2017.1880

38. Brunker K, Mollentze N. Rabies Virus. Trends Microbiol. 2018;26: 886–887. doi:10.1016/j.tim.2018.07.001

39. Barquez, R.M., Perez, S., Miller, B. & Diaz MM. *Desmodus rotundus.* In: The IUCN Red

List of Threatened Species 2015. 2015 [cited 6 Dec 2020] p. e.T6510A21979045. Available: https://dx.doi.org/10.2305/IUCN.UK.2015-4.RLTS.T6510A21979045.en.

40. Páez A, Polo L, Heredia D, Nuñez C, Rodriguez M, Agudelo C, et al. Brote de rabia humana transmitida por gato en el municipio de Santander de Quilichao, Colombia, 2008. Rev Salud Pública. 2009;11: 931–943. doi:10.1590/S0124-00642009000600009

41. Stoner-Duncan B, Streicker DG, Tedeschi CM. Vampire bats and rabies: Toward an ecological solution to a public health problem. PLoS Neglected Trop Dis. 2014;8: e2867. doi:10.1371/journal.pntd.0002867

42. Hayes MA, Piaggio AJ. Assessing the potential impacts of a changing climate on the distribution of a rabies virus vector. PLoS One. 2018;13: e0192887. doi:10.1371/journal.pone.0192887

43. Van de Vuurst P, Qiao H, Soler-Tovar D, Escobar LE. Climate change linked to vampire bat expansion and rabies virus spillover. Ecography. 2023; e06714. doi:10.1111/ecog.06714

44. Benavides JA, Valderrama W, Streicker DG. Spatial expansions and travelling waves of rabies in vampire bats. Proc R Soc B. 2016;283: 20160328. doi:10.1098/rspb.2016.0328

45. Streicker DG, Recuenco S, Valderrama W, Benavides JG, Vargas I, Pacheco V, et al. Ecological and anthropogenic drivers of rabies exposure in vampire bats: Implications for transmission and control. Proc R Soc B Biol Sci. 2012;279: 3384–3392. doi:10.1098/rspb.2012.0538

46. Phillips SJ, Dudík M, Schapire RE. Maxent software for modeling species niches and distributions Version 3.4.1. 2019 [cited 24 May 2021]. Available: http://biodiversityinformatics.amnh.org/open_source/maxent/

47. Phillips SJ, Anderson RP, Schapire RE. Maximum entropy modeling of species geographic distributions. Ecol Modell. 2006;190: 231–259. doi:10.1016/j.ecolmodel.2005.03.026

48. Phillips S. A Brief Tutorial on Maxent. Lessons Conserv. 2010;3: 108–135. Available: http://ncep.amnh.org/linc

49. Bárcenas-Reyes I, Loza-Rubio E, Zendejas-Martínez H, Luna-Soria H, Cantó-Alarcón GJ, Milián-Suazo F. Comportamiento epidemiológico de la rabia paralítica bovina en la región central de México, 2001-2013. Rev Panam Salud Publica/Pan Am J Public Heal. 2015;38: 396–402. doi:10665.2/18398

50. Elith J, Phillips SJ, Hastie T, Dudík M, Chee YE, Yates CJ. A statistical explanation of MaxEnt for ecologists. Divers Distrib. 2011;17: 43–57. doi:10.1111/j.1472-4642.2010.00725.x

51. Merow C, Smith MJ, Silander JA. A practical guide to MaxEnt for modeling species' distributions: What it does, and why inputs and settings matter. Ecography (Cop). 2013;36: 1058–1069. doi:10.1111/j.1600-0587.2013.07872.x

52. Phillips SJ, Dudík M. Modeling of species distributions with Maxent: New extensions and a comprehensive evaluation. Ecography. 2008;31: 161–175. doi:10.1111/j.0906-7590.2008.5203.x

53. Van de Vuurst P, Diaz MM, Rodriguez-San Pedro A, Allendes JL, Brown N, Gutierrez JD, et al. A database of common vampire bat reports. Sci Data. 2021;9: e41597. doi:10.1038/s41597-022-01140-9

54. Wickham H, Francois R, Henry L, Muller K. Package ‘ dplyr ’: A grammar of data manipulation. CRAN. 2020; 3–88.

55. Fick SE, Hijmans RJ. WorldClim 2: new 1-km spatial resolution climate surfaces for global land areas. Int J Climatol. 2017;37: 4302–4315. doi:10.1002/joc.5086

56. Etten J Van, Sumner M, Cheng J, Baston D, Bevan A, Bivand R, et al. Package ‘ raster ’: Geographic Data Analysis and Modeling. CRAN; 2021. pp. 14–64.

57. Peterson AT, Soberón J, Pearson RG, Anderson RP, Martínez-Meyer E, Nakamura M, et al. Ecological Niches and Geographic Distributions. Horn SAL and HS, editor. Ecological Niches and Geographic Distributions (MPB-49). Princeton, New Jersery: Princeton University Press; 2011. doi:10.23943/princeton/9780691136868.001.0001

58. Cobos ME, Townsend Peterson A, Barve N, Osorio-Olvera L. Kuenm: An R package for detailed development of ecological niche models using Maxent. PeerJ. 2019;7: e6281. doi:10.7717/peerj.6281

59. ESRI. ArcGIS Pro (Version 2.5). ESRI Inc.; 2019. Available: https://www.esri.com/en-us/arcgis/products/arcgis-pro/overview

60. Rocha F, Ulloa-Stanojlovic FM, Rabaquim VCV, Fadil P, Pompei JC, Brandão PE, et al. Relations between topography, feeding sites, and foraging behavior of the vampire bat, *Desmodus rotundus*. J Mammal. 2020;101: 164–171. doi:10.1093/jmammal/gyz177

61. Trajano E. Movements of cave bats in southeastern Brazil, with emphasis on the population ecology of the Common Vampire Bat, *Desmodus rotundus* (Chiroptera). Biotropica. 1996;28: 121. doi:10.2307/2388777

62. Rocha F, Dias RA. The common vampire bat *Desmodus rotundus* (Chiroptera: Phyllostomidae) and the transmission of the rabies virus to livestock: A contact network approach and recommendations for surveillance and control. Prev Vet Med. 2020;174: e104809. doi:10.1016/j.prevetmed.2019.104809

63. Warren DL, Seifert SN. Ecological niche modeling in Maxent: The importance of model complexity and the performance of model selection criteria. Ecol Appl. 2011;21: 335–342. doi:10.1890/10-1171.1

64. Morales NS, Fernández IC, Baca-González V. MaxEnt’s parameter configuration and small samples: Are we paying attention to recommendations? A systematic review. PeerJ. 2017;5: e3093. doi:10.7717/peerj.3093

65. Peterson AT, Papeş M, Soberón J. Rethinking receiver operating characteristic analysis applications in ecological niche modeling. Ecol Modell. 2008;213: 63–72. doi:10.1016/j.ecolmodel.2007.11.008

66. Hausfather Z, Marvel K, Schmidt GA, Nielsen-Gammon JW, Zelinka M. Climate simulations: recognize the ‘hot model’ problem. Nature. 2022;605: 26–29.

doi:10.1038/d41586-022-01192-2

67. Meehl GA, Senior CA, Eyring V, Flato G, Lamarque JF, Stouffer RJ, et al. Context for interpreting equilibrium climate sensitivity and transient climate response from the CMIP6 Earth system models. Sci Adv. 2020;6: 1–11. doi:10.1126/sciadv.aba1981

68. Murali G, Iwamura T, Meiri S, Roll U. Future temperature extremes threaten land vertebrates. Nature. 2023;615: 461–467. doi:10.1038/s41586-022-05606-z

69. Meinshausen M, Nicholls ZRJ, Lewis J, Gidden MJ, Vogel E, Freund M, et al. The shared socio-economic pathway (SSP) greenhouse gas concentrations and their extensions to 2500. Geosci Model Dev. 2020;13: 3571–3605. doi:10.5194/gmd-13-3571-2020

70. Tebaldi C, Debeire K, Eyring V, Fischer E, Fyfe J, Friedlingstein P, et al. Climate model projections from the Scenario Model Intercomparison Project (ScenarioMIP) of CMIP6. Earth Syst Dyn. 2021;12: 253–293. doi:10.5194/esd-12-253-2021

71. Mesgaran MB, Cousens RD, Webber BL. Here be dragons: A tool for quantifying novelty due to covariate range and correlation change when projecting species distribution models. Divers Distrib. 2014;20: 1147–1159. doi:10.1111/ddi.12209

72. Peterson AT. Ecological niche conservatism : a time-structured review of evidence. J Biogeogr. 2011;38: 817–827. doi:10.1111/j.1365-2699.2010.02456.x

73. Peterson AT. Mapping Disease Transmission Risk: Enriching Models Using Biology and Ecology. Baltimore: Johns Hopkins University Press; 2014.

74. Carvalho S, Lisboa F. A changing Amazon rainforest : Historical trends and future projections under post-Paris climate scenarios. Glob Planet Change. 2020;195: 103328. doi:10.1016/j.gloplacha.2020.103328

75. Flores BM, Montoya E, Sakschewski B, Nascimento N, Staal A, Betts RA, et al. Critical transitions in the Amazon forest system. Nature. 2024;626: 555–575. doi:10.1038/s41586-023-06970-0

76. Lee DN, Papeş M, Van Den Bussche RA. Present and potential future distribution of common vampire bats in the Americas and the associated risk to cattle. PLoS One. 2012;7: e42466. doi:10.1371/journal.pone.0042466

77. Zarza H, Martínez-Meyer E, Suzán G, Ceballos G. Geographic distribution of *Desmodus rotundus* in Mexico under current and future climate change scenarios: Implications for bovine paralytic rabies infection. Vet Mex. 2017;4: 3–16. doi:10.21753/vmoa.4.3.390

78. Arellano-Sota C. Vampire bat-transmitted rabies in cattle. Rev Infect Dis. 1988;10: 707–709. doi:10.1093/clinids/10.Supplement_4.S707

79. McNab BK. Energetics and the distribution of vampires. J Mammal. 1973;54: 131–144. doi:10.2307/1378876

80. Lyman CP, Wimsatt WA. Temperature regulation in the vampire bat, *Desmodus rotundus.* Physiol Zool. 1966;39: 101–109.

81. Wimsatt WA. Responses of captive common vampires to cold and warm environments. J

Mammal. 1962;43: 185–191. doi:10.2307/1377089

82. Feng X, Porporato A, Rodriguez-Iturbe I. Changes in rainfall seasonality in the tropics. Nat Clim Chang. 2013;3: 811–815. doi:10.1038/nclimate1907

83. Gilbert M, Nicolas G, Cinardi G, Van Boeckel TP, Vanwambeke SO, Wint GRW, et al. Global distribution data for cattle, buffaloes, horses, sheep, goats, pigs, chickens and ducks in 2010. Sci Data. 2018;5: 1–11. doi:10.1038/sdata.2018.227

84. NASA Earth Data. United States Socioeconomic Data and Applications Center (SEDAC). In: Earth Observing System Data and Information System [Internet]. 2022 [cited 17 Aug 2023]. Available: https://sedac.ciesin.columbia.edu/

85. NASA Earth Data. U.S. Social Vulnerability Index Grid 2018. In: Socioeconomic Data and Applications Center [Internet]. 2018. Available: https://sedac.ciesin.columbia.edu/data/set/usgrid-us-social-vulnerability-index/data-download

86. Viana M, Benavides JA, Broos A, Loayza DI, Niño R, Bone J, et al. Effects of culling vampire bats on the spatial spread and spillover of rabies virus. Sci Adv. 2023;9. doi:10.1126/sciadv.add7437

87. O'Neill BC, Tebaldi C, Van Vuuren DP, Eyring V, Friedlingstein P, Hurtt G, et al. The Scenario Model Intercomparison Project (ScenarioMIP) for CMIP6. Geosci Model Dev. 2016;9: 3461–3482. doi:10.5194/gmd-9-3461-2016

88. Owens HL, Campbell LP, Dornak LL, Saupe EE, Barve N, Soberón J, et al. Constraints on interpretation of ecological niche models by limited environmental ranges on calibration areas. Ecol Modell. 2013;263: 10–18. doi:10.1016/j.ecolmodel.2013.04.011

89. Qiao H, Peterson AT, Myers CE, Yang Q, Saupe EE. Ecological niche conservatism spurs diversification in response to climate change. Nat Ecol Evol. 2024;8: 729–738. doi:10.1038/s41559-024-02344-5

90. Bukovsky MS, Gao J, Mearns LO, O'Neill BC. SSP-Based land-use change scenarios: A critical uncertainty in future regional climate change projections. Earth's Futur. 2021;9: e2020EF001782. doi:10.1029/2020EF001782

CONCLUSION

Zoonotic spillover of pathogens from bat reservoirs has given rise to many of the most lethal pandemics to affect humans in recent decades [1–4]. The effective management of spillover transmission of zoonotic pathogens relies upon understanding of how spillover occurs, and how environmental factors modulate the likelihood of transmission. *Desmodus rotundus* is a known reservoir of rabies virus (RABV) [5–7], and recent research has shown that anthropogenic activity impacts the ecology of this species and its ability to transmit RABV to other species [8–10]. The *D. rotundus* RABV disease system exemplifies many of the factors identified as important to the broader elucidation of bat-borne disease emergence, and thus functions as a prime study system [11]. The goal of this dissertation research was to assess how environmental variation may explain the geography and ecology of wildlife hosts across different spatial scales. In doing so, we sought to fill key research gaps in the current understanding of emerging infectious diseases of bat origin.

In Chapter One, our main goal was to assess the distribution of *D. rotundus'* population genetic structure, and the implications of its landscape patterns on *D. rotundus* dispersal. We utilized standard methods for assessment of genetic variation at 12 microsatellite loci developed by Piaggio et al. (2008). We then quantified genetic variance and distribution of genetically clustered individuals across the landscape of Colombia with a comparator group of *D. rotundus* individuals from Mexico. We found that genetic structure was present within our collection of samples from Colombia, with two distinct populations detected. Limited differences were present between the identified populations with regard to genetic variance, climate of occupancy, or landscape characteristics. Our results confirm previous findings of male-biased dispersal for *D. rotundus* [12], and supported previous hypotheses of dispersal for this species through low-

elevation regions [13,14]. Furthermore, our results inform future research on the role of genetic connectivity upon RABV transmission between *D. rotundus* colonies in Colombia.

In Chapter Two, we sought to identify landscape level drivers of RABV spillover risk in Colombia. Results of this study suggested that anthropogenic factors, such as livestock density, are more informative for RABV spillover risk prediction than environmental or climatic variables alone. Our results echoed those of previous research in Colombia suggesting that numbers of cattle correlate with RABV spillover expansion [15]. We found that low chicken density, a proxy of subsistence agriculture, also was an informative variable for prediction RABV spillover transmission risk. In general, our results highlighted the importance of predictor variable selection (e.g., combination of predictor variables and control of sampling bias) in spillover risk estimations. Future research on RABV spillover should further explore the impacts of anthropogenic factors on RABV spillover at the local level, such as socioeconomic conditions.

Finally, in Chapter Three we assessed the potential impacts of future climate on the continent-wide distribution of *D. rotundus*. We found that *D. rotundus* could extend its range in the next 20-80 years into novel areas due to changes in climate. Areas that were vulnerable to a range expansion for *D. rotundus* include the southern United States and south-central portions of Argentina and Chile. Our findings also indicated that, while certain areas may gain climate suitability in the higher latitudes of *D. rotundus*' range, areas in the Amazon rainforest may become unsuitable for this species. It would be beneficial for preventive and educational program on RABV transmission to be implemented in areas predicted as vulnerable to *D. rotundus* range expansion.

The results of this dissertation support the theory that changes to landscape and climate driven by human activity can have tractable impacts in the geography and ecology of bat-disease

reservoirs [8,16–18]. Furthermore, this research fills key research gaps on the ecological dispersal of *D. rotundus* and transmission dynamics of RABV by *D. rotundus*. The methods utilized here could be used to identify similar factors in other bat-borne disease systems, especially within the context of the Anthropocene era. Both infectious diseases of wildlife origin and climate change present imminent threats to human and animal health. As the interactions between climate change, anthropogenic land-use change, and disease emergence continue to advance, it is important for researchers and stakeholders alike to be aware of the risks and impacts that the confluence of these factors can yield. This dissertation contributes to the elucidation of how global change impacts transmission and spillover of wildlife diseases. In an era of climate uncertainty and ecosystem degradation, this research may inform efforts to prevent negative health outcomes for humans and animals alike.

References

1. Shereen MA, Khan S, Kazmi A, Bashir N, Siddique R. COVID-19 infection: Origin, transmission, and characteristics of human coronaviruses. J Adv Res. 2020;24: 91–98. doi:10.1016/j.jare.2020.03.005

2. Plowright RK, Eby P, Hudson PJ, Smith IL, Westcott D, Bryden WL, et al. Ecological dynamics of emerging bat virus spillover. Proc R Soc B Biol Sci. 2014;282. doi:10.1098/rspb.2014.2124

3. Piret J, Boivin G. Pandemics throughout history. Front Microbiol. 2021;11: e631736. doi:10.3389/fmicb.2020.631736

4. Letko M, Seifert SN, Olival KJ, Plowright RK, Munster VJ. Bat-borne virus diversity, spillover and emergence. Nat Rev Microbiol. 2020;18: 461–471. doi:10.1038/s41579-020-0394-z

5. Bárcenas-Reyes I, Loza-Rubio E, Zendejas-Martínez H, Luna-Soria H, Cantó-Alarcón GJ, Milián-Suazo F. Comportamiento epidemiológico de la rabia paralítica bovina en la región central de México, 2001-2013. Rev Panam Salud Publica/Pan Am J Public Heal. 2015;38: 396–402. doi:10665.2/18398

6. Arellano-Sota C. Vampire bat-transmitted rabies in cattle. Rev Infect Dis. 1988;10: 707–709. doi:10.1093/clinids/10.Supplement_4.S707

7. Domenici D, Kurup D, Rupprechet CE, Socholand S, Yankowski C, Schnell M, et al. History of Rabies in the Americas: From the Pre-Columbian to the Present , Volume I. Rupprecht CE, editor. Springer; 2023. pp. 28-57.

8. Streicker DG, Recuenco S, Valderrama W, Benavides JG, Vargas I, Pacheco V, et al. Ecological and anthropogenic drivers of rabies exposure in vampire bats: Implications for transmission and control. Proc R Soc B Biol Sci. 2012;279: 3384–3392. doi:10.1098/rspb.2012.0538

9. Viana M, Benavides JA, Broos A, Loayza DI, Niño R, Bone J, et al. Effects of culling vampire bats on the spatial spread and spillover of rabies virus. 2023. doi:10.1126/sciadv.add7437

10. Van de Vuurst P, Qiao H, Soler-Tovar D, Escobar LE. Climate change linked to vampire bat expansion and rabies virus spillover. Ecography. 2023; e06714. doi:10.1111/ecog.06714

11. Escobar LE, Villa AV, Satheshkumar PS, Nakazawa Y, Van de Vuurst, P. Revealing the complexity of vampire bat rabies “spillover transmission.” Infect Dis Poverty. 2023;12: 1–9. doi:10.1186/s40249-023-01062-7

12. Martins FM, Templeton AR, Pavan AC, Kohlbach BC, Morgante JS. Phylogeography of the common vampire bat (*Desmodus rotundus*): Marked population structure, Neotropical Pleistocene vicariance and incongruence between nuclear and mtDNA markers. BMC Evol Biol. 2009;9: 10–13. doi:10.1186/1471-2148-9-294

13. Benavides JA, Valderrama W, Streicker DG. Spatial expansions and travelling waves of

rabies in vampire bats. Proc R Soc B. 2016;283: 20160328. doi:10.1098/rspb.2016.0328

14. Streicker DG, Winternitz J, Satterfield D, Condori-condori RE, Broos A, Tello C, et al. Host-pathogen evolutionary signatures reveal dynamics of future invasions of vampire bat rabies. Proc Na Acad Sci. 2016; 113:10926-10931. doi: 10.1073/pnas.1606587113

15. Rojas-sereno ZE, Streicker DG, Medina-Rodriguez AT, Benavides JA. Drivers of spatial expansions of vampire bat rabies in Colombia. Viruses. 2022;14. doi:10.3390/v14112318

16. Bolívar-Cimé B, Flores-Peredo R, García-Ortíz SA, Murrieta-Galindo R, Laborde J. Influence of landscape structure on the abundance of *Desmodus rotundus* (Geoffroy 1810) in northeastern Yucatan, Mexico. Ecosistemas y Recur Agropecu. 2019;6: 263. doi:10.19136/era.a6n17.1968

17. Brierley L, Vonhof MJ, Olival KJ, Daszak P, Jones KE. Quantifying global drivers of zoonotic bat viruses: A process-based perspective. Am Nat. 2016;187: E53–E64. doi:10.1086/684391

18. Johnson CK, Hitchens PL, Pandit PS, Rushmore J, Evans TS, Young CCW, et al. Global shifts in mammalian population trends reveal key predictors of virus spillover risk. Proc R Soc B Biol Sci. 2020;287. doi:10.1098/rspb.2019.2736